REVIEW

Aerogels Meet Phase Change Materials: Fundamentals, Advances, and Beyond

Panpan Liu, Xiao Chen,* Yang Li, Piao Cheng, Zhaodi Tang, Junjun Lv, Waseem Aftab, and Ge Wang*

Cite This: https://doi.org/10.1021/acsnano.2c05067

Read Online

ACCESS | Metrics & More | Article Recommendations

ABSTRACT: Benefiting from the inherent properties of ultralight weight, ultrahigh porosity, ultrahigh specific surface area, adjustable thermal/electrical conductivities, and mechanical flexibility, aerogels are considered ideal supporting alternatives to efficiently encapsulate phase change materials (PCMs) and rationalize phase transformation behaviors. The marriage of versatile aerogels and PCMs is a milestone in pioneering advanced multifunctional composite PCMs. Emerging aerogel-based composite PCMs with high energy storage density are accepted as a cutting-edge thermal energy storage (TES) concept, enabling advanced functionality of PCMs. Considering the lack of a timely and comprehensive review on aerogel-based composite PCMs, herein, we systematically retrospect the state-of-the-art advances of versatile aerogels for high-performance and multifunctional composite PCMs, with particular emphasis on advanced multiple functions, such as acoustic−thermal and solar−thermal−electricity energy conversion strategies, mechanical flexibility, flame retardancy, shape memory, intelligent grippers, and thermal infrared stealth. Emphasis is also given to the versatile roles of different aerogels in composite PCMs and the relationships between their architectures and thermophysical properties. This review also showcases the discovery of an interdisciplinary research field combining aerogels and 3D printing technology, which will contribute to pioneering cutting-edge PCMs. This review aims to arouse wider research interests among interdisciplinary fields and provide insightful guidance for the rational design of advanced multifunctional aerogel-based composite PCMs, thus facilitating the significant breakthroughs in both fundamental research and commercial applications.

KEYWORDS: phase change materials, carbon aerogels, silica aerogels, polymer aerogels, metal aerogels, thermophysical properties, thermal energy storage, energy conversion, advanced multiple functions
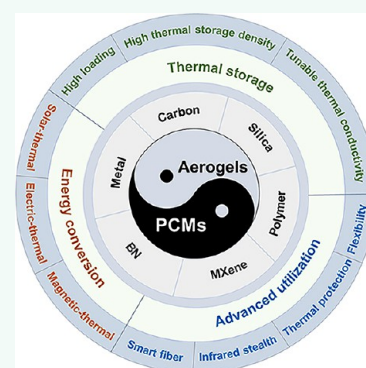
1. INTRODUCTION

Human development is dependent on fossil energy, resulting in climate change and energy shortages, which are already global problems for humankind. Therefore, it is imperative to develop clean, low-cost, and sustainable energy. Thermal energy storage (TES) is one of the key technologies to support the large-scale development of renewable energy. Rapid latent heat energy storage technology advancements have imposed stringent energy efficiency requirements on next-generation shape-stabilized composite phase change materials (PCMs).[1] Maximizing the energy storage efficiency of shape-stabilized composite PCMs is highly dependent on the structure and properties of the supporting materials. Compared to other composite PCMs, aerogel-based PCMs TES is accepted as a cutting-edge concept, enabling the advanced functionality of PCMs.

Aerogels are a class of continuous three-dimensional (3D) porous networked solid materials. Aerogels create a family of solid materials toward versatile application prospects by integrating the attributes of separated solids with macroscopic

morphology.[2,3] Benefiting from ultralow density, ultrahigh porosity and specific surface area, excellent mass transfer properties, and ultralow thermal conductivity, aerogels show great promise in numerous fields, such as high adsorption,[4] thermal insulation,[5] sensors,[6] and energy storage.[7] Aerogels have attracted increasing interest from academia and industry over the past 20 years. With the dramatically increased thermal energy storage demand in recent years, aerogels have been considered promising alternatives to efficiently encapsulate PCMs and rationalize phase transformation behavior.[8−11] The marriage of versatile aerogels and PCMs is a milestone in pioneering advanced multifunctional composite PCMs.

PCMs are functional energy storage materials that achieve reversible storage and release of thermal energy through phase change process and are widely used in thermal energy storage, thermal energy management, and solar energy utilization. The liquid phase leakage of pristine PCMs is a long-standing bottleneck in both industrial and domestic application scenarios. Therefore, infiltrating PCMs into supporting materials to prepare shape-stabilized composite PCMs is a feasible solution, which has become a hot research topic in recent years.[1,12−14] Notably, it is still challenging to balance between shape stability and energy storage density in the shape-stabilized composite PCMs, as the introduced supporting materials are inactive materials without energy storage capacity. Aerogels are considered to be ideal supporting materials to efficiently encapsulate PCMs to prevent leakage for PCMs due to strong capillary forces and surface tension.[15,16] Benefiting from their ultralight weight, ultrahigh specific surface area, and porosity, the maximum loading of PCMs can be achieved in aerogels, thus maintaining ultrahigh energy storage density.[17] More attractively, versatile aerogels can also ameliorate the inherent defects of PCMs, and another advantage is that aerogels impart fascinating properties and advanced multiple functions to PCMs. Specifically, (1) the inherent low thermal conductivity of PCMs limits the heat charging/discharging rates.[18,19] Designing 3D structural highly thermally conductive nanofillers is advantageous to reduce the contact thermal resistance between nanofillers.[20−22] Emerging aerogels with high 3D thermally conductive networks can significantly improve the thermal conductivity of PCMs with little sacrifice in energy storage density. (2) Equally important, the reduction of the thermal conductivity of PCMs plays an important role in thermal protection.[23] Integrating aerogels with low 3D thermally conductive networks with PCMs can design satisfactory thermal protection products. (3) It is imperative to develop multiresponse thermal energy capture and storage systems, including solar energy, electric energy, magnetic energy, and acoustic energy.[24,25] However, pristine PCMs are not conducive to converting these into thermal energy due to inferior solar-trapping capacity, electrical conductivity, and magnetic permeability.[26−30] Integrating PCMs into functional aerogels can respond to multiple energy sources quickly. (4) Interestingly, the ingenious integration of PCMs and aerogels accelerates the development of advanced multifunctional composite PCMs, such as mechanical flexibility, shape memory, thermal infrared stealth, and flame retardancy.[31−35] These advanced functions provide an innovative application platform, such as wearable thermal management, thermoregulating textiles, and intelligent grippers.

To date, many reviews on the application of aerogels for adsorption, battery storage, and sensing are available, and many reviews have also been published on nanoporous supporting materials for the performance enhancement of PCMs, especially various carbon materials. However, a timely and comprehensive review of aerogel frameworks for shape stabilization of PCMs is still lacking, especially focusing on the relationships between the structures of aerogels and the thermophysical performances of composite PCMs. Herein, we provide a timely and comprehensive review highlighting the state-of-the-art advances of aerogel-based composite PCMs. This review retrospectively describes the fundamental development of versatile aerogels, focusing on the relationships between the physical properties of aerogels and the

thermophysical properties of PCMs. This review highlights energy conversion pathways of PCMs responding to multiple energy sources (such as solar energy, electric energy, magnetic energy, and acoustic energy) to harvest thermal energy. In particular, we emphasize the direct power generation energy conversion pathways based on PCMs using solar energy, which is a breakthrough for solar energy utilization. This review also provides particular emphasis on state-of-the-art advances in advanced cutting-edge multifunctional aerogel-based composite PCMs, such as flexible PCMs, thermal infrared stealth, shape memory, and intelligent grippers (Figure 1). The review

Figure 1. Layout structure of this review. Highlighting main advanced multifunctional applications of various aerogel-based composite PCMs.

also showcases the discovery in interdisciplinary research fields combining aerogels and 3D printing technology, which will serve well to pioneer cutting-edge PCMs. Finally, we introduce critical considerations on the opportunities and challenges in the development of advanced high-performance and multifunctional aerogel-based composite PCMs, hoping to provide constructive references for the rational design of advanced multifunctional PCMs and facilitate their significant breakthroughs in both fundamental research and commercial applications.

2. OVERVIEW OF PCMs AND AEROGELS

2.1. Overview of PCMs. *2.1.1. Classification of PCMs.* Phase change materials can absorb and release large amounts of latent heat during the reversible isothermal phase change process.[36−38] PCMs are divided into solid−gas PCMs, liquid−gas PCMs, solid−solid PCMs, and solid−liquid PCMs based on phase transition. Comparatively, solid−liquid PCMs are more practical in TES systems due to their relatively high latent heat and small volume change (approximately 10% or less), stable phase change temperature, and ease of control.[39−41] Furthermore, solid−liquid PCMs are divided into inorganic PCMs, organic PCMs and eutectic PCMs. Organic PCMs exhibit small supercooling degree, noncorrosive and no phase separation, including paraffins, alcohols, and fatty

acids. Inorganic PCMs exhibit high latent heat and relatively high thermal conductivity (0.40−0.70 W/m·K), including hydrated salts, salts or metals. The irreversible salts binding lower hydration numbers emerge due to the inconsistent melting of salt hydrates. Their large phase separation and supercooling degree seriously hinder the far-ranging applications. Comparatively, organic PCMs are more popular in practical applications due to the advantages of easy handling and relatively low cost. Nevertheless, the inherently low thermal conductivity (usually less than 0.40 W/m·K), liquid phase leakage, and flammability seriously hinder their far-ranging applications.[42] To address these issues, the integration of PCMs with various supporting materials has been recognized as an effective way. Good chemical compatibility between PCMs and supporting materials is a prerequisite for maintaining high heat storage. Organic PCMs, such as fatty acids and their derivatives, alkanes and their mixtures, and PEG, have been proven to have good compatibility with inorganic porous materials (including expanded clay, expanded fly ash, and expanded perlite) and organic porous materials (including expanded graphite, carbon nanotubes, graphene, and carbon nanofibers). Certainly, the phase change behavior of PCMs can be regulated by suitable surface functional design, thereby improving the heat storage and release characteristics. Notably, it is a competitive advantage for aerogels that the porous structures can be tailored by modifying the functional groups or the ratio between the precursors to better match PCMs in terms of morphology and surface chemistry.

2.1.2. Confinement Strategies of PCMs. Confinement is defined as encapsulating PCMs into supporting materials for the preparation of shape-stabilized composite PCMs, realizing leakage-proof, corrosion-proof and avoiding reacting with the external environment.[43] Confinement strategies are divided into nanoconfinement, microconfinement, and macroconfinement based on the size of the supporting materials.[44−46] The advent of nanoscience and technology has revolutionized the development of shape-stabilized PCMs. It has been found that adhesion, van der Waals interactions, capillary interactions, and surface chemistry are more effective in the encapsulation of PCMs on the nanoscale. Depending on the dimensions of the supporting materials, confinement strategies are divided into (I) core−shell confinement (0D), (II) longitudinal confinement (1D), (III) interface confinement (2D), and (IV) porous confinement (3D). In core−shell confinement, PCMs are encapsulated by shell materials. Through coaxial electrospinning technology, PCMs are penetrated into the inner cavity of carbon nanotubes (CNTs) (tubular confinement) or nanofibrous materials, realizing the longitudinal or 1D confinement of organic PCMs. In interface confinement, such as MXenes, boron nitride (BN) nanosheets, graphene, or graphene oxide, PCMs are confined between the nanomaterial layers through interfacial interaction. In nanoporous confinement, the nanomaterials self-assemble into interconnected 3D nanoporous frameworks, and PCMs are infiltrated into these nanoporous frameworks. Depending on the confinement steps, confinement strategies can be classified into two-step methods and a one-step in situ synthesis method. The two-step methods refer to the design and synthesis of supporting materials followed by the infiltration of PCMs into the supporting materials. Generally, melt impregnation, solvent impregnation, and vacuum-assisted impregnation methods are very versatile. The one-step in situ synthesis method synchronously completes the generation of shell or nanoporous networks

and the encapsulation of PCMs, meaning that PCMs are encapsulated in situ within the pores during the formation of shell or interconnected nanoporous supporting networks.[47]

Intriguingly, different from traditional manufacturing methods, additive manufacturing methods can produce objects with high precision, shape fidelity, additional functionality, and excellent material properties.[48,49] Strikingly, researchers have applied 3D printing strategies to the preparation of composite PCMs, providing flexible solutions for complex and programmable PCMs.[50−52] 3D printing technology for PCMs pushes their application to the forefront and will allow PCMs to be integrated into advanced multimaterial architectures.

2.2. Overview of Aerogels. *2.2.1. Aerogel Species.* Aerogels are a kind of ultralight nanoporous materials with 3D network structure. Benefiting from their ultralow density, ultrahigh porosity, ultrahigh specific surface area, and excellent mass transfer properties, aerogels integrate a variety of fascinating physical properties.[53] From inception in 1931,[54] Kistler developed the silica aerogels, and since then, aerogels have received continued attention from researchers and engineers. A particularly important contribution to this field was the discovery of polymer-derived carbon aerogels by Pekala in the 1980s.[55] Subsequently, the carbon aerogel family exhibits fascinating developments, including CNT aerogels, carbon nanofiber aerogels, and graphene aerogels.[56−58] In recent years, various aerogels have emerged in an endless stream, and the properties of aerogels have been diversified, mainly including oxides, carbon, polymers, metals, biomass, and non-oxide ceramic aerogels. The most common silica aerogels exhibit good thermal stability and ultralow thermal conductivity. However, traditional silica aerogels usually suffer from weak mechanical strength and high brittleness. Silica aerogels with longer durations and higher strength can be obtained by the appropriate selection of silane precursors and reinforcement with polymers.[59] Comparatively, carbon aerogels have the advantages of mechanical flexibility, high electrical conductivity, and resistance to acid and alkali corrosion.[60] Polymer aerogels, such as polyimide and poly-(vinyl alcohol) aerogels, also exhibit good flexibility. However, polymer aerogels generally suffer from inferior thermal stability.[61] Metal aerogels typically exhibit high electrical conductivity and durability. In 2009, Eychmüller et al.[62] prepared noble metal aerogels, monometal (Pt, Ag, and Au), and bimetal (Pt/Ag and Au/Ag) aerogels composed of metal nanoparticles via sol−gel chemical gelation. Some metal aerogels composed of metal nanowires exhibit good mechanical flexibility.[63] Compared to conventional aerogels, biodegradability is an important feature of biomass aerogels, which are sustainable and more environmentally friendly materials. Biomass aerogels are usually synthesized from extracted biomass through cross-linking reactions. The corresponding raw materials are abundant, sustainable, and environmentally friendly.[64,65] Intriguingly, these biomass aerogels are generally biodegradable and biocompatible. Recently, some non-oxide ceramic aerogels have been developed, such as BN aerogels[66] and MXene aerogels.[67] These 2D lamellar materials no longer undergo restacking and reagglomeration due to 3D structure of aerogels.

2.2.2. Fabrication Strategies of Aerogels. Aerogels are typically prepared via a sol−gel method, a process involving the conversion of molecular precursors into highly cross-linked inorganic or organic gels. Then the liquid components of wet gels are replaced by gas (usually air) using appropriate drying
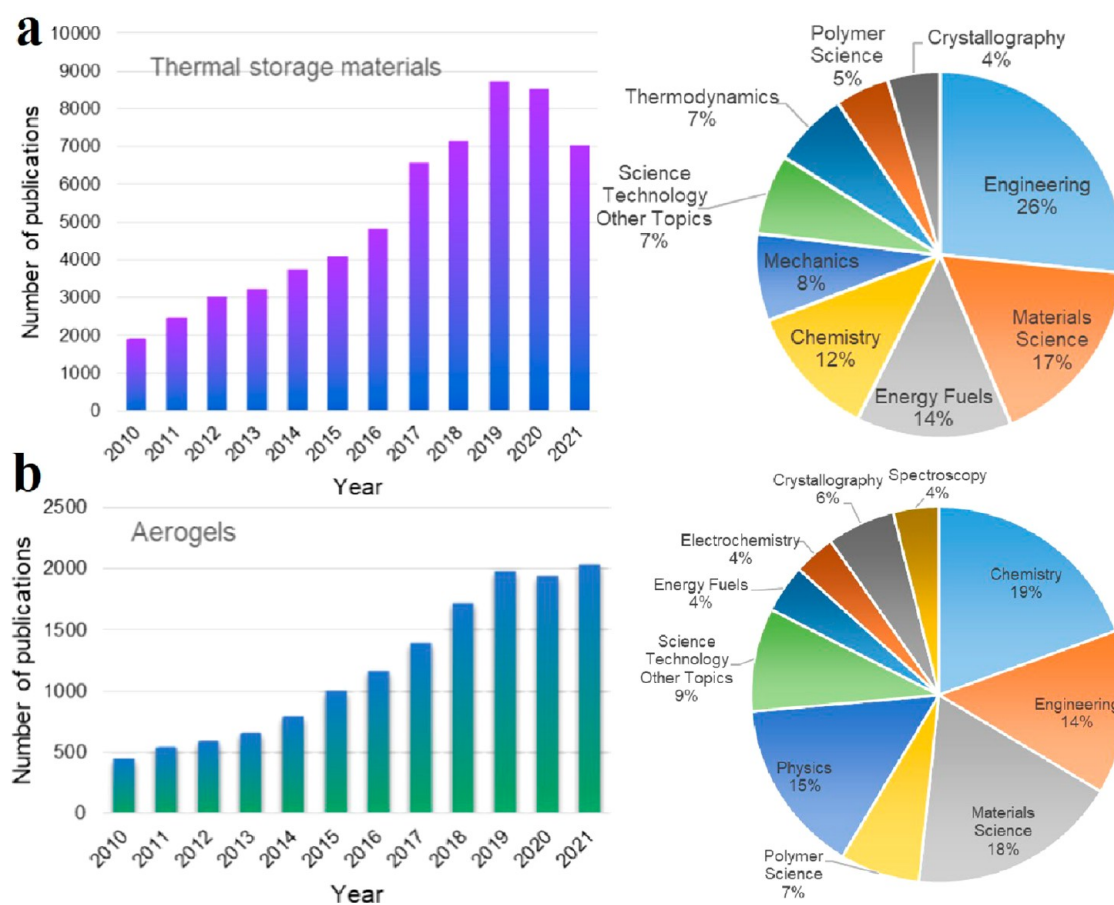
Figure 2. Number of publications of aerogels and thermal storage materials from 2010 to 2021, and data visualization of application fields, data extracted from Web of Science.

techniques (e.g., supercritical drying, freeze-drying, and ambient pressure drying) to obtain a 3D solid network.[68] Classically, the construction of silica aerogels generally requires three steps: (I) gel formation, (II) aging, and (III) drying. The aging step is considered to strengthen the gel after the gelation of silica aerogels.[69] Carbon aerogels are generally prepared by carbonizing organic aerogels, including polymerization, drying and carbonization. CNTs, graphene, and graphene oxide aerogels are usually prepared via a sol−gel method without carbonization. In addition, the preparation methods of graphene aerogels also include a hydrothermal reduction/self-assembly method, a chemical reduction method, and a template-directed reduction method.[60,70] The preparation of nanocellulose aerogels is generally divided into three steps: (I) dispersion of nanocellulose, (II) gelation of nanocellulose, and (III) gel drying process.[71] Traditional preparation methods of metal aerogels include dealloying, powder metallurgy, templating, and sol−gel methods.[72]

Interestingly, 3D-printed aerogels were reported by extrusion 3D printing with GO-based inks in 2015,[73] which overturned traditional preparation technology. This is interdisciplinary research area combining aerogels and 3D printing technology. The feasibility of additive manufacturing of aerogels has been demonstrated for graphene, graphene oxide, carbon nitride, gold, resorcinol formaldehyde, cellulose, and MXenes.[74,75] A recent achievement in additive manufacturing of silica aerogels has been made by Malfait et al. They printed silica aerogels with silica aerogels powders in *n*-pentyl alcohol-based silica sols using direct-write shaping technique.[76]

2.2.3. Properties of Aerogels. Aerogels are more competitive in obtaining high-performance composite PCMs due to their excellent properties in terms of density, porosity, specific surface area, and tunable mechanical properties. Researches related to PCMs and aerogels have been growing in the past decade, and they have been kept hot in multiple fields (Figure 2).

2.2.3.1. Density. One fascinating property of aerogels is ultralow density, making them the lightest solid in the world.[77] Lightweight composite PCMs are the pursuit of the future, and the energy storage density of composite PCMs, expressed as phase change enthalpy, basically decreases as the content of supporting materials increases. Therefore, the weight of supporting materials should be kept to a minimum. Attractively, aerogels are ultralight materials that are suitable to encapsulate PCMs to ensure the high gravimetric energy density of composite PCMs.

2.2.3.2. Textural Properties. Porosity, specific surface area and pore size are particularly important physical parameters in aerogels. A hierarchically porous structure with a high porosity and specific surface area can facilitate the accommodation of large amounts of PCMs, enabling ultrahigh loading of PCMs.[78,79] Generally, the movement of molecular chains of PCMs is restricted in micropores, thus limiting their free crystallization of PCMs, while large macropores are insufficient to accommodate liquid PCMs due to weak capillary forces.[80,81] Comparatively, aerogels with mesopores are more appropriate for adsorption and stabilization of PCMs due to considerable surface tension and capillary force. More importantly, the
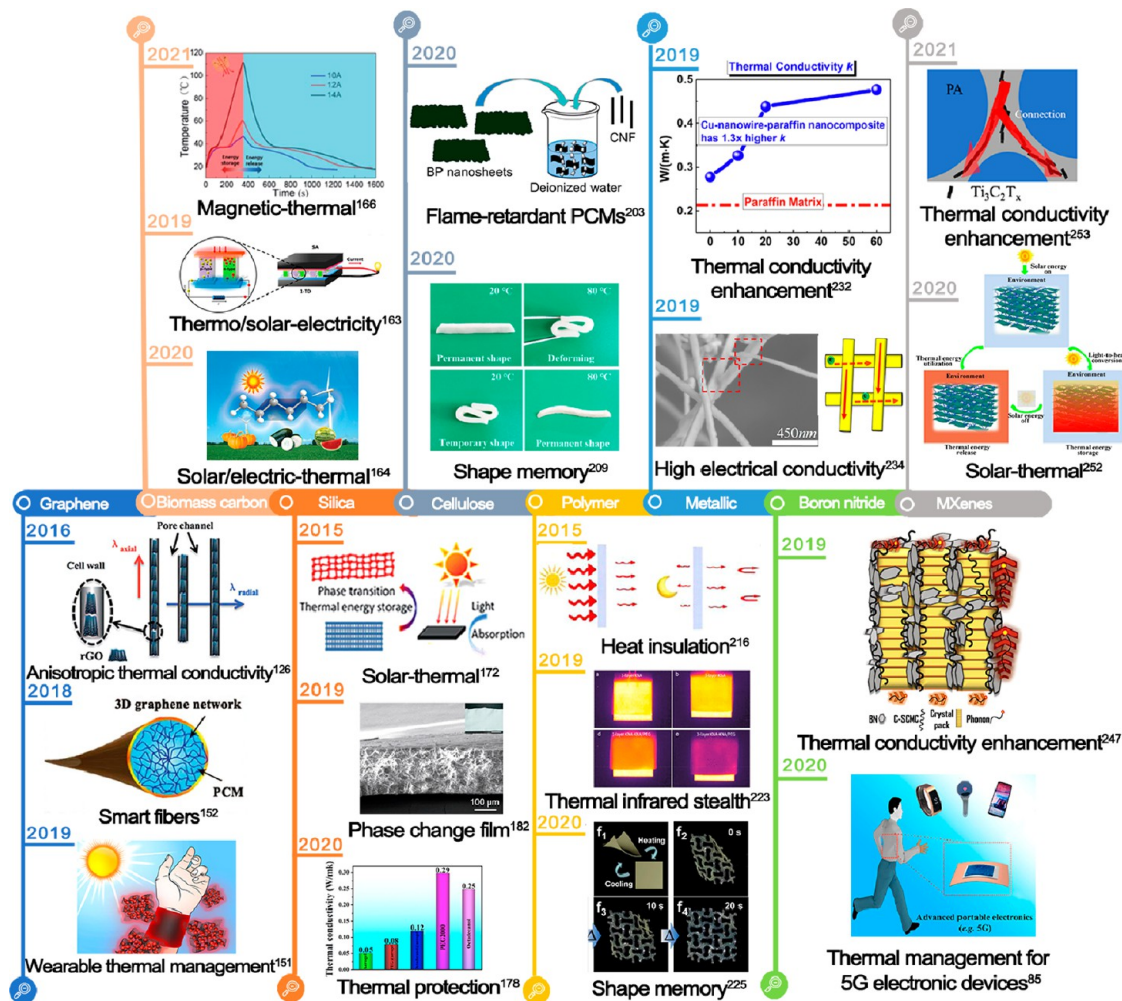
Figure 3. Timeline of major breakthroughs of aerogel-based composite PCMs in recent years.

porous structure of aerogels can be tailored by modifying the functional groups or the ratio between the precursors to better match PCMs in terms of morphology and surface chemistry.

2.2.3.3. Thermal Properties. Depending on the application scenarios of PCMs, thermal conductivity is requisite to be stimulated or suppressed. Aerogels composed of thermally conductive or nonthermally conductive materials are considered as promising supporting materials to regulate the thermal conductivities of PCMs. Highly thermally conductive PCMs can facilitate heat transfer and thermal energy charging/discharging rates, while PCMs with low thermally conductive are suitable candidates for thermal protection.

Generally, the thermal conductivity of aerogels is ultralow due to the severe scattering effect of nanopores on phonons, which reduces the average free path of phonons. The pore walls of nanoporous aerogels with a higher porosity constantly reflect and refract thermal radiation, thus reducing the heat transferred by radiation.[82,83] For instance, 3D graphene aerogels containing a low volume fraction of graphene still exhibit a low thermal conductivity, even though graphene has an extremely high thermal conductivity.[84] However, interestingly, once the air in aerogels is replaced by PCMs, the thermal conductivity of composite PCMs will be effectively enhanced because the heat flow along the interconnected graphene nanosheets is collected at the junctions and is then transported to the adjacent graphene nanosheets, thus forming continuous

heat transfer channels.[85] Therefore, a highly thermally conductive network of graphene aerogels allows rapid heat transfer throughout the PCMs. This concept is also applicable to aerogel-based composite PCMs composed of other highly thermally conductive materials, such as BN aerogels, MXene aerogels, and metal aerogels. Conversely, when PCMs are encapsulated in aerogels composed of low thermally conductive components, such as silica aerogels, polymer aerogels, and cellulose aerogels, the thermal conductivity of aerogel-based composite PCMs will be suppressed.

2.2.3.4. Mechanical Properties. The mechanical properties of traditional silica aerogels can be enhanced with the assistance of nanofillers and polymers. Graphene aerogels, cellulose aerogels, and polymer aerogels generally exhibit outstanding mechanical performance under external forces, including compressive strength and flexibility, due to the high strength of the components and the stable porous structure of the formed aerogels. This is a prerequisite to guarantee excellent shape stability of composite PCMs due to their stable porous structure. Intriguingly, flexible aerogels can also endow composite PCMs with good flexibility. The resulting flexible aerogel-based composite PCMs further broaden advanced multifunctional applications of PCMs. Emerging flexible PCMs offer great application potential in thermal management of wearable devices, thermoregulating textiles, and shape memory materials.[31]

Up to now, carbon aerogel-based, silica aerogel-based, polymer aerogel-based, metal aerogel-based, boron nitride aerogel-based, and MXene aerogel-based composite PCMs have attracted extensive interest from researchers and engineers. Figure 3 shows the timeline of major breakthroughs in various aerogel-based composite PCMs in recent years.

3. CARBON AEROGEL-BASED PCMs

Carbon aerogels (CAs) typically have a continuous 3D network structure composed of interconnected colloidal carbon particles or polymer carbon chains that can be controlled and adjusted on the nanoscale.[86−88] Based on the type of carbon precursors, CAs can be divided into three categories: phenolic resin-derived CAs, carbon nanotubes and graphene CAs, and biomass-derived CAs. Such materials are produced by the pyrolysis process of organic aerogels or the self-assembly route of precursors. Carbon-based aerogels have all the structural properties of aerogels, but also have the ability to conduct electricity. Currently, they have attracted extensive research interest as supporting materials for the encapsulation of PCMs due to their distinct advantages of ultrahigh porosity, ultralow density, and large specific surface area. The high porosity of CAs facilitates the encapsulation of a high fraction of PCMs and ensures the high thermal storage capacity of composite PCMs while preventing leakage of melted PCMs through strong capillary force.[89] Meanwhile, the highly interconnected 3D thermally conductive framework of CAs ameliorates the inherent low thermal conductivity of PCMs for faster heating−cooling response rates. Furthermore, CA-based composite PCMs are considered as promising candidates for photothermal and electrothermal conversion and storage due to their superior solar trapping ability and high electrical conductivity.[90,91] Hence, CAs are promising supporting materials for the preparation of high-performance comprehensive composite PCMs.

3.1. Graphene Aerogel-Based PCMs. Graphene aerogels (GAs) are ultralight porous materials composed of aggregated graphene nanosheets with fascinating properties, including high electrical conductivity, excellent compressibility and high mechanical strength, and outstanding photothermal conversion performance.[92−94] Recently, GAs have been popularly considered as supporting materials for the encapsulation of PCMs, and the corresponding research results have taken a big step forward.

3.1.1. Thermal Storage. In composite PCM systems, increasing the encapsulation content of PCMs is an effective strategy to increase the thermal energy storage density.[1] A compelling advantage of GAs is their high encapsulation capacity for PCMs due to their lightweight, high porosity, and high specific surface area, which solves the problem that the introduction of large amounts of supporting materials significantly reduces the thermal energy storage density of composite PCMs. For example, Xia et al.[95] prepared *n*-octadecane (OD)@GA composite PCMs by a vacuum impregnation method. The composite PCMs presented a high encapsulation efficiency of 96.7 wt % with a high latent heat of 196.7 J/g, which were slightly lower than the theoretical values compared with pristine OD (197.3 J/g). To enhance the shape stability by a few supporting materials without significantly sacrificing the phase change enthalpy, Ye et al.[96] designed core−shell structured paraffin@graphene composite PCMs. Typically, graphene oxide (GO) nanosheets were reduced and self-assembled into 3D GAs consisting of

numerous hollow graphene nanoshells through a modified hydrothermal method. After paraffin molecules were encapsulated into the shells in the form of micron-sized droplets, the resulting composite PCMs exhibited a high paraffin encapsulation of 97 wt % and a large melting enthalpy of 202.2 J/g and freezing enthalpy of 213 J/g, which were even comparable to the enthalpy of pristine paraffin (201.5 and 213 J/g). These results indicated that GAs prepared by a modified hydrothermal method had an enhancement of the phase change enthalpy. For graphene or CNT-based composite PCMs, the additional enthalpy does not depend on the paraffin content and is generally attributed to the interactions between the paraffin and the nanofillers.[97,98] Although many studies have reported enthalpy enhancement of composite PCMs, the enhanced mechanisms have not been fully elucidated and deserve to be explored, which is of great significance for obtaining high enthalpy composite PCMs.

To further enlarge the encapsulation content of PCMs, Zhao et al.[99] prepared reduced graphene oxide aerogels beads (rGOABs) for the infiltration of 1-tetradecanol (TD) by wet spinning and thermal reduction of GO slurry. The rGOABs exhibited a highly porous structure with interconnected micropores, thus providing sufficient capillary forces and permeation pathways for PCMs. The encapsulation fraction of TD in rGOABs was as high as 98.83 wt %, and the obtained TD@rGOAB composite PCMs exhibited a high latent heat of 232.2 J/g. Xie et al.[100] introduced lignin as a modifier to obtain GAs with an ultralow density. Lignin facilitated the support and expansion of the originally significantly shrunken GA skeleton. Lignin-modified graphene aerogels (LGAs) successfully constructed a good 3D porous structure with the help of lignin. The LGA skeleton showed extremely high absorption of PEG (∼99.2 wt %). Qiu et al.[17] developed GO aerogel-based composite PCMs with the highest PCMs loading by improving the pore size and pore ratio of aerogels. The authors proposed a method for the fabrication of composite PCMs by encapsulating PEG in situ in 3D network structural GO aerogels constructed by Ca^{2+} cross-linking. The 3D network space of GO aerogels was maximized by the side-to-side cross-linking mode of GO nanosheets. Ultimately, the PEG loading content in GO aerogels was increased to 99.5 wt %, and the prepared composite PCMs exhibited an ultrahigh thermal energy storage density of 218.9 J/g, which was infinitely close to the theoretical latent heat of pristine PEG (221.7 J/g).

3.1.2. Thermal Conductivity. In general, the thermal conductivity of composite PCMs is enhanced when PCMs are infiltrated into thermally conductive nanofillers.[101] However, the thermal conductivity enhancement is not significant due to the formation of large interfacial thermal resistance of PCMs and conductive nanofillers, as well as conductive nanofillers-nanofillers.[102] Especially, graphene is a well-recognized excellent thermally conductive material with an ultrahigh theoretical thermal conductivity of over 5000 W/m·K at room temperature.[103] Therefore, the construction of 3D highly interconnected GAs can efficiently reduce the interfacial thermal resistance, and this structure is indispensable to substantially improve the thermal conductivity of PCMs. Notably, 3D lightweight GAs can absorb large amounts of PCMs, improve the thermal conductivity, and maintain a high latent heat.

3.1.2.1. Single Graphene Aerogels. The continuous 3D graphene skeleton can provide accelerated heat transfer channels for PCMs.[104] Therefore, GAs can greatly reduce
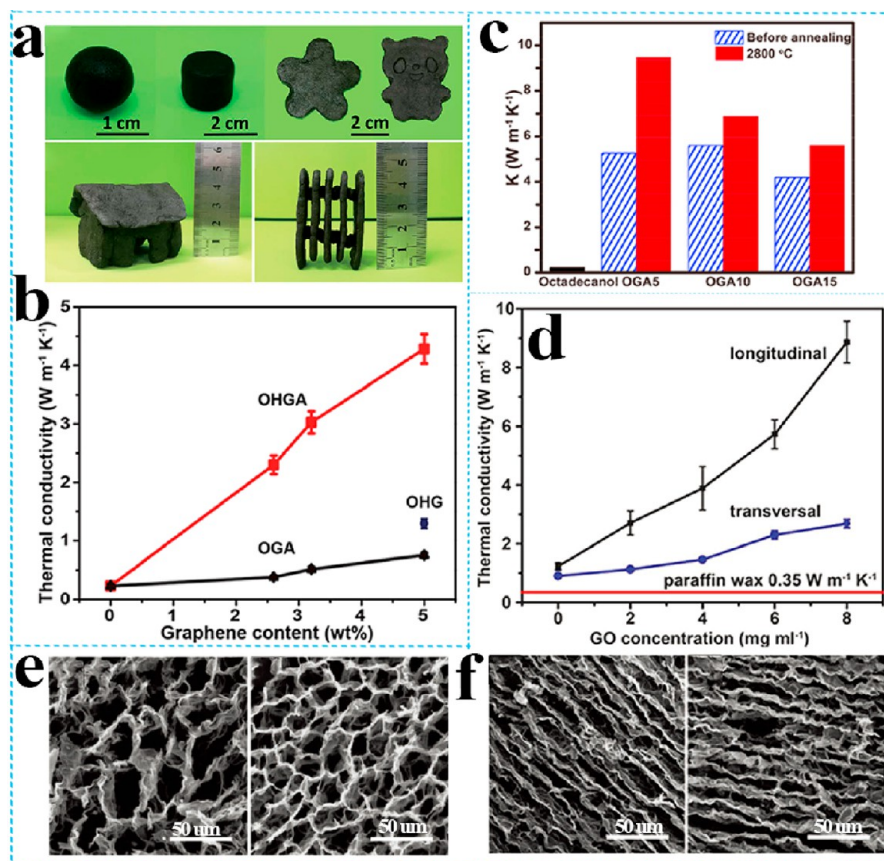
Figure 4. (a) Digital photos of models prepared based on the highly processable GO paste. (b) Thermal conductivities of GA-based composite PCMs. Adapted with permission from ref 107. Copyright 2018 Royal Society of Chemistry. (c) Thermal conductivities of GA-based composite PCMs. Adapted with permission from ref 113. Copyright 2021 Elsevier. (d) Anisotropic thermal conductivities of GA-based composite PCMs. (e,f) Longitudinal view and transversal view SEM images of GA-based composite PCMs. Adapted with permission from ref 125. Copyright 2018 Wiley-VCH.

the internal contact thermal resistance in their continuous 3D architectures. For example, Zhong et al.[105] developed octadecanoic acid (OA)@GA composite PCMs with tightly integrated interfaces due to the good wettability between the two phases. Good continuity at the interfaces and throughout the 3D structure provided excellent heat transfer paths. The thermal conductivity of OA@GA composite PCMs with 15 wt % GAs was 2.64 W/m·K, which was approximately 1332% higher than that of pristine OA (0.18 W/m·K). Furthermore, considering that large interfacial thermal resistance between GAs and PCMs would limit the enhancement of thermal conductivity, Li et al.[106] modified the surface of GAs to reduce the interfacial thermal resistance between GAs and PCMs and further improved the thermal conductivity of GA-based composite PCMs. Specifically, functionalized GAs were obtained by grafting lauric acid (LA) onto GO. The interfacial compatibility was strengthened by the esterification reaction between LA and GAs and reduced the phonon vibration mismatch between the surface of LA−GAs and LA. Attributed to the covalent functionalization, the thermal conductivity of LA@LA−GA composite PCMs was 1.207 W/m K, which was 32.6% higher than that of LA@GAs and 352.1% higher than that of pristine LA. The functionalization of the thermally conductive additive has been demonstrated to be an effective way to reduce interfacial thermal resistance and improve interfacial heat transfer. However, GA-based composite PCMs suffer from unsatisfactory thermal conductivity enhancement

due to residual defects and abundant oxygen-containing groups in rGO nanosheets. Therefore, high-quality GAs with high thermal conductivity were obtained via annealing at 2800 °C to effectively remove the oxygen-containing groups and repair the defects. High-quality GA-based composite PCMs with only 5.0 wt % graphene showed a high thermal conductivity of 4.28 W/m·K, which was approximately 1760% higher than that of pristine 1-octadecanol (Figure 4a,b).[107]

3.1.2.2. Hybrid Graphene Aerogels. Generally, thermally conductive nanofillers, such as CNTs, graphene, expanded graphite (EG), and metal nanoparticles, are used to improve the thermal conductivity of PCMs.[108,109] Benefiting from the advantages of these materials, the compatible incorporation of thermally conductive nanofillers in GAs can yield high-performance thermally conductive frameworks. Liang et al.[110] reported shape-stabilized composite PCMs encapsulated with hybrid graphene aerogels (HGAs) consisting of GO and graphene. In this study, the thermal conductivity of LA@GO composite PCMs was only 0.60 W/m·K due to the abundant oxygenated groups of GO. The introduced graphene enhanced the thermal conduction of HGAs by prompting electron transfer. Ultimately, the thermal conductivity of HGA-based composite PCMs with 1.8 wt % graphene was 1.29 W/m·K, which was 144% higher than that of GO aerogel-based composite PCMs and 227% higher than that of pristine LA. Similarly, Yang et al.[111] reported GO/graphene aerogel-based composite PCMs with a thermal conductivity of 1.43 W/m·K.

Notably, graphene can also act as an enhancer to avoid excessive volume shrinkage during environmental drying, as reported by Yu et al.[112] HGAs exhibited a high modulus of ~23.8 MPa when the ratio of graphene to GO was 5:1. The composite PCMs with 11.4 wt % graphene and 0.6 wt % rGO exhibited a very high thermal conductivity of 5.92 W/m·K, which was 2473% higher than that of pristine 1-octadecanol. Liu et al.[113] designed rGO/graphene hybrid aerogels as a lightweight porous framework to accommodate PCMs and as a thermally conductive network to enhance the thermal conductivity of PCMs. The synthesized composite PCMs exhibited an ultrahigh thermal conductivity of 9.50 W/m·K at a graphene content of 13.3 wt % (Figure 4c). In addition, graphene foam (GF) prepared by the chemical vapor deposition (CVD) technique is a monolith 3D graphene network formed by covalently bound graphene, providing a continuous pathway for phonon transport. Compared with GAs prepared from the self-assembly technique, GF can improve the thermal conductivity of composite PCMs more effectively because the physical cross-linking of GAs is formed by van der Waals contacts, hydrogen bonds, and $\pi-\pi$ superposition interactions, which still generate large interfacial thermal resistance between graphene nanosheets. However, the macropores of GF are not favorable for the shape stability of PCMs. Therefore, Yang et al.[114] integrated rGO/graphene hybrid aerogels (HGAs) into 3D GF by combining self-assembly and CVD to obtain GF/HGA (GH) hybrid structure. The thermal conductivity of paraffin@GH composite PCMs was 1.82 W/m·K, improved by 574% and 98% compared to the pristine paraffin and paraffin@GF, respectively.

CNTs with lightweight and excellent heat transfer properties can serve as secondary heat conductive nanofillers and construct extended surfaces on skeletal structures to further improve the heat transfer performance of GA-based composite PCMs.[115] Cao et al.[116] investigated the effect of 3D thermally conductive skeletons with different ratios of GO and CNTs on the thermal conductivity of composite PCMs. The results indicated that the disorderly arrangement of excess CNTs induced the disorganization of the heat transfer paths of the composite PCMs, resulting in the reduction of thermal conductivity. The optimal thermal conductivity enhancement was achieved when the ratio of GO to CNTs was 2:1. Similarly, Chen et al.[117] prepared GO/CNT hybrid aerogel-based composite PCMs with a thermal conductivity of 0.46 W/m·K when the content of HGAs was 2.2 wt %, which was 76% higher than that of pristine paraffin and 46% higher than that of paraffin@GA. Furthermore, Cao et al.[118] prepared rGO/CNT hybrid aerogel-based composite PCMs with an enhanced thermal conductivity (0.84 W/m·K), which was increased by 318% over pristine paraffin.

Expanded graphite (EG) is also considered one of the best thermally conductive nanofillers because of its low density, high thermal conductivity, excellent chemical stability and compatibility.[19,119] Ren et al.[120] prepared rGO aerogels with the assistance of EG, and the resulting composite PCMs exhibited better thermal properties and shape stability due to the uniformly distributed EG attached on the rGO. As EG content increased to 6.06 wt %, the thermal conductivity of rGO/EG aerogel-based composite PCMs was improved to 0.79 W/m·K, which was about 295% higher than that of pristine paraffin.

Silver (Ag) nanoparticles are also considered for heat transfer applications due to their high thermal conductivity of 429 W/m·K at room temperature.[121] Hu et al.[122] compared the thermal conductivities of rGO aerogel-based composite PCMs and rGO/Ag aerogel-based composite PCMs using a one-pot hydrothermal method. The stearic acid (SA)@rGO composite PCMs with 10 wt % rGO exhibited an obviously enhanced thermal conductivity of 3.21 W/m·K. More interestingly, a fraction of graphene was substituted by Ag nanoparticles, and the thermal conductivity of SA@rGO/Ag composite PCMs can be as high as 5.89 W/m·K. The compared results demonstrated that the synergistic effect of the rGO network and Ag nanoparticles was beneficial to significantly enhance the thermal conductivity of PCMs. However, Ag nanoparticles are not suitable for the thermal conductivity enhancement due to their high cost and the complicated preparation process.

3.1.2.3. Anisotropic Graphene Aerogels. Graphene with highly anisotropic configurations can greatly improve thermal conductivity along a directional path.[123] Thus, some researchers have proposed anisotropic GAs with a regular arrangement of graphene nanosheets to greatly improve thermal conductivity in one direction of composite PCMs. In a study by Huang et al.,[124] they prepared high-quality anisotropic graphene aerogels (AGAs) using a heat flow method with vacuum microwave treatment, which significantly reduced the oxygen and nitrogen contents of AGAs. After impregnation of paraffin, the axial thermal conductivity of the obtained composite PCMs with only 0.32 vol % AGAs reached 1.07 W/m·K, which was increased by 995% compared with pristine paraffin. Min et al.[125] employed high-quality graphene to construct AGAs monoliths by directionally freezing aqueous suspensions of polyamic acid salt and GO, followed by freeze-drying, imidization at 300 °C and graphitization at 2800 °C. The corresponding composite PCMs exhibited a high transversal thermal conductivity (2.68 W/m·K) and a higher longitudinal thermal conductivity (8.87 W/m·K), which were 665 and 2434% higher than pristine paraffin (0.35 W/m·K), respectively (Figure 4d−f). Hence, heat can be easily diffused into the interior of composite PCMs due to high thermal conductivity in the thickness direction. Li et al.[126] designed structurally, mechanically, electrically, and optically AGAs. After infiltration of paraffin, the thermal conductivity of paraffin@AGA composite PCMs significantly increased up to 2.99 W/m·K in the axial direction, which was 1323% higher than pristine paraffin.

In addition to single AGAs, Li et al.[127] prepared anisotropic rGO/EG hybrid aerogels by directional freezing. The longitudinal thermal conductivity of the obtained composite PCMs was 0.79 W/m·K when the content of rGO/EG aerogels was 8.7 wt %, which was almost four times higher than pristine paraffin. Similarly, Zhang et al.[128] prepared anisotropic graphene/silver hybrid aerogels using an ice crystal template method. During the preparation process, silver was tightly attached to the interfaces of graphene nanosheets to reduce the thermal resistance between graphene and PCMs. Significantly, the maximum axial thermal conductivity of composite PCMs was 1.20 W/m·K, which was increased by 362% compared to pristine paraffin. Responding to the time-consuming and complicated ice-crystal template method, Huang et al.[129] proposed a one-step heat flow method to synthesize anisotropic rGO/BN hybrid aerogels. The axial thermal conductivity of the corresponding composite PCMs was 1.68 W/m·K, which was 504% higher than that of pristine paraffin.
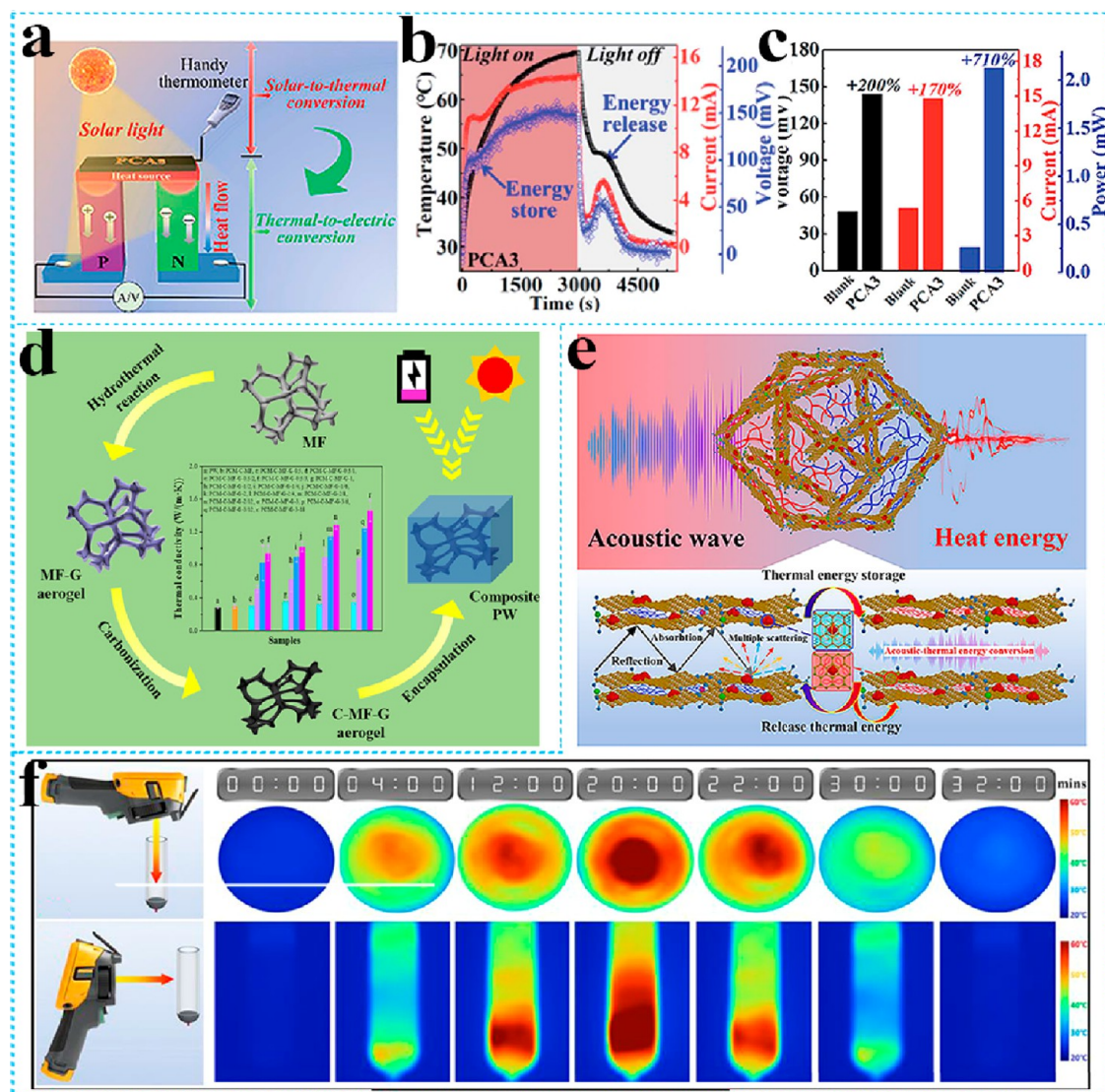
H

Figure 5. (a) Schematic diagram of PCA-loaded TEGs. (b) Temperature/voltage/current–time curves of PCA-loaded TEG. (c) Contrast diagram of electrical properties between PCA-loaded and blank TEG. Adapted with permission from ref 140. Copyright 2020 Royal Society of Chemistry. (d) Schematic diagram of the solar/electric response of composite PCMs based on rGO/graphene/MF. Adapted with permission from ref 145. Copyright 2019 Elsevier. (e) Mechanism schematic of acoustic–thermal conversion of PEG@Fe$_3$O$_4$-GO. (f) Infrared thermal images of PEG@Fe$_3$O$_4$-GO in acoustic–thermal conversion test. Adapted with permission from ref 150. Copyright 2021 Elsevier.

3.1.3. Energy Conversion. To achieve thermal energy conversion from solar energy, electric energy, magnetic energy, or acoustic energy, energy conversion systems based on functional responsive materials should be constructed to respond to various energies rapidly and convert those energy sources into thermal energy. The smart integration of graphene and PCMs can realize multiple energy conversion and storage, including solar–thermal conversion, solar–thermal–electric conversion, electric–thermal conversion, and acoustic–thermal conversion.

3.1.3.1. Solar–Thermal Conversion. Inexhaustible solar energy is the cheapest and most environmentally friendly; however, the intermittence of sunlight hinders its effective utilization. In this regard, PCMs have triggered considerable attention as candidates for solar–thermal energy storage. However, pristine PCMs are not conducive to storing solar energy due to their inferior solar-capturing ability.[130,131] At present, various photothermal materials have been investigated

for driving solar–thermal conversion, especially carbon materials due to their structures and properties in sunlight absorption and conversion.[131] Due to high thermal conductivity and light absorbing nature, GA-based composite PCMs are considered as solar–thermal conversion materials for real-time energy storage. For example, Tang et al.[132] employed GAs as photonic antennas to achieve photon capture and solar–thermal conversion. Xue et al.[133] prepared GAs by co-mediating melamine foam (MF) and cellulose nanofibers. After paraffin was impregnated into GAs, the obtained composite PCMs exhibited a good photothermal conversion efficiency of 78%. Graphene aerogels can further improve the photothermal conversion performance by modification with metal nanoparticles. Yu et al.[134] improved the optical properties of composite PCMs using oxygen-deficient TiO$_2$ (TiO$_2$-x) and increased the thermal conductivity of composite PCMs to 1.22 W/m·K. The solar–thermal conversion efficiency of the composite PCMs was 89.9% due to the

broad-spectrum absorption of TiO_2-x. TiO_2-x/rGO aerogels will bring a paradigm for PCMs as a working medium for solar energy absorption. Furthermore, Yang et al.[114] prepared rGO/graphene hybrid aerogels into 3D GF for the encapsulation of paraffin to realize efficient solar−thermal conversion and storage. The rGO/graphene/GF hybrid aerogels behaved as effective photon traps and molecular heaters that absorb and convert solar radiation into thermal energy due to their low reflection and effective light capture. As a result, the composite PCMs achieved a high solar−thermal conversion efficiency of above 90%. Fang et al.[135] encapsulated paraffin into a copper foam (CF) containing GAs to improve the solar−thermal conversion capacity. The composite PCMs showed excellent solar−thermal conversion efficiency (up to 97%).

3.1.3.2. Solar−Thermal−Electric Conversion.

Recently, thermoelectric power generation from solar radiation or waste heat has attracted great attention. In particular, solar thermoelectric generators (TEGs) are expected to be a promising technology for collecting and converting clean solar energy.[136] Integrating TEGs with GA-based composite PCMs is more advantageous because of their long-lasting energy generation, regardless of the variation of actual solar energy over time and weather.[137−139] In addition, GA-based composite PCMs can maximize the average temperature difference (ΔT) of thermoelectric devices due to their excellent solar energy absorption and solar−thermal conversion capability. For example, Cao et al.[140] prepared TEGs based on phase change aerogels (PCAs) to improve the solar−thermal−electricity energy conversion. Under simulated solar light radiation, the voltage (144 mV) and current (14.8 mA) output of the PCA-loaded TEGs were approximately 3 and 2.7 times higher than those of the blank TEGs (48 mV, 5.4 mA), respectively. The optimal solar−thermal−electric conversion efficiency was increased by approximately 61.3% compared to that of blank TEGs (Figure 5a−c). Using waste heat as a source, the thermoelectric energy-harvesting system was optimized by Yu et al.[141] The thermoelectric energy harvesting was achieved by placing two different PCMs (PEG and 1-tetradecanol) on both sides of the N-type and P-type semiconductors. The maximum output current was 10 mA during both heating and cooling, and the calculated thermoelectric conversion efficiencies were 52.81 and 30.29%, respectively. Song et al.[142] prepared graphene/cysteamine cross-linked aerogels (GCAs) by a cysteamine vapor method. The GCAs could accommodate a large amount of PCMs in the internal space due to their high specific surface area. The harvesting solar−thermal−electric conversion efficiencies of the TEG with composite PCMs were 67.92 and 41.72% under light irradiation and light source removal conditions, respectively.

3.1.3.3. Electric−Thermal Conversion.

Similar to solar−thermal conversion, it is difficult to drive pristine PCMs with electricity as the heat source due to their low electrical conductivity.[143,144] Supporting materials with superior electrical conductivity are applied to encapsulate PCMs, which can effectively manage the conversion from electric energy to thermal energy. Xue et al.[145] prepared composite PCMs based on GO/graphene aerogel-decorated MF (Figure 5d). The results showed that paraffin was completely insulated, while the electrical conductivity of GA-based composite PCMs was 278.7 S/m when the GA content was 4.89 wt %. However, the electric−thermal conversion efficiency was only 62.5%. To further improve the electric−thermal conversion efficiency of

GA-based composite PCMs, Li et al.[126] prepared structurally and electrically anisotropic GA-based composite PCMs. The electrical conductivity reached 341.3 S/m in the axial direction, which was approximately 4 times that of the isotropic GAs (87 S/m). Attractively, the composite PCMs can be driven for electric−thermal conversion by applying a small voltage (1−3 V) with a high electric−thermal efficiency of 85%.

Generally, GA-based composite PCMs can achieve simultaneous integration of solar−thermal and electric−thermal conversion functions. Zhou et al.[146] prepared halloysite nanotube (HNT)-GA/polyurethane-based composite PCMs. The HNTs not only promoted the reduction of GAs, but also enhanced the latent heat of the system through heterogeneous nucleation effects. The HNT-GA system exhibited a solar−thermal efficiency of 75.6% and an electric−thermal efficiency of 67.2%. Furthermore, they[147] prepared polyurethane-based composite PCMs containing ZnO nanoparticles and GAs. The solar−thermal and electric−thermal conversion efficiencies of the systems were 80.1% and 84.4%, respectively, due to the excellent light absorption of ZnO nanoparticles and GA as well as the excellent electrical conductivity of GA.

3.1.3.4. Acoustic−Thermal Conversion.

As a kind of mechanical wave, acoustic wave with high energy and high penetration can be converted into thermal energy by the ultrasound thermal effect, showing important applications in the fields of denoising and minimally invasive thermal therapy.[148] GO nanomaterials are capable of absorbing acoustic waves and converting them into thermal energy through the molecular friction in solid domains in vibrational mode.[149] Based on this mechanism, Tang et al.[150] developed advanced PEG@Fe_3O_4-GO aerogel-based composite PCMs for acoustic−thermal conversion (Figure 5e). The 3D network structure of GO aerogels not only improved the thermal conductivity but also effectively enhanced the acoustic absorption capacity. In addition, the vibrational heat generation of Fe_3O_4 nanoparticles further enhanced the acoustic−thermal conversion capacity. As shown in Figure 5f, the temperature of the sample steadily increased with increasing sonication time. In this process, the mechanical energy caused by acoustic waves was converted into thermal energy by reflection, scattering and microvibrations in the tortuous network structure of GO-Fe_3O_4.

3.1.4. Advanced Utilization.

Compared with nonflexible PCMs, flexible PCMs can withstand a certain degree of deformation and guarantee closer contact with complex structural surfaces, which can improve the thermal management capability of complicated device surfaces. In addition, flexible PCMs are also applied in smart wearable thermal management devices, which is a very promising direction.[151] Pristine PCMs are well-known to be inherently highly rigid and inferiorly processable. Therefore, most of the developed composite PCMs insufficiently satisfy the flexible requirements due to their high mechanical rigidity.

To solve the rigid problem of PCMs, Sun et al.[152] designed a flexible GA-based composite phase change film with excellent thermal performance, advanced flexibility, and outstanding solar−thermal conversion capability for wearable personal thermal management. GAs were synthesized by lyophilization and high-temperature reduction of GO. Then polyvinylidene fluoride−hexafluoropropylene (PVDF−HFP) was introduced to form a flexible film. Finally, the obtained flexible GA-based phase change film exhibited a high phase change enthalpy of 154.64 J/g, and a high solar−thermal conversion efficiency of
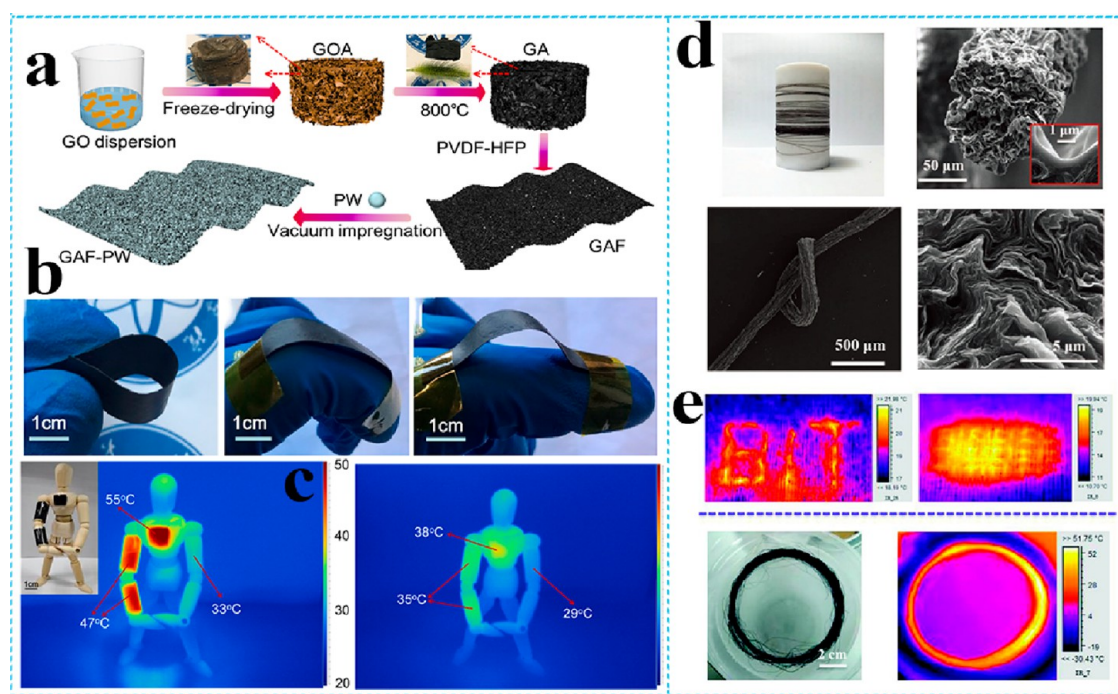
Figure 6. (a) Synthesis procedure of GA-based phase change film. (b) Images of flexible phase change film. (c) Infrared thermal images of human model with phase change film. Adapted with permission from ref 152. Copyright 2021 Elsevier. (d) Aerogel-directed smart fiber and SEM images of the cross section of PEG@ASF. (e) Infrared thermal images of PEG@ASF fabric under solar illumination. Adapted with permission from ref 153. Copyright 2018 Wiley-VCH.

95.98%. More importantly, the phase change film showed excellent and stable flexibility even after extensive bending and can be further customized to for humans (Figure 6a−c). The flexible phase change film showed great application potential in the field of wearable thermal management and the thermal management of complicated surfaces on devices. In another study, Li et al.[153] developed flexible, strong, self-cleaning graphene aerogel-directed phase change smart fibers (ASF) with thermal storage ability under multiple stimuli. The graphene nanosheets were stacked and wrapped in parallel, aligned with the long axis of the fibers, and the nanopores were filled with PEG (Figure 6d). The obtained PEG@ASF can produce a warm surface at a comfortable human temperature of approximately 19−21 °C when exposed to the sun (Figure 6e). Furthermore, PEG@ASF showed good multiple response properties to external stimuli (electrons/photons) with reversible energy storage and conversion. Such graphene aerogel-oriented smart fibers are expected to be widely used in next-generation wearable thermal management systems.

3.2. Biomass-Derived Carbon Aerogel-Based PCMs. Typically, the synthesis of GAs involves complex processes, high cost and harmful precursors. Therefore, it would be advantageous to develop more economical and environmentally friendly high-performance CAs by convenient strategies.[154,155] Recently, the exploration of biomass-derived CAs using easily available and inexpensive biomass raw materials has been of great practical value. The direct conversion of biomass materials to CAs provides a low-cost method for the development of supporting materials for PCMs.

3.2.1. Thermal Storage. Biomass-derived CAs ensure high loading of the PCMs in the substrate and significantly improve the thermal stability of the composite PCMs. Fang et al.[156] carbonized chitosan to synthesize biomass-derived CAs, which

was a low-cost and eco-friendly approach. The loading of 1-hexadecanol in CAs was approximately 98.08 wt %. The melting enthalpy of the composite PCMs was approximately 220 J/g, which was only 8% lower than that of pristine 1-hexadecanol. Similarly, Sheng et al.[157] prepared CAs by the direct carbonization of sustainable biomass cotton. The obtained hollow carbon fiber aerogels exhibited a high paraffin loading of 95.5 wt % by capillary and intermolecular forces, and a high melting enthalpy of 209.3 J/g. In another study, by combining flexible carbon resources from biomass guar gum with hard brittle carbon from polyimide, Zhang et al.[158] constructed homogeneous reinforced CAs with well-interconnected porous structure to overcome the severe shrinkage and poor mechanical properties of conventional CAs. The results showed that the compressive strength of the composite PCMs was 1.60 MPa. Moreover, PEG can be uniformly dispersed in CAs to form dense a 3D network. Therefore, the composite PCMs with a high loading of 95 wt % PEG exhibited high energy storage capacities of 171.50 and 169.50 J/g, which were very close to the theoretical values (171.57 and 169.48 J/g).

3.2.2. Thermal Conductivity. Biomass-derived CAs usually possess outstanding thermal conductivity, which benefits the high heat transfer efficiency of PCMs. Zou et al.[159] fabricated pumpkin-derived carbon aerogels (PCAs) via a hydrothermal and postsintering method, and the corresponding composite PCMs were prepared by infiltrating palmitic acid (PA)/thiol−ene resin (TE). The thermal conductivity of PA/TE@PCAs (0.149 W/m·K) was 60.5% higher than that of PA/TE (0.093 W/m·K). Wei et al.[160] used succulent-based carbon aerogels (SCAs) to stabilize paraffin by vacuum impregnation. In the composite PCMs, the carbon network was the key factor maintaining leakage-proof performance and enhancing thermal conductivity (0.427 W/m·K). To simultaneously achieve a
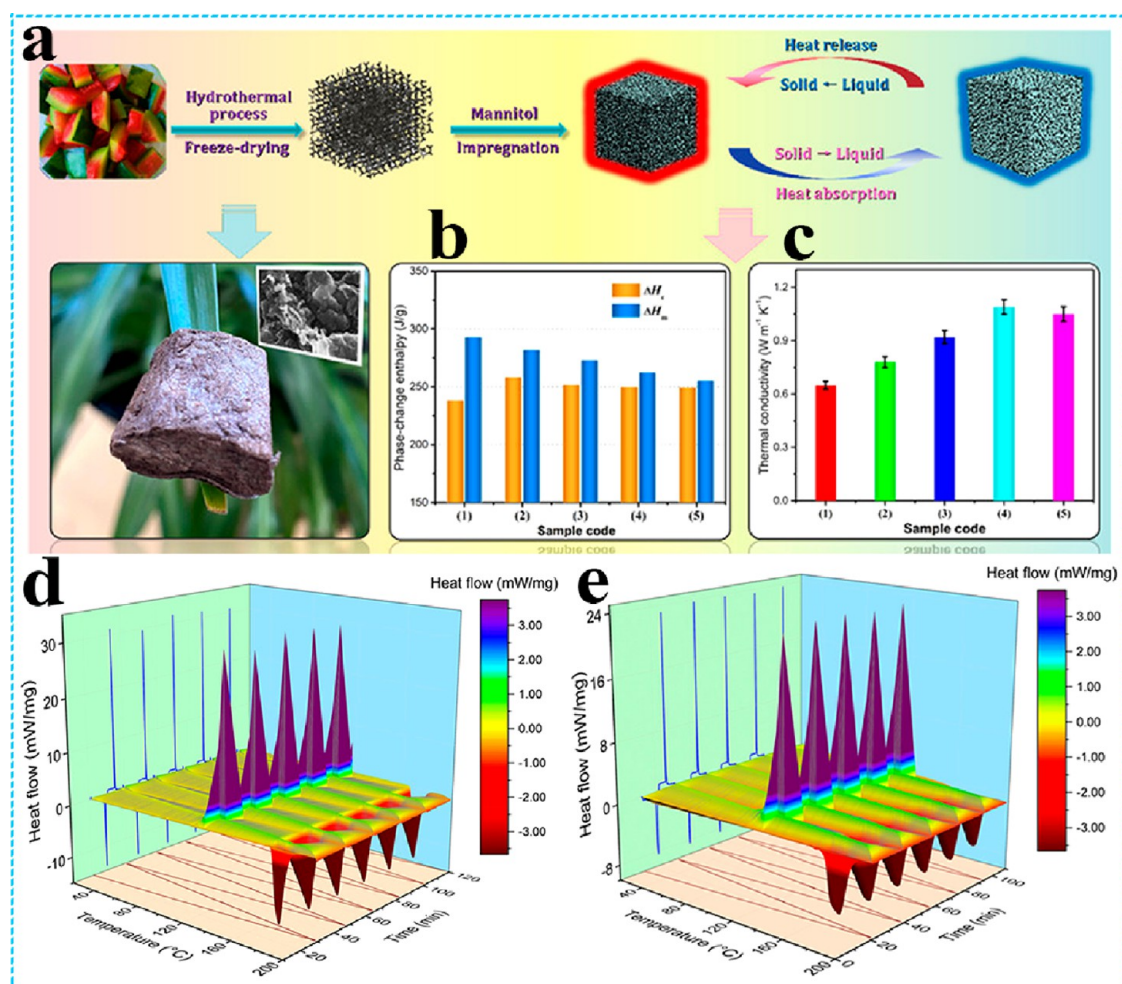
Figure 7. (a) Schematic synthetic route and digital photograph of biomass-derived CAs. (b) Phase change enthalpies of pristine mannitol and mannitol@CAs. (c) Thermal conductivities of pristine mannitol and mannitol@CAs. (d,e) Nonisothermal 3D heat flowcharts of pristine mannitol and mannitol@CAs. Adapted from ref 161. Copyright 2021 American Chemical Society.

high thermal energy density and a high thermal conductivity, Liu et al.[161] prepared composite PCMs by combining mannitol with CAs derived from watermelon rinds (Figure 7a). The mannitol@CA composite PCMs had a high latent heat of more than 280 J/g, and a reduced supercooling degree. Importantly, mannitol@CA composite PCMs exhibited a high thermal conductivity of 1.09 W/m·K, which was 67.6% higher than that of pristine mannitol at the CA loading of 12 wt % (Figure 7b,c). The 3D heat flow diagram of mannitol@CAs was slightly different from that of pristine mannitol. Compared to pristine mannitol, the much broader heat flow peak of mannitol@CAs indicated a longer heat charging−discharging period during the heating and cooling processes (Figure 7d,e).

3.2.3. Energy Conversion. 3.2.3.1. Solar−Thermal Conversion. CAs are used as the sunlight-driven heating unit of the composite PCMs, which can effectively capture photons and subsequently transform solar energy to thermal energy. As reported by Wang et al.,[162] sunflower receptacle sponge carbon aerogels (r-CAs) and sunflower stem carbon aerogels (s-CAs) served as porous supporting materials for PCMs. The obtained CA-based composite PCMs exhibited a solar−thermal conversion efficiency of 75.6% for 1-hexadecanamine@r-CAs and 67.8% for 1-hexadecanamine@s-CAs. Furthermore, Wei et al.[160] reported composite PCMs based on CAs derived from succulents for solar−thermal conversion. The solar−thermal

conversion efficiency of composite PCMs was approximately 82%.

3.2.3.2. Solar−Thermal−Electric Conversion. It is a challenge to harvest thermoelectric energy in a uniform environment temperature without an appropriate temperature gradient that is necessary for the Seebeck effect.[163] Considering this issue, Niu et al.[164] designed a sustainable and highly efficient thermal-driven and solar-driven energy-harvesting system composed of two different PCM@carbon nanofiber aerogels (CNFAs) from wood-derived cellulose nanofibers. The prepared composite PCMs can instantly convert thermal energy into electric energy in a suitable temperature environment or under sunlight radiation. As the temperature increased, 1-tetradecanol@CNFA composite PCMs underwent a melting transition process due to the lower melting temperature, while the temperature of stearic acid@CNFA composite PCMs continued to increase. This created a temperature difference between the two ends of the semiconductor, and the collected thermal energy could be converted into electric energy at a uniform environmental temperature. The maximum voltages generated by the energy-harvesting system were 55 and 80 mV, respectively, corresponding to the thermally driven thermoelectric and solar-driven thermoelectric energy conversion process, and the

L
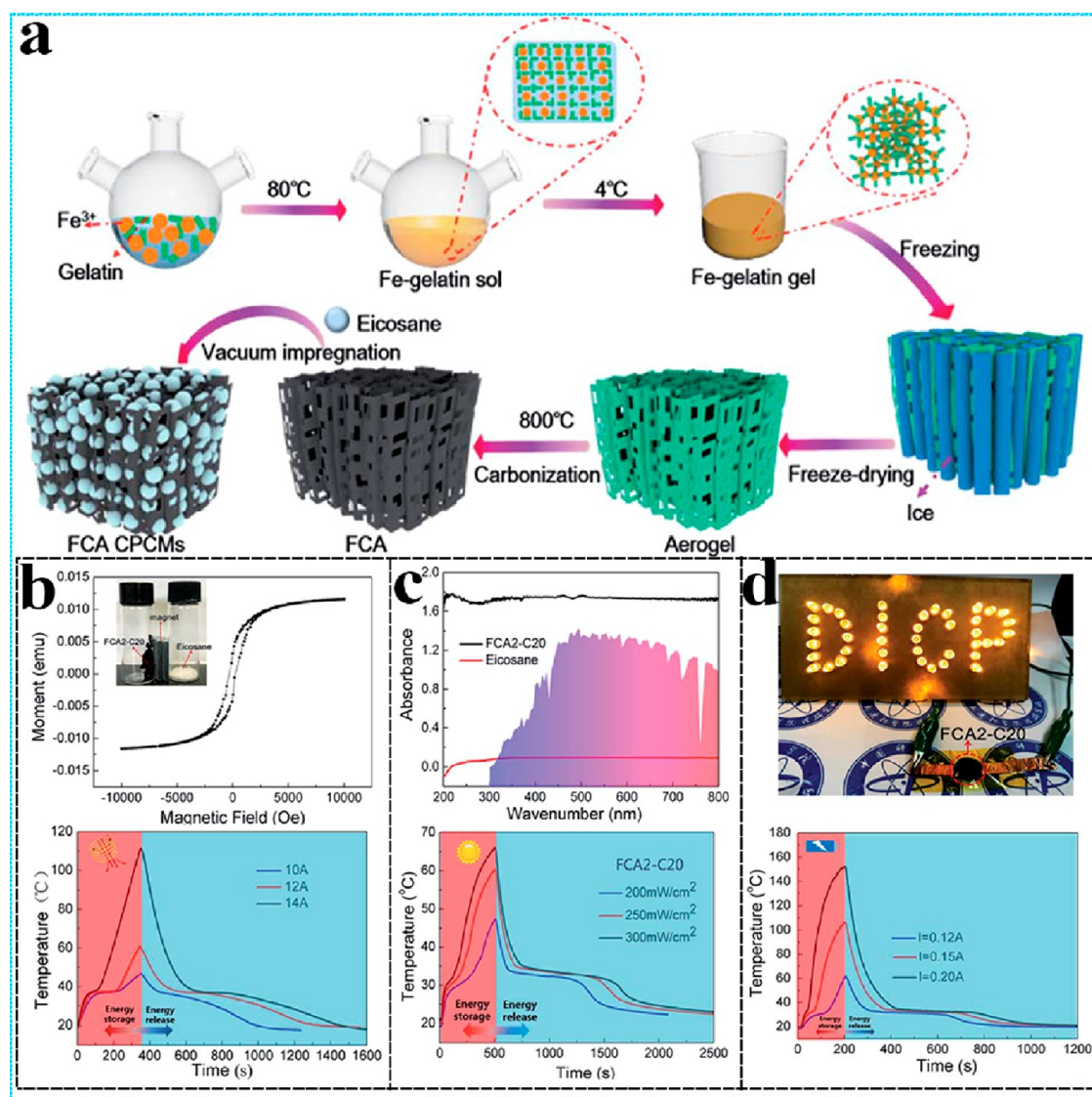
Figure 8. (a) Synthesis schematic of composite PCMs. (b) Magnetic property curves and magnetic−thermal conversion curves of composite PCMs. (c) UV−vis absorption spectra of and solar−thermal conversion curves of eicosane and composite PCMs. (d) LED lights of "DICP" characters with composite PCMs and electric−thermal conversion curves of composite PCMs. Adapted with permission from ref 167. Copyright 2021 Royal Society of Chemistry.

maximum power densities of each process were 0.5 and 1.2 W/m², respectively.

3.2.3.3. Electric−Thermal Conversion. Biomass-derived CAs can also improve the electrical conductivity of PCMs. In view of this advantage, Li et al.[165] reported the composite PCMs with the dual functions of solar−thermal and electric−thermal conversion. CAs were derived from various melon (winter melon, watermelon, and pumpkin) via a hydrothermal carbonization and a postpyrolysis process, followed by the encapsulation of paraffin using a vacuum infusion method. The obtained paraffin@CA composite PCMs exhibited high solar adsorption capacity (96%) over the whole ultraviolet−visible−near-infrared (UV−vis−NIR) range because biomass-derived black CAs served as an effective photon captor and molecular heater. Therefore, biomass-derived CA-based composite PCMs can effectively absorb solar radiation to convert solar energy into heat energy and store it in the form of latent heat in PCMs. In addition, paraffin was an excellent insulator with an electrical conductivity of only 10^{-14} S/m, while the electrical

conductivity of biomass-derived CA-based composite PCMs was as high as 3.4 S/m, an increase of 14 orders of magnitude over that of paraffin. Hence, biomass-derived CA-based composite PCMs can be triggered for electric−thermal conversion, and the electric−thermal conversion efficiency was 71.4%.

3.2.3.4. Magnetic−Thermal Conversion. Magnetic energy is also a source of energy, which can be converted into thermal energy by a composite PCMs system.[28,29,166] For example, Sun et al.[167] designed biomass-derived CA-based composite PCMs with multifunctional energy conversions, such as solar−thermal, electric−thermal, and magnetic−thermal (Figure 8a). Surprisingly, the solar−thermal and electric−thermal conversion efficiencies reached 93.32 and 94.83%, respectively (Figure 8b,c). In the preparation process, the chelation of Fe^{3+} with gelatin was utilized to enhance the carbon skeleton, and the magnetic network was from the introduction of Fe_3O_4 nanoparticles. The magnetic hysteresis loop of composite PCMs indicated their superparamagnetic behavior. When the
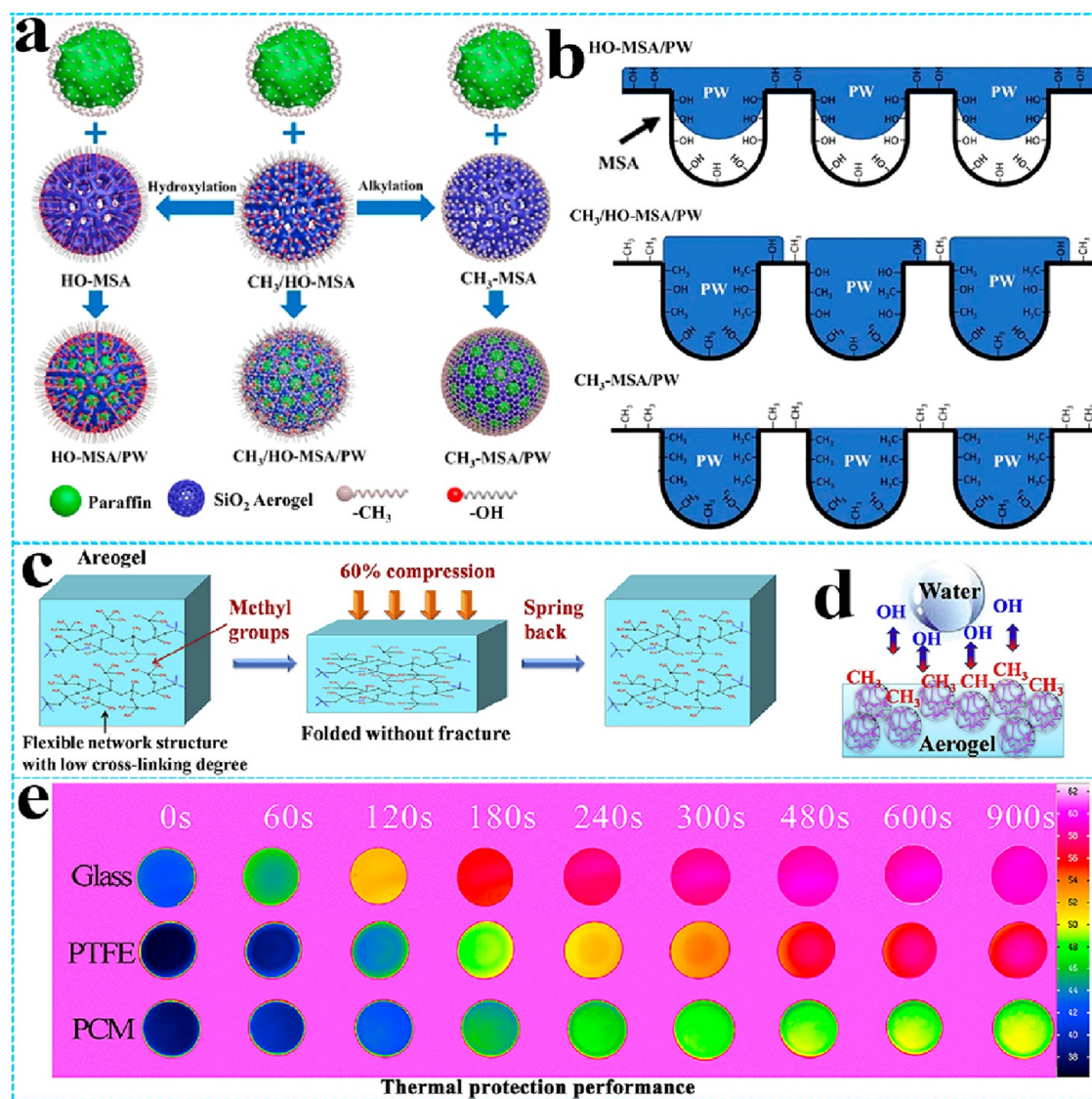
Figure 9. (a) Synthesis schematic of functionalized MSA and composite PCMs. (b) Schematic comparison of paraffin penetration in MSA with various surface properties. Adapted with permission from ref 173. Copyright 2020 Springer. (c) Structural change schematic of aerogels during compression−decompression. (d) Schematic of hydrophobic interaction of aerogels. Adapted with permission from ref 179. Copyright 2019 Elsevier. (e) Thermal protection of silica aerogel-based PCMs. Adapted with permission from ref 180. Copyright 2020 Elsevier.

sample was exposed to an alternating magnetic field for 350 s, the temperature increased to approximately 47, 60, and 111 °C with the alternating input currents at 10, 12, and 14 A, respectively. The platform occurred from 33 to 40 °C in the heating process, corresponding to the latent heat storage process (Figure 8d). These results indicated that biomass-derived CA-based composite PCMs can convert magnetic energy into thermal energy and store it in the phase change system. Song et al.[168] reported that carbonized kapok fiber aerogel (CKF)-based composite PCMs incorporating Fe_3O_4 nanoparticles as magnetic guest and lauric acid as thermal guests. The obtained composite PCMs achieved efficient solar−thermal conversion and magnetic−thermal conversion. Our group[169] integrated polypyrrole/Fe_3O_4 into hollow kapok fiber (KF) aerogels and encapsulated paraffin to prepare composite PCMs with enhanced thermal conductivity. The resulting composite PCMs exhibited high-efficiency solar/magnetic−thermal energy conversion properties.

3.2.4. Advanced Utilization. Electronic devices are increasingly miniaturized, integrated, functional, and networked. Heat dissipation and electromagnetic pollution of electronic devices have become urgent problems to be solved with the improvement of operating speed and efficiency.[170] Therefore, it is critical to develop functional materials with both thermal management and electromagnetic interference (EMI) shielding capabilities. Song et al.[168] fabricated carbonized kapok fiber (CKF) aerogel-based composite PCM by decorating Fe_3O_4 nanoparticles on the microtubule as multifunctional supporting materials and encapsulating lauric acid (LA). The integration of Fe_3O_4 contributes to the composite PCMs with excellent microwave absorption performance by achieving an optimal balance between impedance matching and high loss characteristics. The minimum reflection loss for composite PCMs was −17.3 dB at 8.4 GHz within a thickness of 5.5 mm, far exceeding the practical demand of −10 dB. Furthermore, the composite

PCMs can also realize efficient solar/magnetic—thermal conversion.

In summary, the porous structure of CAs can accommodate PCMs by capillary force and surface tension to ensure the maximum loading ratio of PCMs in composites due to their ultrahigh specific surface area and porosity. CA-based composite PCMs can achieve both enhanced thermal and electrical conductivity. Generally, there is a trade-off between the thermal storage capacity and thermal conductivity of composite PCMs. A high thermal storage capacity requires a high loading of PCMs, while small thermally conductive supporting material content usually yield limited thermal conductivity enhancement. Therefore, it is imminent to develop CA-based composite PCMs integrating high thermal storage capacity and high thermal conductivity. More appealingly, CA-based composite PCMs can also realize multiple energy conversions, including solar—thermal, electric—thermal, magnetic—thermal, acoustic—thermal, and solar—thermal—electrical energy conversions. Among these conversions, the combination of high-performance PCMs and N/P-type semiconductors has made a breakthrough in thermoelectric conversion systems, which can convert low grade waste heat and solar energy into electricity. Although thermoelectric technology based on PCMs is a promising conversion method, its conversion efficiency is still low and urgently needs to be enhanced. In addition, it is worthy of attention that emerging highly thermally conductive GA-based flexible PCMs have broad prospects for thermal management of complex surfaces and wearable thermal management as well as thermal management of electronic devices in the 5G era.

4. SILICA AEROGEL-BASED PCMs

Silica aerogels are promising inorganic porous materials with ultralow thermal conductivity, high specific surface area and excellent thermochemical stability.[171] In recent years, silica aerogels have been used as supporting materials to maintain the shape stability of PCMs and prevent leakage throughout the phase change process due to their large porosity and high specific surface area. Benefiting from ultralow thermal conductivity of silica aerogels and the high thermal storage capacity of PCMs, silica aerogel-based composite PCMs have great potential in thermal protection applications.

4.1. Thermal Storage. According to reports, the hydroxyl ends of silica aerogels have a significant impact on the infiltration fraction and thermal storage capacity of organic PCMs.[172] It is essential to investigate the effect of the interaction between the surface properties of silica aerogels and PCMs on the thermal storage properties of composite PCMs, especially in extreme environments, such as high humidity environments. With respect to this problem, Yu et al.[173] engineered mesoporous SiO_2 aerogels (MSA) to regulate the interactions between paraffin and SiO_2 aerogels. MSA were modified with various functional terminals, such as HO-MSA, CH_3/HO-MSA, and CH_3-MSA (Figure 9a). The authors found that molten paraffin spontaneously adhered to the surface of HO-MSA due to the high surface energy and interfacial tension of the polar surface of HO-MSA. Additionally, the pore size shrank to some extent during the hydroxylation modification process, resulting in increased capillary blood flow. As a result, paraffin molecules were firmly adsorbed on the surface of HO-MSA, but poorly adsorbed within the pores. For paraffin@CH_3-MSA, the molten paraffin was penetrated into the pores of MSA due to the low surface

energy of CH_3-MSA. The adsorption state of paraffin in CH_3/HO-MSA was between HO-MSA and CH_3-MSA (Figure 9b). In conclusion, the modified alkyl groups on the pore surface of MSA eliminated the separation of PCMs caused by the hydrogen bonding interaction between MSA and water molecules. The enthalpy of paraffin@CH_3-MSA was 154 J/g, and there was no liquid leakage above the melting point of paraffin in a high humidity environment. As reported by Huang et al.,[174] to overcome the moisture absorption problem of SiO_2 aerogels, the surface of hydrophilic SiO_2 aerogels was alkylated for the effective impregnation of hydrophobic PCMs. The adsorption capacity of PCMs was increased by 20.9—34.7%, and the corresponding thermal energy storage capacity was 153.7 J/g.

In addition, some researchers pay attention to high-temperature PCMs. Wu et al.[175] developed Al_2O_3—SiO_2 hybrid aerogel-based composites PCMs with high heat resistance. The obtained high-temperature composite PCMs was composed of a core—shell structured Na_2SO_4@SiO_2 PCMs with high melting temperature (878 °C) and Al_2O_3—SiO_2 aerogels with high thermal resistance (about 1000 °C). The latent heat of Na_2SO_4@SiO_2@Al_2O_3—SiO_2 was 153.8 J/g when the mass percentage of Na_2SO_4@SiO_2 PCMs was 36.7 wt %. This designed Na_2SO_4@SiO_2@Al_2O_3—SiO_2 can store thermal energy under high-temperature conditions. However, there are still relatively few research studies on aerogel-based high-temperature PCMs, and further systematic research is needed in the future.

4.2. Thermal Conductivity. As mentioned previously, many studies have focused on improving the thermal conductivity of PCMs, while relatively few studies have been conducted to reduce the thermal conductivity of PCMs. Similarly, reducing the thermal conductivity of PCMs is also important for thermal protection applications. An effective method to reduce the thermal conductivity of PCM is to apply porous substrates with low thermal conductivity.[23] Fittingly, silica aerogels with ultralow thermal conductivity have been used to encapsulate PCMs for thermal insulation. Zhou et al.[176] adopted silica aerogels to impregnate erythritol to obtain composite PCMs with a high heat storage capacity of 289.9 J/g. The authors simulated a thermal measurement device for an aircraft thermal environment and confirmed that the erythritol@silica aerogel-based composite PCMs accomplished thermal protection. The temperature of the cold side of the erythritol@silica aerogels was kept below 150 °C for 1600 s at a hot surface temperature of 600 °C. In another study, Shaid et al.[177] prepared eicosane@silica aerogel microparticles by dispersing silica aerogels in liquid eicosane via melt-infiltration, solvent dissolution and combined melt dissolution, which can serve as thermal protective textile coating additives over a wide temperature range. Based on surface modification techniques, Wang et al.[178] employed short chain alkyl-modified SiO_2 (M-SiO_2) aerogels to encapsulate technical grade paraffin (RT). The adsorption rate of RT in SiO_2 aerogels was increased by 38%, and the obtained RT@M-SiO_2 aerogel exhibited a high latent heat of 180 J/g and a lower thermal conductivity of 0.17 W/m·K compared to that of RT. The low thermal conductivity of RT@M-SiO_2 aerogels was caused by the lower thermal conductivity of SiO_2 aerogels (0.02 W/m·K).

However, the above silica aerogels still have the disadvantages of poor mechanical properties and high production cost due to the complex preparation technology. Regarding these problems, our group[179] prepared flexible monolithic silica

aerogels using low-cost ambient pressure drying by controlling the cross-linking degree of the network and in situ modification of methyl groups to the siloxane backbone (Figure 9c). The aerogels were strongly hydrophobic (contact angle was 140°) because of abundant methyl groups on the siloxane backbone (Figure 9d). The monolithic paraffin@ aerogels exhibited a reduced thermal conductivity of 0.13 W/ m·K. To enhance the compressive strength of silica aerogel-based PCMs, our group[180] further developed monolithic silica aerogel-based composite PCMs by a in situ one-step strategy. This method ensured uniform distribution of PCMs inside the pores of silica aerogels and the stable interconnected network of silica aerogels. Importantly, the resulting monolithic octadecanol@silica aerogels exhibited a low thermal conductivity of 0.12 W/m·K and large compressive strength of ~11 MPa. The monolithic silica aerogel-based composite PCMs showed potential promise for direct application to the thermal insulation and thermal protection devices due to the synergistic effect of low thermal conductivity and high latent heat (Figure 9e).

4.3. Energy Conversion. Solar thermal collection systems based on silica aerogel-based composite PCMs are usually designed by introducing high-performance photosensitive materials. Dye molecules can be used as a sunlight capturer. Yan et al.[181] prepared PEG@SiO$_2$−dye composite PCMs based on dye-grafted silica aerogels using a sol−gel method for solar−thermal conversion and storage. The dye molecules captured UV−vis sunlight well and efficiently converted light into heat through nonradiation thermal decay under solar irradiation, and the generated heat energy was stored in PEG through the phase change process. Moreover, PEG@SiO$_2$−dye composite PCMs were more homogeneous and stable due to the grafting of dye molecules onto the inorganic supporting material through chemical bonding. PEG@SiO$_2$−dye composite PCMs exhibited high solar−thermal conversion and storage efficiencies (85−88%). In another study, Huang et al.[174] carbonized silica aerogels to better capture solar energy for solar−thermal conversion and storage.

In addition, the loss of stored heat is inevitable as the heat transfer rate increases. The solar heat collection can be increased by reducing the heat loss of the solar receiver. Silica aerogels are used in solar energy storage systems to ensure that the stored heat does not diffuse too much to the outside environment. As reported by Zhang et al.,[182] porous GO/silica aerogels with a low thermal conductivity were prepared by a sol−gel method. The prepared GO/silica aerogel-based composite PCMs exhibited ultralow thermal conductivity of only 0.08 W/m·K, which was 72% lower than that of pristine *n*-octadecanol (0.30 W/m·K). The low heat transfer rate ensured that the stored heat was not easily diffused outward. Nonetheless, harvesting solar energy and suppressing heat loss remains a technical challenge. In a study, Zhao et al.[183] fabricated a silica aerogel-based solar thermal receiver that was capable of reaching stagnation temperatures exceeding 265 °C at a unconcentrated solar flux (1000 W/m^2). The device consisted of a blackbody absorber covered with optimized silica aerogels as a solar−thermal receiver. Silica aerogels with low-scattering and highly transparent simultaneously transmitted sunlight and suppressed heat loss by conduction, convection, and radiation. This study provides ideas for the design and fabrication of silica aerogel-based composite PCMs for photothermal conversion, which is promising to promote the application of medium-temperature PCMs in photothermal conversion.

4.4. Advanced Utilization. Currently, most aerogel-based composite PCMs are monolithic blocks. Compared with aerogel-based monolithic block composite PCMs, aerogel-based phase change films may yield more fascinating properties, such as low area density and good flexibility. Lyu et al.[184] reported a free-standing and form-stable energy storage PCMs film composed of paraffin and polytetrafluoro-ethylene/silica (PTFE/SiO$_2$) aerogels. Interestingly, the phase change film had multiple responsiveness to thermal stimuli, including wettability, transmittance, and mechanical evolutions. For instance, the contact angle decreased when paraffin in the laminate film was heated and melted. The UV−vis transmittance of the phase change film increased with the increase of temperature. The intelligently responsive phase change aerogel films have potential applications such as thermal management of small electronic devices and shape memory materials.

In summary, porous silica aerogels can stabilize PCMs without leakage through surface tension. Intriguingly, silica aerogels can reduce the thermal conductivity of PCMs, so that silica aerogel-based composite PCMs can effectively retard the surface temperature rise through the synergistic effect of insulation from silica aerogels and latent heat absorption from PCMs when subjected to high heat fluxes. Furthermore, the smart combination of high light transmission and low heat transfer of silica aerogels can increase the temperature of solar absorbers under unconcentrated sunlight and may unexpectedly improve the effect of energy conversion and storage of silica aerogel-based composite PCMs.

5. POLYMER AEROGEL-BASED PCMs

Polymer aerogels have become competitive candidates for energy storage due to their properties of ultralow thermal conductivity, ultralight density, high porosity, low dielectric constant, excellent mechanical properties, and flexible molecular design.[185−187]

5.1. Cellulose Aerogel-Based PCMs. Environmental issues have stimulated researchers to utilize native biobased materials for the development of advanced materials and applications. Cellulose aerogels derived from cellulose nano-fibers (CNFs), cellulose nanocrystals (CNCs), or bacterial cellulose (BC) have received wide attention because of their abundant resources, good biodegradability, easy degradation, and environmental friendliness.[188−190] Cellulose aerogels combine the lightweight, high porosity and large specific surface area of conventional aerogels with the excellent properties of cellulose itself (good biocompatibility and degradability, high mechanical strength).[191] Impregnating PCMs into cellulose aerogels is considered an effective technology to prevent liquid leakage due to the superior surface tension and capillary force. Most notably, cellulose aerogels have attractive mechanical properties, such as large compressibility and excellent flexibility. The smart integration of cellulose aerogels and PCMs can yield advanced flexible multifunctional composite PCMs.

5.1.1. Thermal Storage. Incorporating PCMs into robust cellulose aerogels can develop high-density thermal storage composite PCMs. For example, Wang et al.[192] improved the thermophysical properties of PEG via a surface functional strategy. In this work, PEG@cellulose aerogel−dopamine composite PCMs were constructed using a simple in situ
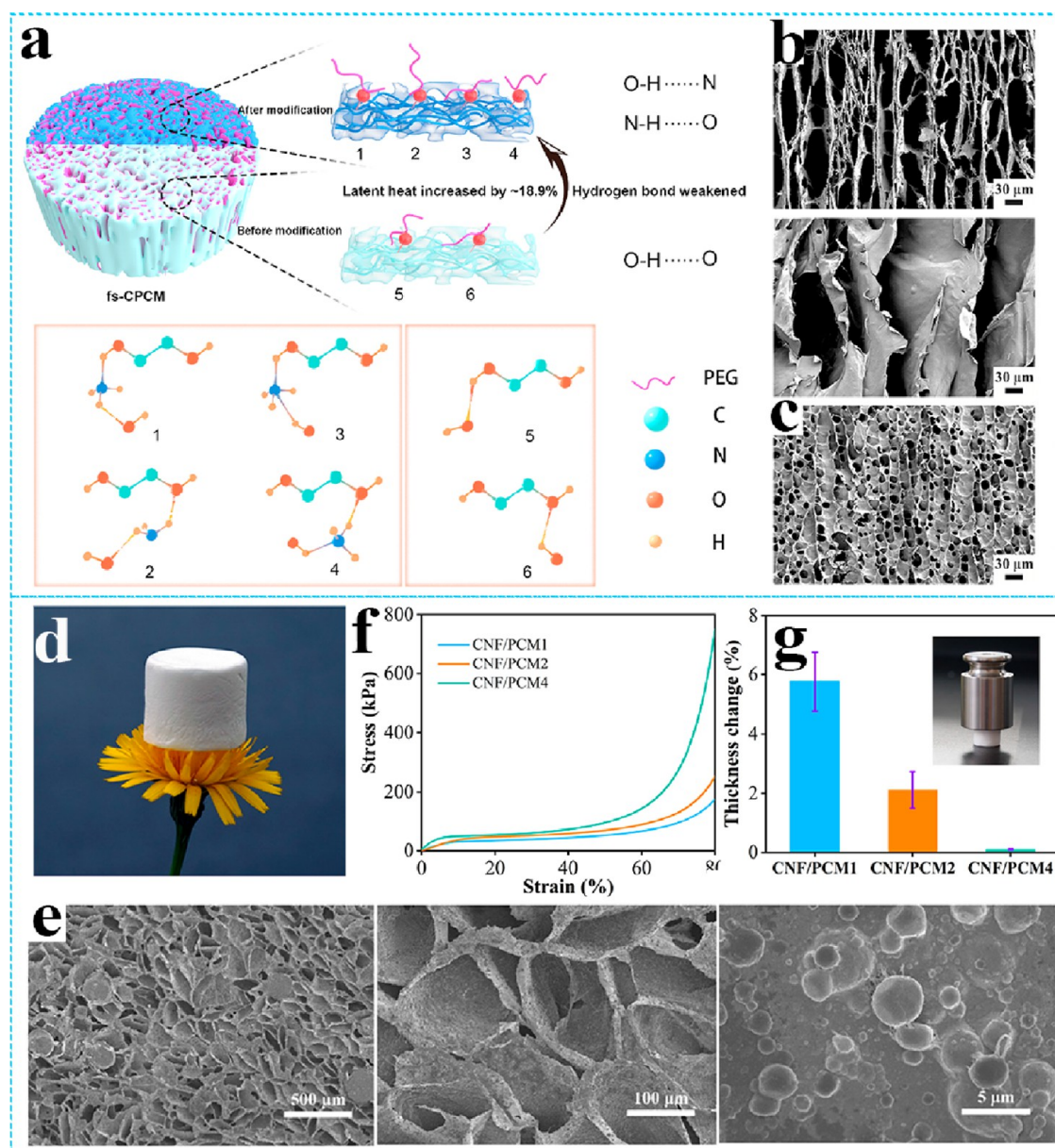
Figure 10. (a) Schematic diagram of latent heat enhancement after dopamine modification. (b) SEM images of cellulose aerogels and modified cellulose aerogels, respectively. (c) SEM image of composite PCMs. Adapted with permission from ref 192. Copyright 2021 Elsevier. (d) Digital image of CNF aerogels. (e) SEM images of paraffin@CNF composite PCMs. (f,g) Mechanical properties of paraffin@CNF composite PCMs. Adapted with permission from ref 193. Copyright 2021 Elsevier.

preparation method based on freeze casting. The morphology and structure of the cellulose aerogels did not change significantly after dopamine modification. The cellulose aerogels with well-aligned porous structures provided a large encapsulation space for PEG, and the encapsulation capacity reached 95 wt %. The abundant hydroxyl groups on the cellulose aerogels surface tended to form strong hydrogen bonds (O−H···O) with the hydroxyl groups of PEG, which was not conducive to the phase transition and latent heat release of PEG. After dopamine modification, the functional groups of cellulose aerogels (−OH), dopamine (N−H), and PEG (−OH) formed weaker hydrogen bonds (O−H···N and N−H···O) (Figure 10a−c). The latent heat of composite PCMs was further increased from 172.2 to 194.3 J/g.

For loading alkanes, Song et al.[193] prepared CNF aerogel-based PCMs by oil-in-water Pickering emulsion using paraffin as the oil phase based on the amphiphilic nature of 2,2,6,6-tetramethylpiperidine 1-oxyl (TEMPO)-oxidized CNFs (Figure 10d,e). The obtained paraffin@CNF aerogels can withstand loads over 3000−5000 times their own weight with little shape change due to the enhanced mechanical properties and good shape stability (Figure 10f,g). Nevertheless, the loading of *n*-alkanes in cellulose aerogels is much lower than the theoretical value due to the poor affinity between cellulose aerogels and *n*-alkanes, and the latent heat of composite PCMs was 173.59 J/g, approximately 84.4% of paraffin. To improve the affinity between cellulose aerogels and *n*-alkanes, Du et al.[194] prepared composite PCMs by impregnating *n*-octacosane into the alkylated nanofibrillated cellulose (NFC)/CNT hybrid aerogels. NFC/CNT aerogels were functionalized by grafting with organic acid chloride via an esterification reaction. The affinity between NFC/CNT aerogels and *n*-alkanes was
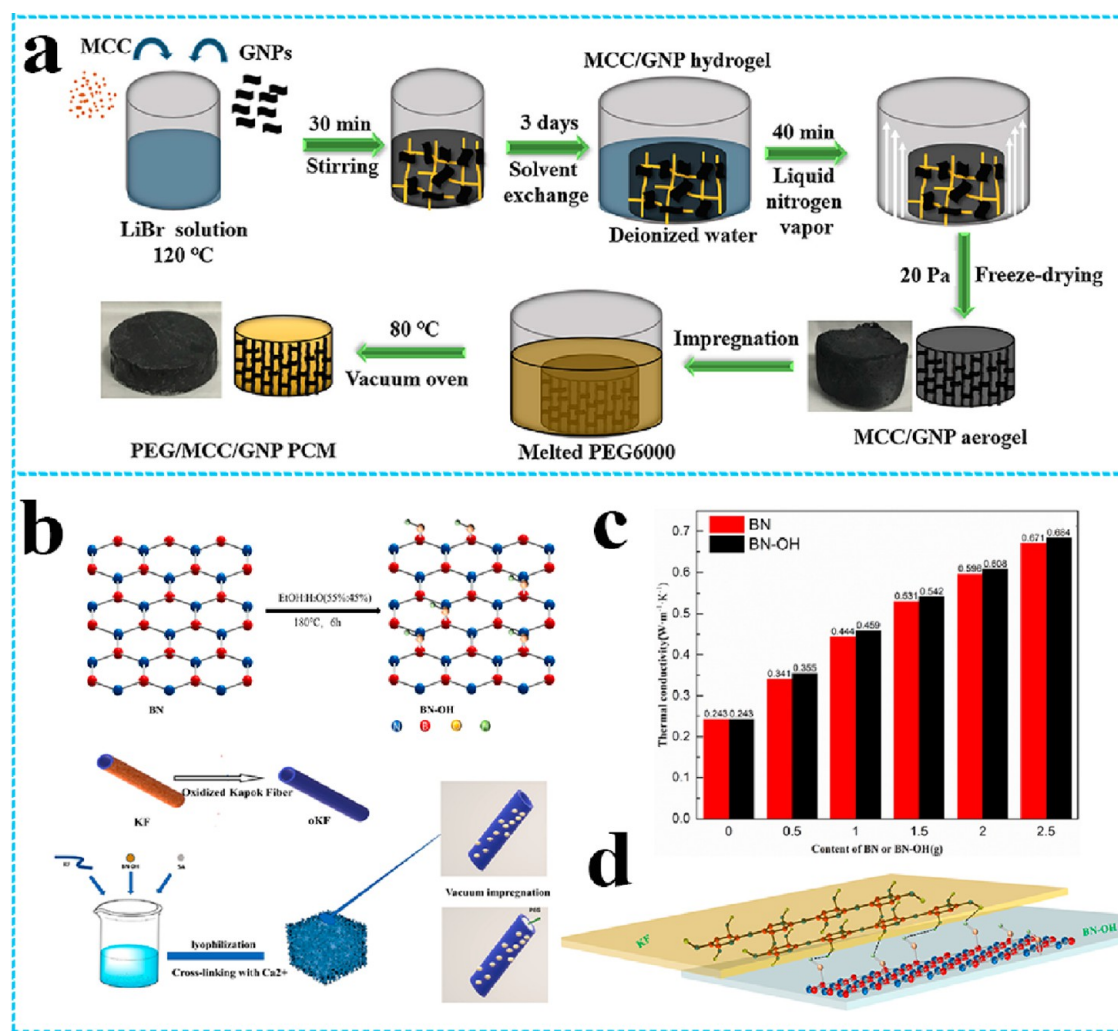
Figure 11. (a) Schematic diagram of the fabrication procedures of the PEG@MCC/graphene PCMs. Adapted with permission from ref 196. Copyright 2019 Elsevier. (b) Schematic diagram of kapok fiber-based aerogels. (c) Thermal conductivities of composite PCMs with different BN content. (d) Schematic diagram of hydrogen bond formation. Adapted with permission from ref 197. Copyright 2021, Elsevier.

significantly improved after modification by alkylation, and the alkane encapsulation ratio of NFC/CNT aerogels reached 94.9 wt %. Moreover, the resulting composite PCMs exhibited extremely high phase change enthalpies ranging from 250.9 to 252.9 J/g. It can be concluded that favorable surface modification can fully induce the phase transition behavior of PCMs and achieve high phase change enthalpy.

5.1.2. Thermal Conductivity. Generally, the thermal conductivity of cellulose aerogel-based composite PCMs is relatively low. To meet the unremitting pursuit of improving the thermal conductivity of PCMs, the combination of thermally conductive nanofillers and cellulose aerogels was considered. On the one hand, the governing cellulose aerogels ensure uniform dispersion of thermally conductive nanofillers due to the high porosity, high specific surface area, and thermally conductive nanofillers are not easily agglomerated. On the other hand, cellulose aerogel-based composite PCMs exhibit enhanced thermal conductivity without significantly sacrificing heat storage capacity because of their ultralow density. Yang et al.[195] fabricated lightweight cellulose/graphene aerogels by combining defect-free graphene and microcrystalline cellulose (MCC), and the corresponding composite PCMs by a vacuum-assisted impregnation method

(Figure 11a). Graphene annealed at 2200 °C was used as thermally conductive nanofiller. The thermal conductivity of composite PCMs with 5.3 wt % graphene was 1.35 W/m·K, which was 463% higher than that without graphene. Moreover, the latent heat of composite PCMs was 156.1 J/g, which was very close to the theoretical enthalpy of 159.5 J/g, indicating that the mass specific heat loss of PEG was negligible after adding cellulose/graphene aerogels. Wei et al.[196] also prepared porous MCC/graphene hybrid aerogels, followed by impregnation with PEG. When the graphene content was 1.51 wt %, the thermal conductivity of PEG@MCC/graphene increased to 1.03 W/m·K, which was 232% higher than PEG@MCC. Furthermore, PEG@MCC/graphene had a high latent heat of 182.6 J/g, which was 99.84% of pristine PEG.

Additionally, considering hydroxylated boron nitride (BN−OH) as a thermally conductive nanofiller, Zhang et al.[197] prepared porous sodium alginate/Kapton fiber (KF)/BN−OH aerogels (Figure 11b). BN−OH was attached to the surface of KF and sodium alginate to form a highly thermally conductive network, thus reducing the interfacial thermal resistance. Consequently, the thermal conductivity of composite PCMs increased to 0.671 W/m·K for 10 wt % BN and 0.684 W/m·K for 10 wt % BN−OH, which were 179 and 181% higher than
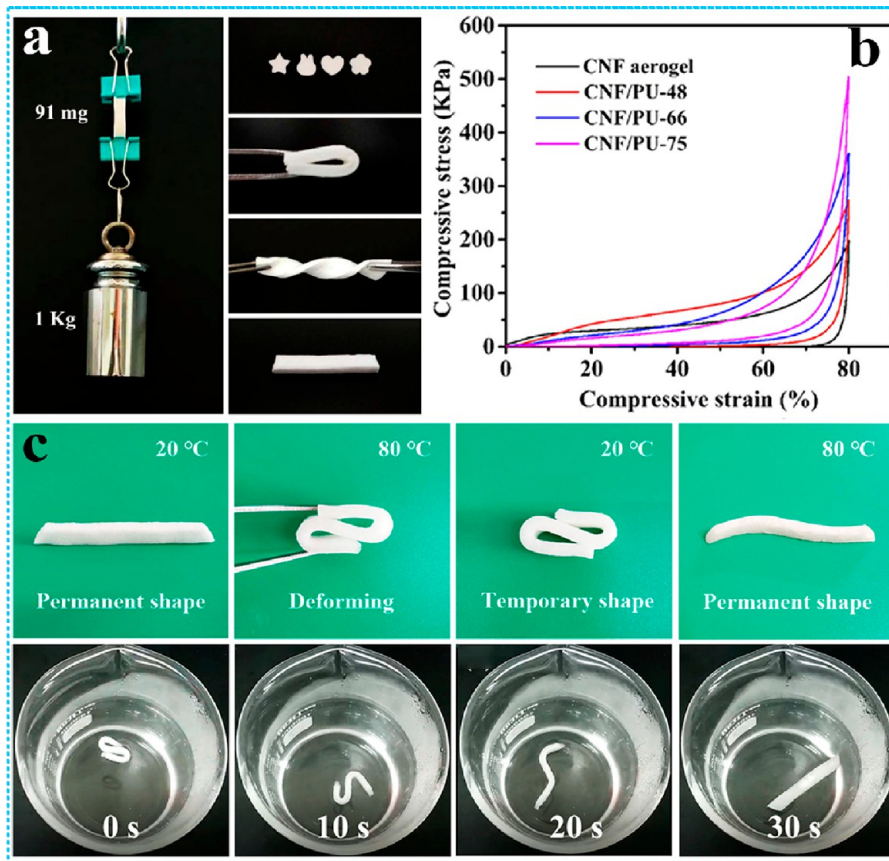
Figure 12. (a) Mechanical property of CNF/PU. (b) Compressive stress−strain curves of CNF aerogels and the CNF/PU hybrid aerogels. (c) Shape recovery process of octadecane@CNF/PU composite PCMs in hot water at 80 °C. Adapted from ref 212. Copyright 2020 American Chemical Society.

that of PEG, respectively. The thermal conductivity of KF/ BN−OH aerogel-based composite PCMs was enhanced because BN−OH can adhere more tightly to the surface of the gel skeleton, and the hydroxylation of BN facilitated the formation of hydrogen bonds between sodium alginate and KF with polyhydroxy structures, thus reducing the interfacial thermal resistance and accelerating the heat transfer (Figure 11c,d).

5.1.3. Energy Conversion. Cellulose aerogels can effectively encapsulate solid−liquid PCMs to overcome the liquid leakage of PCMs during the phase change process. Unfortunately, inferior solar−thermal conversion performance of PCM@ cellulose aerogels still severely limits their direct response to solar energy. The photothermal materials exhibit effective broadband absorption and high solar−thermal conversion efficiency across the whole solar spectrum.[198−201] Therefore, integrating photothermal materials (such as MXenes, graphene, black phosphorus, polypyrrole, and polydopamine) and cellulose aerogel-based composite PCMs can realize effective solar−thermal conversion.

5.1.3.1. MXenes/Cellulose Aerogels. 2D transition-metal carbides/carbonitrides (MXenes) exhibit excellent solar− thermal conversion performance due to their strong light absorption and localized surface plasmon resonance (LSPR) effect.[202] Therefore, MXenes can be introduced into cellulose aerogel-based composite PCMs to improve the solar−thermal conversion and storage efficient. Tang et al.[203] employed MXene/BC hybrid aerogels to prepare solar-driven composite PCMs. A very low concentration of BC with large aspect ratio

can build a 3D porous supporting skeleton, and the PEG loading in BC aerogels was up to 97.9 wt %. Under light conditions, pristine PEG could not undergo phase change due to weak light absorption. The MXene/BC hybrid aerogel-based composite PCMs with only 0.2 wt % MXene rapidly increased in temperature and underwent a phase transition. Du et al.[204] synthesized 2D-layered polymerized dopamine-decorated $Ti_3C_2T_x$ MXene (P-Mxene) and cellulose hybrid nanofiber aerogels. The solar−thermal conversion efficiency of composite PCMs was significantly improved due to the introduction of P-Mxene. In addition, composite PCMs exhibited solar−thermal−electricity conversion capacity with a maximum output voltage of 0.63 V.

5.1.3.2. Graphene/Cellulose Aerogels. Graphene as an effective photon trap can effectively improve the solar−thermal conversion efficiency of cellulose aerogel-based composite PCMs. Du et al.[205] synthesized PEG-grafted nanofibrillated cellulose (NFC-*g*-PEG) aerogels and PEG@NFC-*g*-PEG/ graphene composite PCMs. The added graphene greatly improved the solar−thermal conversion efficiency (84.7%) and the thermal conductivity (0.76 W/m·K) of composite PCMs due to the excellent affinity between PEG and PEG-*g*-NFC/graphene aerogels. Additionally, the phase change enthalpy of PEG-grafting composite PCMs was increased to 185.9 J/g compared with unmodified NFC/graphene aerogel-based composite PCMs (183.2 J/g).

5.1.3.3. Black Phosphorus/Cellulose Aerogels. Black phosphorus (BP) nanosheets, a two-dimensional (2D) nano-material, have superior photothermal effect, large specific

surface area and high thermal conductivity, as well as flame retardancy.[206] Du et al.[207] impregnated *n*-octacosane into CNF/BP aerogels to form composite PCMs. The addition of BP not only significantly enhanced the solar—thermal conversion efficiency of CNF/BP aerogel-based composite PCMs (up to 87.6%), but also increased the thermal conductivity by 87% than without BP. The flame retardancy property of CNF/BP aerogel-based composite PCMs was significantly improved due to the formation of protective carbon layers by BP.

5.1.3.4. Polypyrrole/Cellulose Aerogels. Polypyrrole (PPy) has a high molar absorption efficiency in the NIR region, which can significantly improve the solar—thermal conversion capability of cellulose aerogel-based composite PCMs.[208] Xu et al.[209] introduced PPy into porous CNF aerogels to prepare composite PCMs for solar—thermal conversion through in situ polymerization. The solar—thermal conversion efficiency of PPy/CNF-based composite PCMs was improved to 85.9% due to the presence of PPy. Moreover, PPy/CNF-based composite PCMs exhibited high latent heat of 239.4—258.4 J/g and high loading rate of up to 96 wt %.

5.1.3.5. Polydopamine/Cellulose Aerogels. Polydopamine (PDA) has high photothermal effects in broad sunlight spectrum and can be used for near-infrared photothermal therapy of cancer.[210] Tan et al.[211] prepared NFC/PDA hybrid aerogels (NPAs) by cation-induced gelation of NFC/PDA suspension. Then NPA-based composite PCMs were synthesized by impregnating *n*-octadecane into NPAs. In the photothermal experiments, PDA acted as a photon trap to effectively improve the solar—thermal conversion efficiency of composite PCMs (up to 86.7%). The NPA-based composite PCMs exhibited an extremely high thermal energy storage density of 248 J/g.

5.1.4. Advanced Utilization. Flexibility is a very attractive property of cellulose aerogels. Infiltrating rigid PCMs into flexible cellulose aerogels can yield flexible composite PCMs. Wang et al.[212] reported CNF/PU hybrid aerogels with robust mechanical properties as an efficient supporting material for octadecane. The latent heat of octadecane@CNF/PU composite PCMs can reach 223.3 J/g. CNF/PU hybrid aerogels had outstanding flexibility with a compressive stress of 510 KPa and a tensile strength of 247 KPa at 80% strain (Figure 12a,b). The octadecane@CNF/PU composite PCMs presented excellent shape memory function due to the synergistic effects of the elastic CNF/PU framework and octadecane. The samples could be fixed to the temporary shape of "S" below melting temperature and quickly recovered to the original shape within 30 s at 80 °C (Figure 12c). In addition, CNF/PU hybrid aerogel-based composite PCMs could reduce installation difficulties in thermal management owing to excellent flexibility and toughness.

In summary, cellulose aerogels possess inherent excellent properties, such as good biocompatibility, degradability, and high mechanical strength. They usually exhibit good mechanical properties under external forces, showing high encapsulation ability for PCMs. In addition, cellulose aerogels can also be used as compatible carrier for compounding thermally conductive nanofillers and photothermal conversion materials, which is conducive to improving the thermal conductivity and solar—thermal conversion capacity of cellulose aerogel-based composite PCMs. Surprisingly, advanced composite PCMs with mechanical flexibility and shape memory function have been prepared by smart integration of

high-strength and flexible cellulose aerogels and PCMs with soft and hard state changes. This integration strategy can effectively overcome the inherent rigidity and brittle failure of pristine PCMs.

5.2. Synthetic Polymer Aerogel-Based PCMs. A synthetic polymer aerogel combines the benefits of an aerogel with the conveniences of a plastic process route (i.e., poly(vinyl alcohol), polypropylene, and polyimide). They are very promising for exploring advanced multifunctional composite PCMs such as flexible PCMs, infrared stealth, shape memory, and thermal protection.

5.2.1. Thermal Storage. Poly(vinyl alcohol) (PVA) aerogels, which are easily cross-linked, water-soluble, biodegradable, and biocompatible polymers, are competitive supporting materials for the encapsulation of PCMs.[213] Yang et al.[214] prepared PVA aerogels with hierarchically porous structures by freezing/thawing and introduced PEG into the prepared PVA aerogels by vacuum impregnation. The prepared PVA aerogels can effectively accommodate PEG with leakproof due to their suitable pore size, large specific surface area and hydrogen bonding interactions. The melting enthalpy of PEG@PVA aerogel was 146.7 J/g, which was 95.6% of pristine PEG. Additionally, PEG@PVA aerogel exhibited pronounced shape stability at 80 °C for 60 h. Furthermore, Hong et al.[215] reported polypropylene aerogels with superwetting property as a porous scaffold for the fabrication of composites PCMs. The polypropylene aerogels were easily obtained from bulk chemical materials or industrial polypropylene wastes through dissolution, precipitation and lyophilization processes. The latent heat of polypropylene aerogel-based composite PCMs ranged from 141.1—159.5 J/g, and the latent heat remained almost constant even after 50 melting/freeze cycles, indicating the excellent thermal cycling stability.

5.2.2. Thermal Conductivity. Polymer aerogels are considered very attractive insulation materials due to low thermal conductivity coupled with their great flexibility and mechanical strength.[216−218] The combination of PCMs and polymer aerogels with low thermal conductivity provides interesting benefits for heat insulation and preservation. For conventional thermal insulation materials, heat is not preserved because conventional insulation materials cannot store and retain heat. In contrast, polymer aerogel-based composite PCMs are used as thermal insulation materials, in which heat can be retained and released from the insulation materials due to the presence of PCMs. As reported by Wang et al.,[219] single-component supramolecular aerogels (SMAs) were synthesized from supramolecular hydrogels formed by the self-assembly of R-/ γ-cyclodextrin and PEG by supercritical liquid drying (SCLD). The surface temperature of SMAs was below 60 °C due to their low thermal conductivity (0.05 W/m·K) after operating on a heater at 100 °C for 0.5 h, while PEG was melted after only 10 min due to the high thermal conductivity (0.31 W/m· K). The thermal conductivity of SMAs was only slightly higher than silica aerogels (0.04 W/m·K). For SMA insulation materials, most of the heat was not only insulated, but the heat of the insulation materials was preserved at high temperatures and heat was released at low temperatures due to the presence of PEG.

Attractively, aerogel fiber-based composite PCMs can be an alternative to synthetic fibers for thermal insulation due to their excellent thermal regulation properties. Liu et al.[220] prepared phase change aerogel fibers by incorporating PEG into Kevlar (KNF) aerogel fibers (Figure 13a). The aerogel
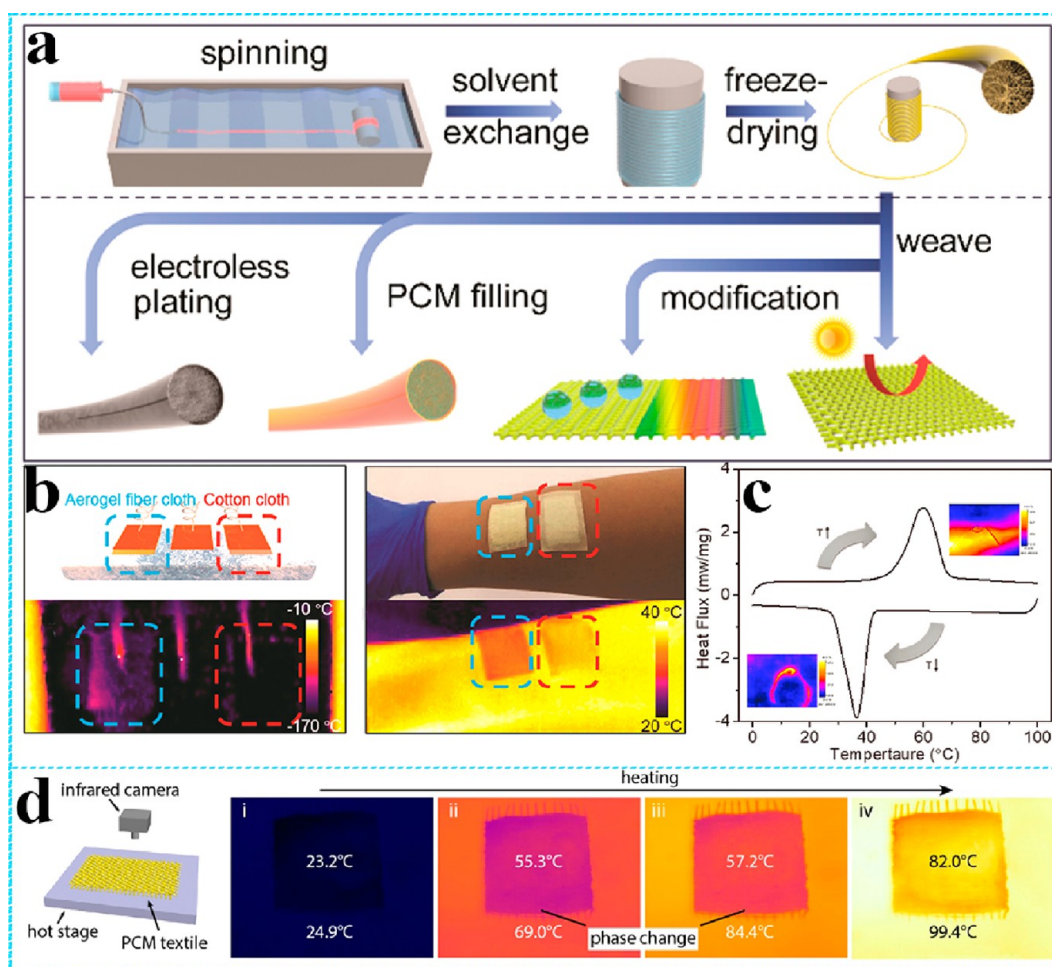
Figure 13. (a) Fabrication schematic of KNF aerogel fibers and their various applications. (b) Thermal insulation property of aerogels textile and cotton cloth. (c) Differential scanning calorimetry curve of phase change aerogels fibers. Adapted from ref 220. Copyright 2019 American Chemical Society. (d) Infrared images showing the thermoregulating function of PI textile infiltrated with PCMs during heating. Adapted with permission from ref 221. Copyright 2020 Elsevier.

fibers were promising fibers for heat insulation, and the thermal conductivity of the prepared aerogel fiber mats was 0.04 W/m·K. The aerogel fabrics provided better insulation than cotton fabrics whether at liquid nitrogen temperature or at room temperature (Figure 13b). The phase change fibers showed a high energy storage density with a phase change enthalpy of 162 J/g (Figure 13c). Inspired by polar bear hair for thermoregulation in extreme environments, Wang et al.[221] reported polyimide (PI) aerogel fibers as protective clothing in high-temperature environments by a facile freeze-spinning method. The obtained PI aerogel fibers exhibited a high tensile strength (14.7 MPa) and an excellent thermal insulation performance due to the aligned porous structure, especially at high temperature. In particular, the thermal conductivities of the PI aerogel fibers were only 0.04 and 0.16 W/m·K at 25 and 300 °C, respectively. The aligned porous structure of PI aerogel fibers facilitated the encapsulation of PCMs. The temperature regulation ability of PI aerogel fibers can be further enhanced by osmotic treatment with *n*-octadecanols. As the temperature increased to 100 °C, a delay and narrow temperature fluctuation was clearly displayed, reflecting the temperature regulation function of the PCMs textiles. The temperature of the PCMs textiles finally did not reach the temperature of the hot stage due to the heat insulation of PI

aerogels (Figure 13d). Therefore, multifunctional PI aerogel fibers show great application potential in intelligent textiles and high-temperature protective clothing.

5.2.3. Energy Conversion. The design of aerogel-based composite PCMs for solar−thermal conversion energy storage has been receiving much attention. Polymer aerogels possess excellent mechanical properties, such as high flexibility, and high-temperature stability compared to traditional inorganic aerogels. The polymer aerogels are expected to serve as an ultralight and robust supporting material to fabricate highly flexible photothermal conversion composite PCMs. Zheng et al.[222] fabricated a composite PCMs based on polyimide (PI)/phosphorene (PR) hybrid aerogels and PEG to realize effective photothermal energy conversion. The introduction of PR nanosheets effectively enhances the solar−thermal conversion and energy storage capacity of the composite PCMs due to their excellent infrared absorption and internal photothermal conversion capability. The resultant PEG@hybrid aerogel composites exhibited a high solar−thermal conversion efficiency of 82.5%. The composites also demonstrated good thermal impact resistance, maintaining high thermal cycle stability after 500 cycles of thermal cycling. In another report, they[223] also developed PI/MXene hybrid aerogel-based composite PCMs for sustainable seawater desalination. The
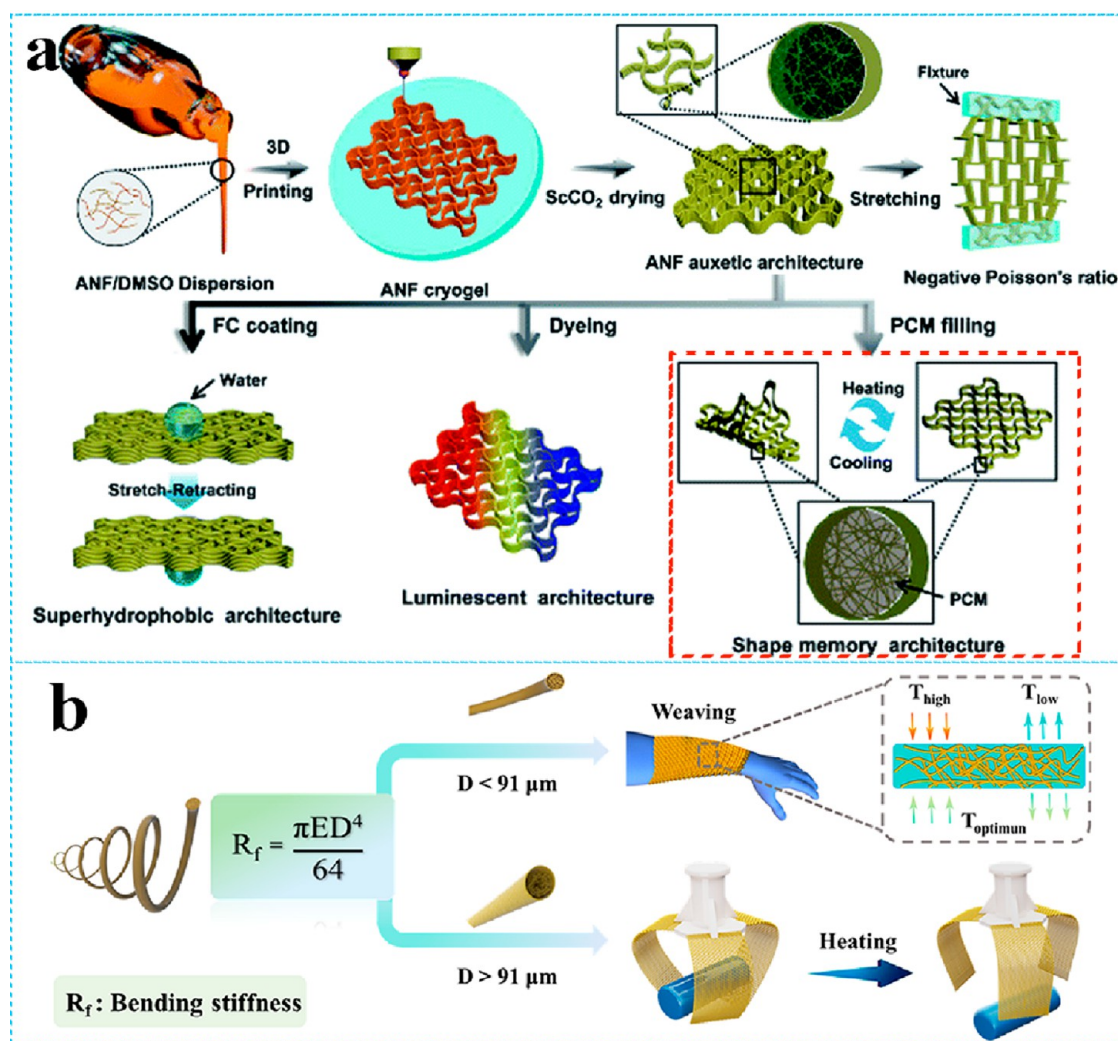
Figure 14. (a) Schematic illustration of 3D printing process and further functionalization. Adapted with permission from ref 229. Copyright 2020 Royal Society of Chemistry. (b) Schematic description of the applications of paraffin@H-KAFs. Adapted from ref 230. Copyright 2021 American Chemical Society.

introduction of MXene nanosheets as a high-efficiency sunlight absorber significantly improved the solar–thermal conversion efficiency (87.28%) of composite PCMs. In the absence of sunlight, thermal energy was released into the desalination system through the crystalline phase transition of PEG, thereby realizing continuous production of pure water for a long time. Cao et al.[224] prepared MXene/PI aerogel-encapsulated PEG composite PCMs with excellent solar–thermal conversion capability. In addition, the composite PCMs possessed good flame retardancy because MXene promoted charring of the pyrolysis products of PEG through catalysis, thus facilitating the formation of stable graphitized char and reducing heat release. Interestingly, the integration of luminescent particles into PCMs to prepare self-luminescent composites expands its applications in the optical field. Zhou et al.[225] introduced luminescent particles into aerogel-based composite PCMs, realizing the dual storage of heat and light energy. Composite PCMs absorbed and stored ultraviolet and visible light during the day, and then emitted fluorescence slowly in the dark for long periods of time. This work provides the basis for research on solar energy acquisition, thermal and light storage.

5.2.4. Advanced Utilization. 5.2.4.1. Thermal Infrared Stealth. Infrared stealth technology has received increasing

attention in recent decades because of its commercial and military value. Reducing the temperature of surface and modulating the infrared emissivity of surface are the two main ways to achieve thermal camouflage. Previous studies have established that PCMs have been explored as tunable infrared emission materials. Attractively, compared with other infrared stealth materials, aerogel-based composite PCMs show better infrared stealth performance due to the excellent thermal insulation of aerogels and temperature regulation of PCMs. As reported by Zhang et al.,[226] flexible Kevlar nanofiber aerogel (KNA) films were employed to infiltrate PEG to fabricate composite PCMs. The KNA films had a high porosity (~98%) and a high specific surface area (~365.99 m^2/g) as well as excellent thermal insulation performance (0.04 W/m· K). The infrared emissivity of the obtained PEG@KNA films was 0.94, which was comparable to the IR emissivity of most backgrounds. Thus, targets covered with PEG@KNA films can incorporate their thermal appearance into the background in the outdoor environment with varying solar illumination. To further achieve the concealment of thermal targets from IR detection, they proposed a hybrid structure consisting of insulation layer (KNA films) and ultralow IR transmittance layer (PEG@KNA), which has promising application in the
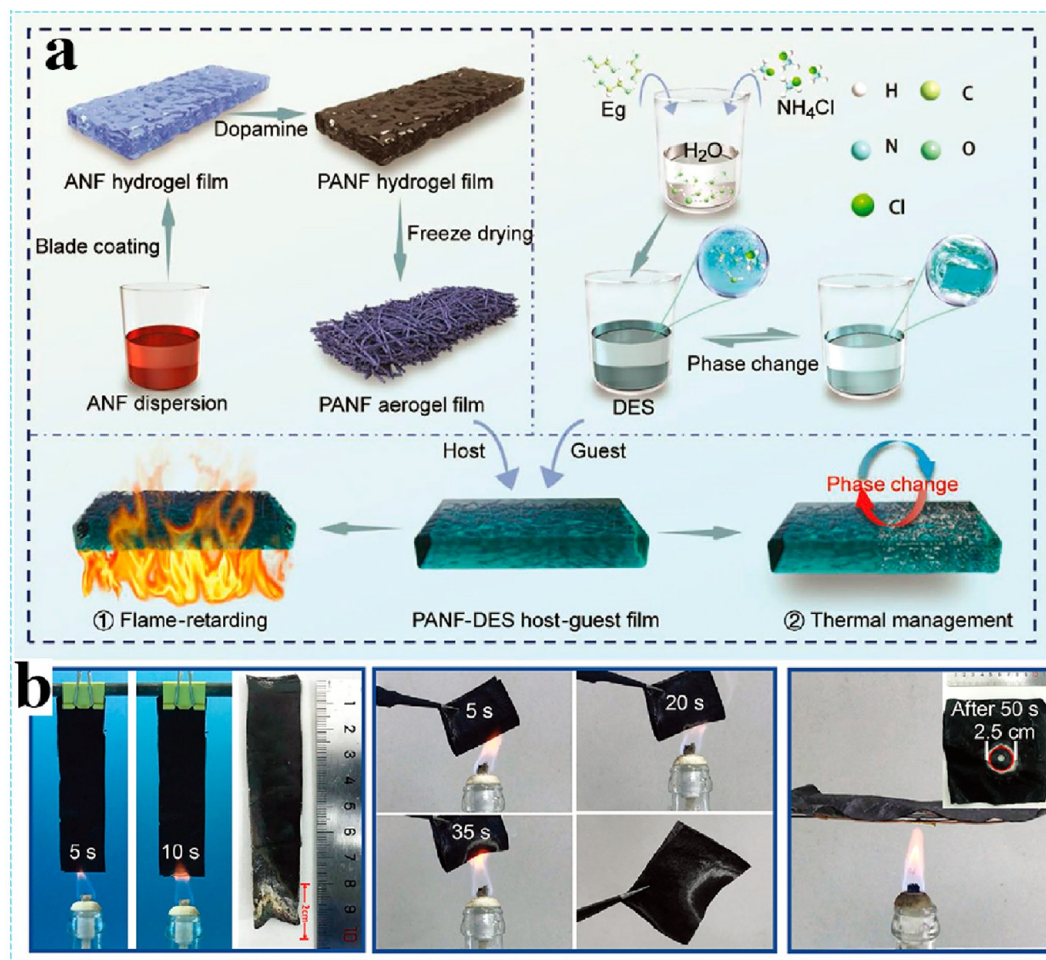
Figure 15. (a) Schematic description of flame retardancy PANF-DES host−guest film. (b) Photographs of PANF-DES host−guest film in combustion. Adapted with permission from ref 232. Copyright 2021 Wiley-VCH.

field of infrared thermal stealth. In another study, Hu et al.[227] synthesized low molecular weight poly(p-phenylene tereph-thalamide) (PPTA) aerogels with adjustable thermal conductivity and superior mechanical properties. The content of PEG in PPTA aerogels was as high as 95.2 wt %, exhibiting superior infrared stealth performance. The infrared radiation was absorbed by PEG to prevent the target from radiating outward when heat radiated to the PEG@PPTA composite PCMs. Shi et al.[228] prepared flexible and foldable composite PCMs films based on the PI/phosphorene (PR) hybrid aerogels and PEG. Thermal insulation and cooling effects are generated through thermal shielding of aerogels and thermal buffering of PCMs, resulting in a synergistic effect of reducing the surface temperature of the thermal target. It can be concluded that polymer aerogel-based composite PCMs show great potential for industrial applications, such as thermal insulation and infrared stealth.

5.2.4.2. Thermoresponsive Shape Memory. Considering the good flexibility of polymer aerogels and the response of PCMs to heat stimulus, it is envisaged that polymer aerogel-based composite PCMs will be endowed with thermoresponsive shape memory function by external thermal stimulation. Thermally induced shape memory and powerful thermo-mechanical conversion technologies are expected to be applied to artificial muscles, actuators, and soft robotics, Cheng et al.[229] developed Kevlar aerogel-based composite PCMs with

thermoresponsive shape memory function. 3D Kevlar aerogel auxetic architectures (3D-KAAA) with excellent mechanical properties were fabricated by a 3D printing technology that combined direct ink writing (DIW) and freeze-casting with dimethyl sulfoxide (DMSO)-based inks, followed by a special drying technology (Figure 14a). Finally, thermally responsive shape memory composite PCMs were prepared by impregnating PCMs (PEG or paraffin) into 3D-KAAA. The highly interconnected 3D architectures of 3D-KAAA retained a high percentage of PCMs (93.5 wt % for PEG and 91.8 wt % for paraffin) due to 3D-KAAA induced strong capillary force. Base on the response of the soft and hard states of PCMs to phase transition temperatures, PEG@3D-AAA exhibited thermally responsive shape memory behavior driven by external thermal stimuli. Interestingly, PCMs and 3D printing technology were linked together, which provided an advanced on-demand manufacturing platform for developing more versatile synthetic structures and devices for advanced multifunctional applications.

Shape memory functional materials offer promising possibility for the design of intelligent grippers. As reported by Bao et al.,[230] hydrophobic Kevlar aerogel-encapsulated paraffin fibers (paraffin@H-KAFs) were prepared using hydrophobic KAFs (H-KAFs) as a porous host and paraffin as a functional guest. The prepared paraffin@H-KAFs exhibited high tensile strength of 30 MPa. The paraffin@H-
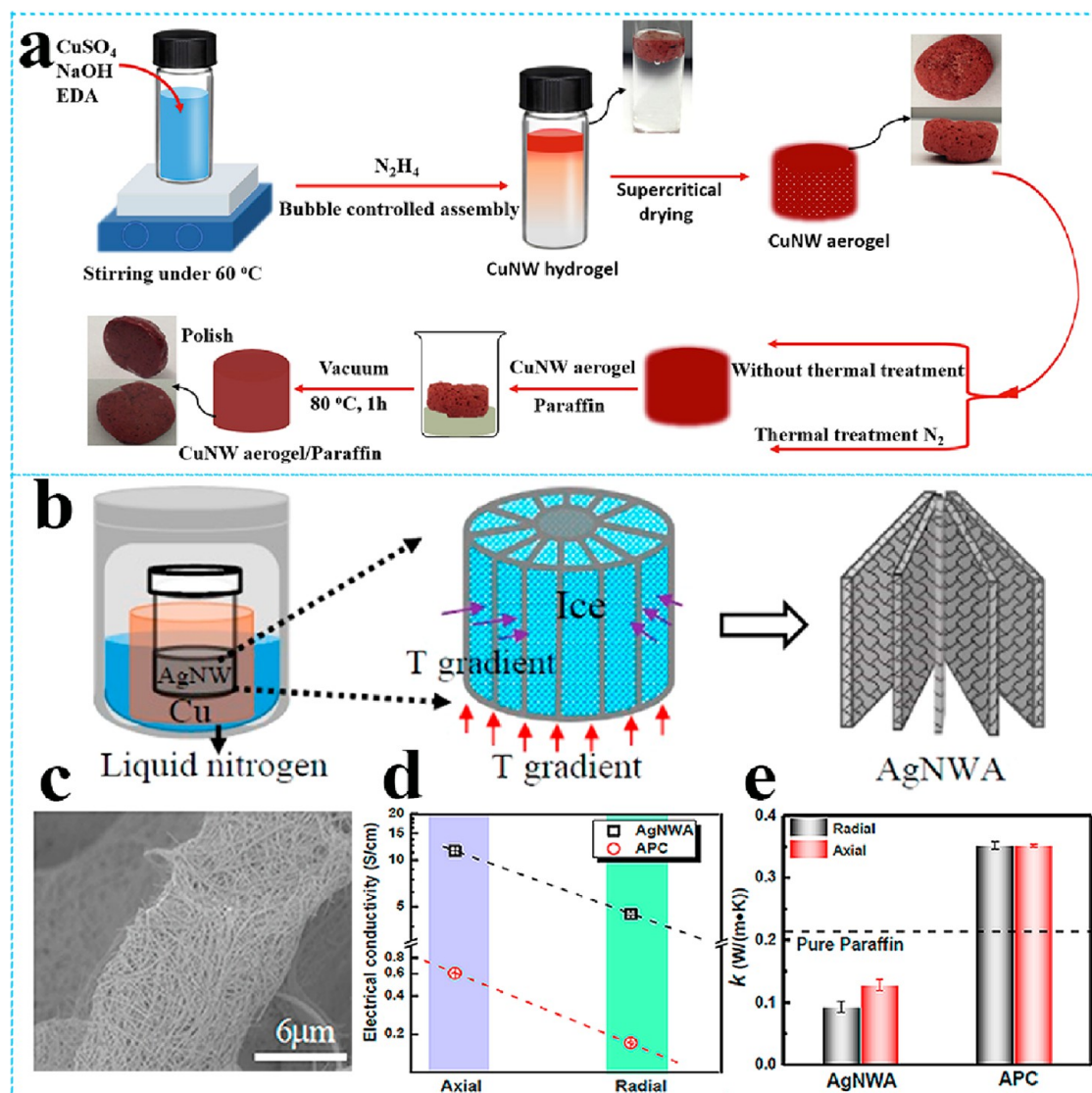
Figure 16. (a) Synthesis schematic of CuNW aerogels and composite PCMs. Adapted with permission from ref 236. Copyright 2019 Elsevier. (b) Fabrication illustration of AgNWAs by bidirectional freezing. (c) SEM image of AgNWAs. (d,e) Electrical and thermal conductivities of AgNWAs and paraffin@AgNWAs along axial and radial directions. Adapted from ref 238. Copyright 2019 American Chemical Society.

KAFs with bending stiffness higher than the critical stiffness in a solid state of paraffin can be used as shape memory materials due to the transition between stiffness and flexibility caused by phase change. To demonstrate shape memory function, paraffin@H-KAFs (400 μm in diameter) as a dynamic gripper was developed for low-temperature gripping and high-temperature release items. In addition, paraffin@H-KAFs showed great application potential in smart thermoregulated scenarios due to their low bending stiffness at room temperature (Figure 14b), such as intelligent temperature-regulated fabrics and automatic temperature-controlled systems.

5.2.4.3. Flame Retardancy. Flammability is a severe problem associated with organic PCMs and the preparation of flame-retardant phase change films is still challenging.[231] To address flammability issue, Yang et al.[232] developed polydopamine—aramid nanofiber (PANF) aerogel films by in situ polymerization of dopamine on ANFs, and nonflammable deep eutectic solvent (DES) served as PCMs (Figure 15a). Interestingly, PANF-DES host—guest films exhibited fast self-extinguishing property and good shape retention property, and

no collapse in fire, thus ensuring safety in the actual application (Figure 15b). Another advantage was that PANF-DES films had excellent temperature regulation capacity in low temperature environments. Specifically, the prepared PANF-DES films had a high energy storage capacity of 225 J/g and a low phase transition temperature of −21 °C.

In summary, flexible polymer aerogels are intriguing candidates to stably encapsulate PCMs. Polymer aerogel-based composite PCMs are very suitable for making temperature-regulating fibers and heat-insulating fibers, bringing people more comfortable and intelligent lives. In addition, some advanced fascinating features of polymer aerogel-based composite PCMs have been proposed, especially to take advantage of the superflexibility of polymer aerogels. Since the report on 3D-printed aerogels in 2015, an interdisciplinary research field combining aerogels and printing technologies has emerged, pushing the boundaries of their structure and property, and further broadening their applications. In follow-up studies, more attention should be given to
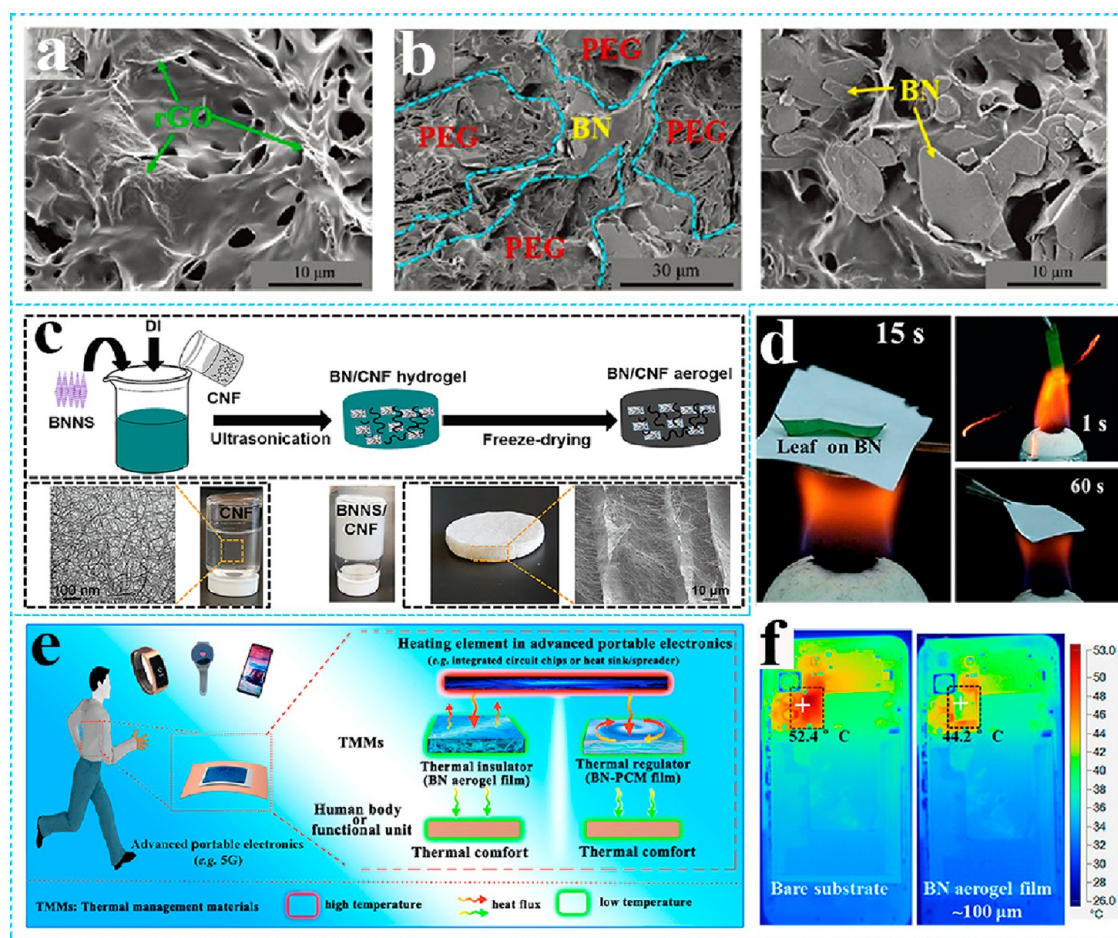
Figure 17. (a) SEM image of PEG@MF/rGO composite PCMs. (b) SEM images of PEG@MF/rGO/BN composite PCMs. Adapted with permission from ref 248. Copyright 2019 Royal Society of Chemistry. (c) Preparation schematic of BNNSs-g/CNF aerogels. Adapted from ref 250. Copyright 2020 American Chemical Society. (d) Flame retardancy of BN aerogel films. (e) Schematic of thermal management mechanisms based on thermal insulation of BN aerogels film and paraffin@BN composite film. (f) Infrared images of the backside of working 5G smart phone. Adapted from ref 85. Copyright 2020 American Chemical Society.

integrating PCMs into 3D-printed materials to develop advanced multifunctional aerogel-based composite PCMs.

6. OTHER AEROGEL-BASED PCMs

6.1. Metal Aerogel-Based PCMs. Metal aerogels are 3D porous materials made of metal nanomaterials. They combine the porous features of aerogels with the typical properties of certain metals, which are highly desirable in energy storage, piezo electronics, and electro-optical sensors.[233−235] A key motivation for using metal aerogels to improve the performance of PCMs is attributed to their very high intrinsic thermal conductivity and electrical conductivity. Feng's group[236] pioneered copper nanowire (CuNW) aerogels to improve the thermal conductivity and electrical conductivity of PCMs. In this work, CuNW aerogels were fabricated based on the "bubble-controlled assembly" mechanism, then the corresponding composite PCMs were prepared by impregnating paraffin (Figure 16a). Compared to pristine paraffin, CuNW aerogel-based composite PCMs with 2.0 wt % CuNW showed an increased thermal conductivity from 0.21 to 0.28 W/m·K and an increased electrical conductivity from 0 to 3.03 S/m, as well as a slight change in latent heat (<1%). Furthermore, the authors systematically studied the influence of filler−filler and filler−matrix interfacial interactions on the thermal perform-

ances of composite PCMs. To obtain the optimal thermal conductivity enhancement for PCMs, it is necessary to achieve advantageous interfacial interactions not only between fillers but also, more importantly, between filler and matrix.

Notably, silver possesses the highest electrical conductivity (6.3×10^7 S/m) and the thermal conductivity (429 W/m·K) among all the metals.[237] Therefore, silver nanowires (AgNWs) have great potential to improve the electrical conductivity and the thermal conductivity of PCMs. In particular, silver nanowire aerogels (AgNWAs) are independent 3D networks, which contribute to the formation of a continuous heat conduction and electrically conductive channel. Feng et al.[238] developed bidirectionally aligned AgNWAs via a bidirectional freeze-casting technique and synthesized paraffin@AgNWA composite PCMs (APC) by vacuum impregnation (Figure 16b,c). Paraffin had no measurable electrical conductivity (σ), while the σ along the axial and transverse directions of AgNWAs and APC showed strong anisotropy. For APC, the axial σ (∼0.6 S/cm) was 3.5× of the radial σ (∼0.17 S/cm) (Figure 16d). Compared to pristine paraffin, the thermal conductivity of APC with 5 wt % AgNWs was increased by 67% due to the anisotropic thermal property of AgNWAs (Figure 16e). Given that one-step synthesis of AgNW aerogels has never been realized, Feng et al.[239] developed a one-step hydrothermal synthesis to directly fabricate Ag/polyvinylpyr-

rolidone (PVP) nanowire aerogels (AgPNWAs) with ultrahigh porosity (~99.4%) and ultralight density (61.5 ± 6.4 mg/cm³). Compared with pristine paraffin, the thermal conductivity of AgPNWA-based composite PCMs containing 5.4 wt % AgPNWAs was increased by ~133% due to the superior thermal conductivity of AgPNWAs. Yi et al.[240] prepared montmorillonite nanosheet and silver nanowire aerogel as supporting material for PCMs. The supporting material provided heat transfer path constructed of cross-linked thermal filler, which greatly enhanced the heat transfer capacity and contributed to excellent solar energy collection performance.

In summary, metal aerogels have the characteristics of metals (such as high electrical conductivity and thermal conductivity), as well as continuous thermal and electrical conduction paths. Benefiting from these advantages, metal aerogels are promising candidates to prepare highly thermally and electrically composite PCMs. However, to date, there are still few studies on metal aerogel-based composite PCMs. Therefore, more systematic studies on metal aerogel-based composite PCMs are urgently needed, especially energy conversion and advanced function.

6.2. Boron Nitride Aerogel-Based PCMs. Hexagonal boron nitride (h-BN) with similar structure to graphite, also called white graphite, exhibits excellent electrical insulation properties, high thermal conductivity, high thermal stability and oxidation resistance.[241−245] Unlike carbon-based nanofillers for the enhancement of both thermal and electrical conductivities of PCMs, BN usually imparts higher electrical insulation properties and thermal conductivity to PCMs.[246] Therefore, infiltrating PCMs into BN aerogels will help to prepare highly thermally conductive but electrically insulating composite PCMs, which are expected to be used in microelectronic devices. However, it is still difficult to construct BN aerogels due to inert surface feature of BN and weak interactions between the networks. Recently, BN aerogels have been popularly constructed by using compatible binders, such as polymers, graphene oxide and cellulose nanofibers, to assist h-BN or boron nitride nanotubes (BNNTs) or boron nitride nanosheets (BNNSs).

GO-assisted dispersion technology was proposed for the preparation of BNNT aerogels. The BNNTs/rGO aerogels were obtained by taking full advantage of the stable dispersion of GO nanosheets in water and the self-assembly ability during the subsequent reduction process.[247] The obtained BNNTs/rGO aerogels exhibited good elasticity and fatigue resistance, which could recover to the original volume and remain more than 85% of the maximum stress even after 100 cycles of 50% compression. The thermal conductivity of PEG@BNNTs/rGO with a low filler content of 1.5 wt % was improved to 0.43 W/m·K. In addition, the phase change enthalpy of PEG@BNNTs/rGO reached 195.6 J/g, which was higher than rGO/PEG of 182.3 J/g. Similarly, GO was used to assist the impregnation of BN nanosheets into MF framework and then deposited on the surface of MF, as reported by Xue et al.[248] The MF/rGO/BN aerogels were fabricated via hydrothermal reaction, freeze-drying and carbonization treatment. The thermal conductivity (0.35 W/m·K) of PEG@MF/rGO composite PCMs was enhanced by 16.67%, while the thermal conductivity (0.79 W/m·K) of PEG@MF/rGO/BN composite PCMs was increased by 163% compared to PEG (0.3 W/m·K), indicating the significant synergistic enhancement effect of rGO and BN (Figure 17a,b). In addition, the fabrication of BN aerogels can also be tactfully achieved by combination of

cellulose. Lei et al.[249] fabricated robust cellulose/BNNS aerogels via a self-assembly strategy. High-strength cellulose/BNNS aerogels displayed an excellent compressive strength of 3.03 MPa due to the synergistic reinforcement of cellulose nanofibers and BNNSs. The composite PCMs with 10 vol % BNNSs showed a significantly enhanced in-plane thermal conductivity (4.76 W/m·K), which was about 1300% higher than that of pristine PEG. To make BNNSs disperse in water well, Wan et al.[250] functionalized BNNSs with amino acid and carboxyl groups. The L-glutamine-grafted BNNSs (BNNSs-g) dispersed well in water at a concentration of above 30 mg/mL. Subsequently, cellulose nanofibers as cross-linking agents were added to form robust aerogels (Figure 17c). The PEG@BNNS-g composite PCMs showed excellent shape stability due to the hydrogen bonding interaction between PEG and the functional groups of CNF and BNNSs-g. In addition, composite PCMs exhibited a high phase change enthalpy of 150.1 J/g, which reached about 94% of pristine PEG. In another study, Kashfipour et al.[251] applied sodium carboxymethyl cellulose (SCMC) to improve the mechanical strength of BN aerogels. In this work, isotropic composites were prepared by incorporating xylitol crystals into to BN aerogels via an ice template method, and exhibited a high thermal conductivity of 4.53 W/m·K at BN loading of 18.2 wt %.

With the advent of the 5G era, the thermal management of electronic systems requires higher efficiency and more functionality. As mentioned above, BN is a promising candidate for thermal management of microelectronic device due to the insulating property. In this regard, Wang et al.[85] proposed two thermal management strategies (thermal insulator and thermal regulator) based on BN aerogel films. The flexible BN aerogel films were prepared through molecular precursor assembly, sublimation drying, and pyrolysis reactions. The obtained BN aerogel films showed high porosity (~96%), large specific surface area (~982 m²/g), controllable thickness (50−200 μm), low thermal conductivity (0.06 W/m·K) and excellent flame retardancy (Figure 17d). Subsequently, BN phase change composite films were prepared by impregnating paraffin into BN aerogel films (Figure 17e). The thermal conductivity of BN phase change composite films was higher than pristine paraffin because the air in BN aerogel films was replaced by paraffin. The low thermal conductivity of the BN aerogel films could be mainly attributed to that the nanoribbons could partition the 3D aerogels into nearly isolated cells to efficiently mitigate the air conduction and convection. However, once the air in aerogels was replaced by PCMs, the heat flow along the interconnected BN nanosheets was collected at the junctions and was then transported to the adjacent BN nanosheets; therefore, the thermal conductivity of composite PCMs will be enhanced. The thermal conductivity of the BN aerogel phase change composite films was 0.29 W/m·K, which was larger than that of pristine paraffin (0.2 W/m·K). Interestingly, paraffin@BN aerogel films were capable of absorbing large amounts of heat and suppressing electron overheating due to enhanced thermal conductivity and large latent heat. Therefore, BN phase change composite films can be used as a thermal protection layer for portable electronics and significantly reduce the heat transfer from electronics to skin (Figure 17f).

In summary, the application of PCMs can be surprisingly broadened by masterly designing the supporting materials and their existing forms. It is meaningful to develop an appropriate strategy for design and synthesis of porous BN aerogels. BN
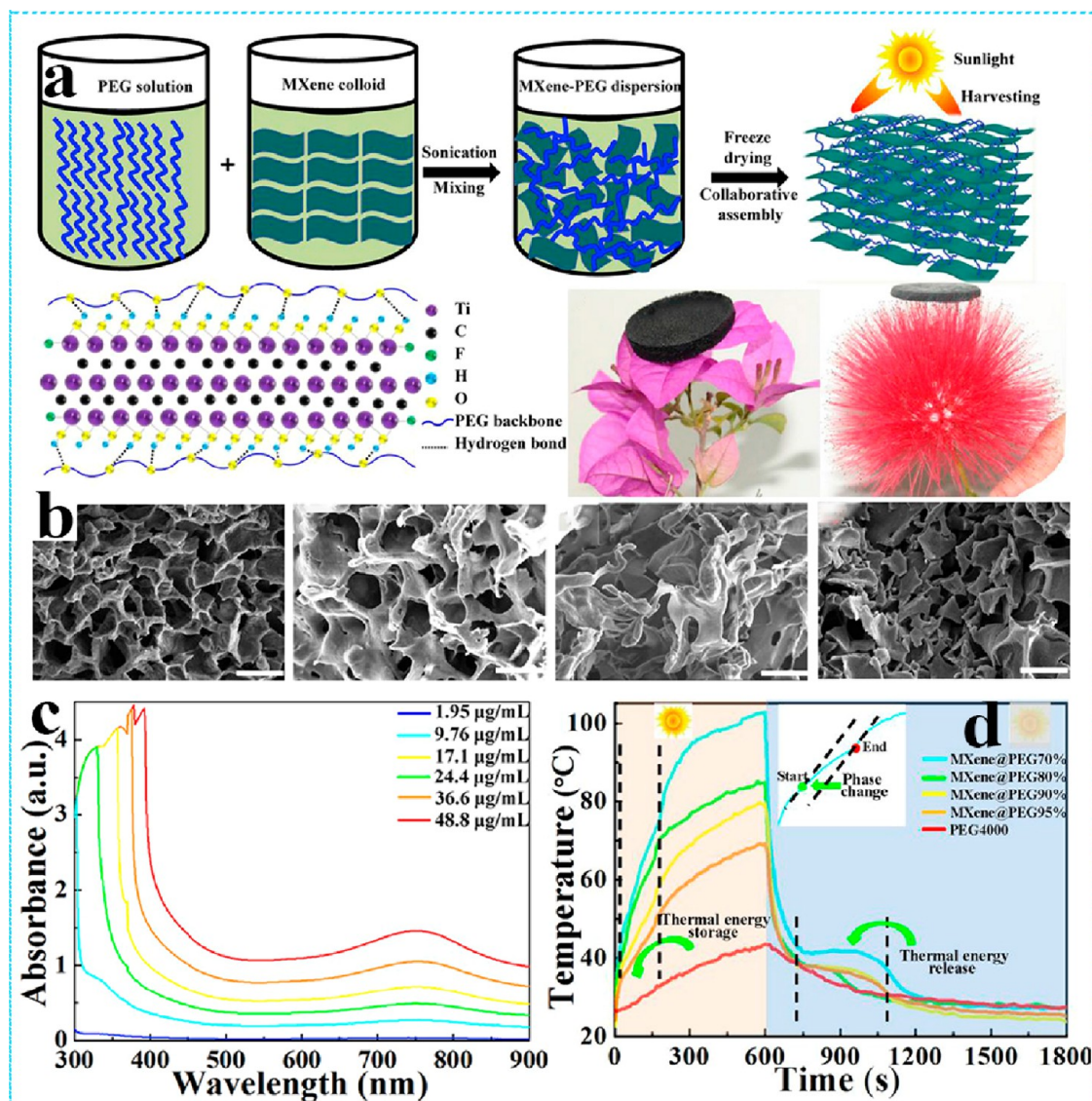
Figure 18. (a) Preparation schematic of PEG@MXene aerogels. (b) SEM images of PEG@MXene aerogels; the loadings of PEG4000 were 70, 80, 90, and 95% (from left to right). (c) UV−vis−NIR absorption spectra of MXene. (d) Solar−thermal conversion curves of PEG@MXene aerogels. Adapted with permission from ref 256. Copyright 2020 Elsevier.

can significantly enhance both the thermal conductivity and the solar−thermal conversion capability of PCMs, therefore thermal storage systems based on BN aerogels for solar−thermal conversion are worthy of further development. BN also significantly enhance electrical insulation of PCMs, which has vigorous competency in thermal management of electronic devices.

6.3. MXene Aerogel-Based PCMs. MXenes are emerging two-dimensional materials derived from MAX phases, or layered hexagonal carbides and nitrides, where A is an A-group element, usually aluminum or gallium. MXenes are defined by a general formula $M_{n+1}X_nT_x$, wherein M represents an transition metal, X is carbon or nitrogen, T represents the surface termination group (−O, −OH, and/or −F), and x represents the number of termination functional groups.[252−254] MXenes have sparked various emerging research hotspots in fundamental theory and engineering applications since they were creatively synthesized by Gogotsi in 2011. Recently, MXene aerogels have become fascinating supporting materials for PCMs to harness the efficient use of solar energy due to

high thermal stability, high thermal conductivity and nearly 100% internal photothermal conversion efficiency.[255] MXenes exhibit prominent photothermal conversion performance by virtue of their excellent electromagnetic wave absorption, LSPR, and interlayer structures. Lin et al.[256] constructed MXene aerogel-based composite PCMs for solar−thermal conversion and storage (Figure 18a,b). MXene nanosheets were attractive photothermal agents due to their characteristic absorption bands in the NIR region from 750−800 nm and high extinction coefficients in the UV−vis−NIR region (Figure 18c). The solar−thermal conversion efficiency of PEG@MXene aerogel was as high as 92.5% (Figure 18d). Similarly, taking advantage of effective photothermal conversion and the high thermal conductivity of MXene, Liu et al.[257] prepared MXene/gelatin hybrid aerogels by a freeze-drying method, and then paraffin was impregnated into the aerogels by vacuum impregnation. The resulting composite PCMs exhibited a high loading rate (96.3−97.7 wt %) and large thermal storage density (184.7−199.9 J/g). The thermal conductivity of paraffin@MXene/gelatin aerogels was 0.92 W/m·K, which

Table 1. Versatile Aerogel PCMs for Thermal Energy Storage[a]

aerogels	PCMs	PCM loading (wt %)	K of PCMs (W/m·K)	composite PCMs K (W/m·K)	η (%)	T_m/T_f (°C)	$\Delta H_m/\Delta H_f$ (J/g)	ref
	paraffin	92.42	0.20	0.79	295	52.9/46.2	210.6/209.2	120
	paraffin		0.35	8.87/2.68	2434/665		179.0/—	125
	paraffin	97	0.207	0.274	32	41.0/58.0	202.2/213.0	96
	paraffin	97.8	0.26	0.46	77	50.8/45.8	121.0/116.9	117
	paraffin	98.15	0.2	0.836	318	46.6/—	245.5/-	118
	paraffin	99.83				40.0/—	232.2/228.4	99
graphene aerogels	n-octadecane	96.7	0.15	0.47	215	35.1/13.8	195.7/196.7	95
	PEG10000	97.75	0.31	1.43	361	64.8/41.8	185.6/177.8	111
	PEG2000	98.79	0.227	0.760	235	53.8/—	162.2/—	116
	PEG4000	99.2		0.384		61.0/42.0	168.7/165.1	100
	PEG6000	99.5	0.211	0.344	63	42.0/61.0	218.9/213.2	17
	1-octadecanol	86.7	0.21	9.50	4423	62/48,53	196.2/234.1	113
	1-octadecanol	88	0.23	5.92	2473	59.0/53.9,49.3	202.8/250.8	112
	1-octadecanol	95	0.23	4.28	1761	61.0/53.9	225.3/289.0	107
	lauric acid	94.31	0.267	1.207	352	43.3/40.6	207.3/205.8	106
	paraffin	95	0.248	0.427	72	63.5/54.5	83.6/98.8	160
	paraffin	95.5	0.250	0.358	43	74.5/58.0	202.2/200.2	157
bioderived carbon aerogels	eicosane	97	0.46	0.53	15	40.0/29.0	211.7/209.8	167
	PEG6000	95	0.31	0.62	100	58.2/37.4	171.5/169.5	158
	mannitol	97	0.65	0.78	20	160/114	281.9/258.3	161
	1-hexadecanol	98.08	0.24	0.50	108		220/—	156
	stearic acid	99.1	0.333	0.621	86	71.4/66.8	223.1/221.6	164
	paraffin	70	0.25	0.13	−48	59.2/49.8	112.9/122.7	179
	paraffin	80.42				65.0/43.2	154.0/131.6	173
	eicosane	84.3				36.8/33.7	198.4/197.4	177
silica aerogels	erythritol	85				123.8/—	289.2/—	176
	PEG2000	60	0.29	0.08	−72	57.4/25.1	90.6/83.1	180
	PEG6000	88.5	-	-	-	58.4/40.6	167.0/168.2	181
	octadecanol	60	0.25	0.12	−52	60.1/53.1	127.7/129.9	180
	n-octadecanol	75	0.3	0.08	−72	52.5/42.3	145.6/126.3	182
	paraffin			0.037		55.4/48.1	173.6/171.9	193
	n-alkanes	94.9	0.23	0.58	152	68.5/48.3	252.9/252.3	194
	n-octacosane		0.228	0.448	96	66.0/52.2	251.6/250.2	207
cellulose aerogels	n-octacosane	96				65.6/50.9	239.4/235.3	209
	PEG6000		0.31	1.03	232	62.0/—	182.6/—	196
	PEG6000	89.2	0.24	1.35	463	63.0/44.3	156.1/148.9	195
	PEG2000	95				59.3/40.9	194.3/193.3	192
	PEG4000	97.9				67.0/41.5	196.7/191.7	203
	PEG10000	52.8	0.307	0.052	−83		71.8	219
	PEG2000	93.5				50.2/40.9	186/135	229
polymer aerogels	PEG1500	94.3				49.9/—	162.9/—	226
	PEG1000	95.6				39.0/19.4	146.7/140.4	214
	deep eutectic solvent	92				−21.0/—	225.0	232
metal aerogels	paraffin	94.6	0.21	0.49	133	55.0/—		239
	paraffin	94.99	0.21	0.35	67	55.0/—		238
	paraffin	98	0.21	0.277	32	55.0/—	173.0/—	236
	paraffin	79.3	0.2	0.29	45	42.4/47.0	183/—	85
BN aerogels	PEG10000		0.33	4.764	1344	60.2/41.6	136.8/122.8	249
	PEG1500		0.28	0.59	110	42.3/15.2	143.5/136.1	250
	PEG4000	98.5	0.29	0.43	48	59.1/38.5	195.6/175.9	247
MXene aerogels	paraffin	97.7	0.26	0.92	248	60.1/38.3	191.7/192.9	257
	PEG4000	95				57.5/33.8	112.3/108.5	256
	phosphorus-modified stearyl alcohol	80	0.353	0.486	37	79.2/50.7	120.1/122.7	258

[a]K, thermal conductivity; η, growth rate of thermal conductivity, $\eta = K_c − K_m/(K_m)$, where K_c and K_m are the thermal conductivity of composite PCMs and pristine PCMs, respectively; T_m, melting point; T_f, freezing point; ΔH_m, melting enthalpy; ΔH_f, freezing enthalpy.

was 3.48 times higher than that of pristine paraffin. Moreover, the solar−thermal conversion efficiency of paraffin@MXene/

gelatin aerogels was greatly improved due to the introduced MXene nanosheets as efficient photon trapper. In another

Table 2. Thermal Properties of Aerogel-Based Composite PCMs for Energy Conversion and Storage

aerogel-based composite PCMs for solar−thermal conversion and storage						
solar absorber	PCMs	absorber loading (wt %)	melting point (°C)	latent heat (J/g)	light intensity (mW/cm^2)	efficiency (%)	ref
graphene aerogels	paraffin	4.1	52.4	154.3	100	78	133
rGO/graphene aerogels	1-octadecanol	13.3	48/53	196.2	100	84	113
TiO$_2$-x/rGO aerogels	paraffin	7.6	55.7	127.8	100	89.9	134
RGO/GF/CAs	paraffin		57.3	145.2	100	90	114
graphene/copper foam aerogels	paraffin	5.19/29.34	45.6/60	133.6	100	97	135
sunflower-derived CAs	hexadecanamine		50.13	239.4	100	75.6	162
sunflower-derived CAs	hexadecanamine		49.33	271	100	67.8	162
succulent-derived CAs	paraffin	37	63.5	83.6	125	82	160
gelatin-derived CAs	eicosane		40	211.7	300	93.32	167
carbon nanofiber aerogels	1-tetradecanol		38.93	262.2		96.2	164
SiO$_2$−dye aerogels	PEG6000	2.7	58.3	158.3	100	88.1	181
graphene/cellulose aerogels	PEG6000		68.8	185.5	300	84.7	205
BP/cellulose aerogels	n-octacosane		66	251.6	250	87.6	207
PPy/cellulose aerogels	n-octacosane		65.6	239.4	300	85.9	209
PDA/cellulose aerogels	n-octacosane		64.3	250.4	250	86.7	211
PI/PR aerogels	PEG10000	16	65	174.4	300	82.5	222
PI/MXene aerogels	PEG10000	20	62.45	177.1	300	87.28	223
MXene aerogels	PEG4000	30	-	72.8	100	92.5	256

aerogel-based composite PCMs for solar−thermal−electric conversion and storage						
solar absorber	PCMs	absorber loading (wt %)	melting point (°C)	latent heat (J/g)	light intensity (mW/cm^2)	output U (mV)/I (mA)/P (μW)	ref
graphene aerogels	m-PEGMA		58.7	177	200	144/14.8/2130	140
graphene/cysteamine aerogels	1-tetradecanol		42.87	213.7	15	−/11/511.58	142
graphene aerogels	1-tetradecanol		44.68	220.4		−/10/437	141
carbon nanofiber aerogels	1-tetradecanol		38.93	262.2		80/13.5/1080	164
MXene/cellulose aerogels	erythritol		125.3	330.6	250	630/−/−	204

aerogel-based composite PCMs for electric−thermal conversion and storage						
conductive additives	PCMs	additives loading (wt %)	melting point (°C)	latent heat (J/g)	input voltage	efficiency (%)	ref
GO/graphene aerogels	paraffin	0.38/4.51	62.4	155.5	2.9	62.5	145
graphene aerogels	PEG4000	1.2	57.4	92.1	10	67.2	146
graphene aerogels	paraffin	6	64.7	193.7	3	85	126
ZnO/graphene aerogels	PEG4000	0.97/1.32	57.1	108.1	15	84.4	147
melon-derived CAs	paraffin	5	53.5	115.2	15	71.4	165
gelatin-derived CAs	eicosane		40	211.7		94.83	167

study, MXene aerogel-based flame retardant composite PCMs were designed by chemically modifying stearyl alcohol with phosphorus-containing molecules (P-SAL) by Luo et al.,[258] which can be utilized for safe and efficient solar storage application. Hu et al.[259] fabricated photodriven and flexible composite PCMs based on a flexible water-borne polyurethane (WPU)/MXene aerogels. The obtained PEG@WPU/MXene composite PCMs possessed excellent dimension retention along with a high phase change enthalpy value (154.6 J/g). The composite PCMs realized excellent light-actuated shape memory and self-healing functions due to excellent photo-absorption ability of MXene combined with the elasticity of the WPU/MXene aerogel and the solid−liquid phase change of PEG.

In summary, benefiting from their high thermal stability, high thermal conductivity and nearly 100% internal photo-thermal conversion efficiency, MXenes are very promising for solar energy storage. It is worth noting that assembling MXene nanosheets into aerogels has more fascinating advantages, including low density, high porosity, and large specific surface area. Importantly, MXene nanosheets no longer undergo restacking and reagglomeration. Recently, solar energy-harvesting and utilization strategies are mainly focusing on carbon nanotubes, graphene, graphite, and BN. However, the composite PCMs for solar energy storage based on MXene aerogels are relatively less discussed, deserving further attention and research.

In this review, Table 1 summarizes various aerogel-based composite PCMs for thermal energy storage. Table 2 summarizes the various forms of energy-harvesting performances of composite PCMs. Among them, solar energy is abundant, clean and sustainable, and it is one of the important clean energy sources that is easy to popularize and popularize. Therefore, the solar−thermal conversion is the most economical and safe among the various energy conversion, and has the highest energy conversion efficiency. However, solar energy suffers from intermittent, unstable disadvantages, which requires additional charging modes, such as electric or magnetic, to keep the energy storage system working continuously. The electric−thermal conversion and storage technology can store thermal energy by using low-cost electric energy for heating during the valley electricity period at night,

Table 3. Comparison of Thermal Properties of Aerogel-Based Composite PCMs and Other Composite PCMs

supporting materials	PCMs	loading (wt %)	latent heat (J/g)	K (W/m·K)	ref	review
expanded graphite	paraffin	90	117.5	3.83	260	Huang et al.[80]
carbon foam	paraffin		164.98	1.19	261	Wu et al.[46]
graphene foam	paraffin		153.1	2.28	262	Yang et al.[263]
biological porous carbon	PEG4000	85.36	175.6	4.48	264	Yang et al.[263]
silica	PEG10000	85	162.9	0.36	265	Wu et al.[46]
cellulose network	paraffin	72.2	139	-	266	Zou et al.[31]
high density polyethylene	paraffin	77	162.2	0.26	267	Wu et al.[46]
olefin block copolymer/EG	paraffin	80	176.7	5.5	268	Zou et al.[31]
copper foam	paraffin	98.6	132.5	4.9	269	Huang et al.[80]
BN scaffolds	paraffin	74	135.1	1.33	270	Yang et al.[263]
MXene	PEG6000	85	171.5	0.293	271	Tang et al.[201]
expanded perlite/CNT	paraffin	60	157.3	0.32	272	Huang et al.[80]
graphene aerogels	PEG6000	99.5	218.9	0.344	17	this review
graphene aerogels	1-octadecanol	86.7	196.2	9.50	113	this review
bioderived carbon aerogels	stearic acid	99.1	223.1	0.333	164	this review
silica aerogels	octadecanol	60	127.7	0.12	180	this review
cellulose aerogels	n-alkanes	94.9	252.9	0.58	194	this review
polymer aerogels	PEG2000	93.5	186		229	this review
metal aerogels	paraffin	98	173	0.277	236	this review
BN aerogels	PEG4000	98.5	195.6	0.43	247	this review
MXene aerogels	paraffin	97.7	191.7	0.92	257	this review

and then release the thermal energy for heating during the day, which plays the role of shaving peaks and filling valleys, and reducing economic costs. However, the electric−thermal conversion efficiency is not high enough, resulting in a part of the electrical energy wasted. Magnetic−thermal conversion can not only be used for energy supply, but also to control temperature in specific field, such as magnetothermal therapy. Specifically, the magnetic energy is stored in the form of latent heat, and the temperature of the material is controlled to prevent excessive temperature from causing damage to the body. However, the conversion efficiency of magnetic−thermal composite PCMs is still relatively low and needs to be further improvement. Solar−thermal−electric conversion is a secondary application of solar−thermal composite PCMs. Solar energy is converted and stored by the PCMs, and then thermal is utilized to generate electricity via thermoelectric modules. The composite PCMs exhibit excellent solar energy absorption and solar thermal conversion capability, which can maximize the average temperature difference (ΔT) of thermoelectric devices, and when the external energy source disappears, the PCMs-based TEGs can still achieve sustainable power output because the accumulated heat in the PCMs can be released for thermoelectric power generation. TEGs have the advantages of quiet operation, high reliability, low production cost, long operating life, and environmental friendliness, however, low thermoelectric conversion efficiency has been considered a major obstacle to the development of thermoelectric power generation. In addition, acoustic−thermal energy conversion and storage is another emerging energy-harvesting application of composite PCMs, and its specific conversion principle and preparation need further study.

The most popular nanoencapsulated composite PCMs have always been an effective means to overcome the disadvantages of using PCMs alone for energy storage systems. Research so far, porous materials such as natural minerals, metal foams, expanded graphite, porous carbon-based materials, aerogels, polymers, BN and MXenes emerging materials have been chosen as shape stabilizing supporting materials. Taking the

widely used paraffin and PEG as examples, the thermophysical properties of aerogel-based composite PCMs are compared with those of other commonly used porous material-based composite PCMs (Table 3). Notably, it is challenging to balance between shape stability and high energy storage density in the preparation of composites PCMs, since energy-free supporting materials energy storage replaces part of the workpiece. Among these supporting materials, benefiting from the inherent properties of ultralight, ultrahigh porosity, ultrahigh surface area, aerogel-based composites PCMs have extremely high loading capacity and large energy storage density.

In terms of improving the thermal conductivity of PCMs, metal foam can significantly enhance the thermal conductivity of the composite PCMs, but its relatively large pores exhibit poor binding force on the PCMs, which leads to the easy leakage of the PCMs during melting. Generally, there is a trade-off between the thermal storage capacity and thermal conductivity of composite PCMs. High thermal storage capacity requires a high loading of PCMs, while thermally conductive supporting materials with small content usually yield limited thermal conductivity enhancement. Therefore, it is imminent to develop aerogel-based composites PCMs integrating high thermal storage capacity and high thermal conductivity.

7. CONCLUSION AND FUTURE PROSPECTS

Aerogels are porous solid materials with ultralow density, high porosity, large specific surface area, and tailorable properties and are ideal substrates for encapsulating PCMs. This review systematically summarizes the state-of-the-art research progress of aerogel-based composite PCMs. In this review, aerogel-based composite PCMs are divided into: (I) carbon aerogel-based, (II) silica aerogel-based, (III) polymer aerogel-based, (IV) metal aerogel-based, (V) boron nitride aerogel-based, and (VI) MXene aerogel-based. Most importantly, 3D interconnected porous aerogels can prevent melted PCM leakage due to strong capillary forces and surface tension. Benefiting from
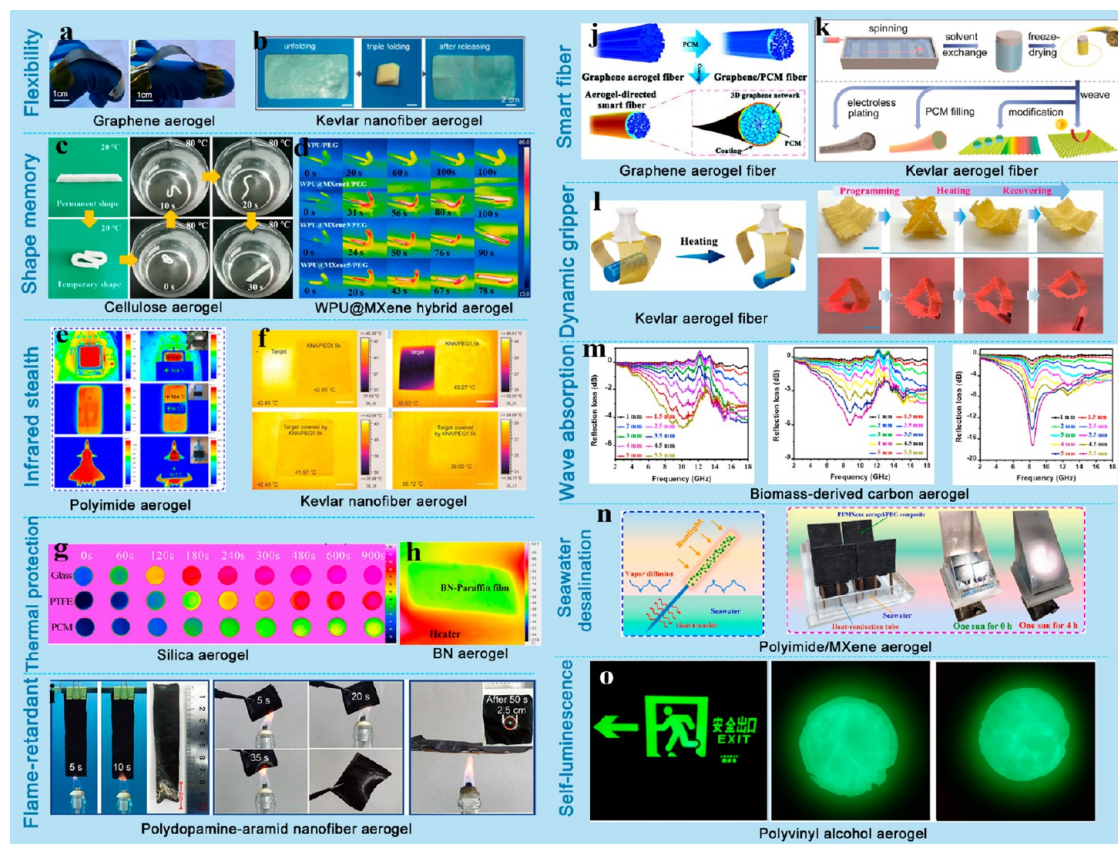
Figure 19. Advanced multifunctions of aerogel-based composite PCMs. (a) Images of flexible paraffin@graphene aerogels. Adapted with permission from ref 152. Copyright 2021 Elsevier. (b) Photographs of the folding and releasing of PEG@Kevlar aerogels. Adapted from ref 226. Copyright 2019 American Chemical Society. (c) Photos showing the shape recovery process of octadecane@cellulose aerogels. Adapted from ref 212. Copyright 2020 American Chemical Society. (d) Light-actuated shape fixing and recovery behaviors of PEG@WPU and PEG@WPU/MXene. Adapted with permission from ref 259. Copyright 2021 Elsevier. (e) Infrared thermographic images of PEG@PI/PR aerogels film. Adapted with permission from ref 228. Copyright 2022 Elsevier. (f) Infrared stealth synergistic performance of PEG@Kevlar aerogels. Adapted from ref 226. Copyright 2019 American Chemical Society. (g) Thermal protection performance of octadecanol@silica aerogels. Adapted with permission from ref 180. Copyright 2020 Elsevier. (h) Thermal protection performance of paraffin@BN aerogels. Adapted from ref 85. Copyright 2020 American Chemical Society. (i) Flame retardancy of polydopamine—aramid nanofiber aerogels. Adapted with permission from ref 232. Copyright 2021 Wiley-VCH. (j) PCM@graphene aerogels smart fibers. Adapted with permission from ref 153. Copyright 2018 Wiley-VCH. (k) Fabrication of Kevlar aerogel fibers and applications. Adapted from ref 220. Copyright 2019 American Chemical Society. (l) Dynamic gripper. Adapted from ref 230. Copyright 2020 American Chemical Society. (m) Microwave absorption performance. Adapted with permission from ref 168. Copyright 2021 Elsevier. (n) Solar-driven evaporation device. Adapted with permission from ref 223. Copyright 2022 Elsevier. (o) Luminescence application of PEG@functionalized PVA aerogels. Adapted with permission from ref 225. Copyright 2022 Elsevier.

the ultralight weight, high porosity, and large specific surface area of aerogels, aerogel-based composite PCMs have extremely high load-bearing capacity and large energy storage density. In addition, versatile aerogels ameliorate the inherent inferior defects of low thermal and electrical conductivities, and the weak solar-capturing capacity of pristine PCMs. Aerogel-based composite PCMs integrate multiple energy conversion and storage models, such as acoustic—thermal and solar—thermal—electricity energy conversion and storage. More importantly, the smart marriage of aerogels and PCMs endow PCMs with advanced multiple functions, such as mechanical flexibility, flame retardancy, shape memory, intelligent grippers, and thermal infrared stealth. Figure 19 summarizes the various emerging advanced functions of aerogel-based composite PCMs.

Specifically, (1) carbon, BN, metal, and MXene aerogels can greatly improve the thermal conductivity of PCMs without sacrificing much latent heat due to high thermally conductive paths. Meanwhile, carbon and metal aerogels can improve the

electrical conductivity of PCMs, which are conducive to the fast response of PCMs to electric energy for electric—thermal conversion and storage. BN aerogels enhance the electrical isolation and thermal conductivity of PCMs, showing great application potential in microelectronic devices. (2) Silica and polymer aerogels with low thermal conductivity can reduce the thermal conductivity of PCMs and realize their application in heat insulation and heat preservation. (3) To allow PCMs to harvest thermal energy generated by other alternations apart from temperature, PCM systems can be designed based on functional aerogels with the ability to respond to solar energy, electric energy, magnetic energy, and acoustic energy and are converted into thermal energy in the form of latent heat. Specifically, carbon, MXene, and BN aerogel-based composite PCMs can realize solar—thermal energy conversion and storage due to their excellent solar-absorbing ability. In addition, CAs also effectively improve the electrical conductivity of PCMs, so CA-based composite PCMs simultaneously integrate solar—thermal and electric—thermal conversion functions. Further-

• Aerogels	• Pros and Cons	• Energy Conversion and Storage	• Advanced Utilization
Carbon aerogels • Graphene aerogels • Biomass-derived carbon aerogels	✓ Tailorable properties ✗ Costly ✗ Environmentally hazardous ✓ High loading PCM ✓ High thermal/electrical conductivity ✓ Excellent high temperature stability ✓ Good mechanical strength ✓ Good photothermal conversion capacity ✓ Environmental-friendly ✓ Abundant source ✓ Low-cost ✗ Larger aperture	• Solar-thermal • Solar-thermal-electric • Electric-thermal • Magnetic-thermal • Acoustic-thermal	• Flexible PCM • Phase change smart fiber • Microwave absorption
Silica aerogels	✓ Thermal conductivity reduction ✓ Ease of preparation ✓ High insulation performance ✗ Non-electrical conductive ✗ Relatively low loading PCM ✗ Inferior mechanical strength	• Solar-thermal	• Thermal protection
Polymer aerogels • Cellulose aerogels • Synthetic polymer aerogels	✓ Good degradability ✓ Environmental-friendly ✓ Abundant source ✓ Low-cost ✗ Relatively strong surface restriction ✓ High loading PCM ✓ High flexibility ✓ Thermal conductivity reduction ✓ Flame-retardant ✗ Non-electrical conductive ✗ Inferior photothermal conversion ✗ Environmentally hazardous ✗ Complex of preparation	• Solar-thermal • Solar-thermal-electric	• Flexible PCM • Infrared stealth • Shape memory • Flame-retardant PCM • Thermal protection • Seawater desalination
Metal aerogels	✓ High thermal conductivity ✓ High electrical conductivity ✗ Relatively high-cost ✗ Harsh manufacturing conditions	• Solar-thermal	• Future direction: Electromagnetic shielding
BN aerogels	✓ High thermal conductivity ✓ Excellent electrical insulation ✓ Good antioxidative abilities ✗ Difficulty of preparation ✗ Poor water dispersity	• Solar-thermal	• Thermal protection for electronic equipment
MXene aerogels	✓ High thermal conductivity ✓ Broad light absorption ✓ High photothermal conversion capacity ✓ High affinity ✗ Difficulty of preparation ✗ Water solution instability ✗ Costly ✗ Low production rate	• Solar-thermal	• Light-actuated shape memory • Flame-retardant PCM • Future direction: Electromagnetic shielding

Figure 20. Summary of different aerogel-based composite PCMs in terms of their advantages, challenges, energy conversion, and advanced utilizations.

more, magnetic−thermal and acoustic−thermal conversion and storage are achieved by introducing magnetic particles into the carbon aerogels. (4) To better accommodate electronic devices and wearable thermal management, the flexibility of PCMs is a key feature. For example, graphene and BN aerogel-based composite PCMs can be designed as flexible phase change films. Attractively, highly flexible cellulose and polymer aerogel-based composite PCMs also exhibit shape memory function due to their excellent mechanical properties and flexibility, which are expected to be used for intelligent grippers. (5) Phase change aerogels can be made into different dimensions. Shaping phase change aerogels into 1D fibers can facilitate the design and manufacturing of smart thermoregulating textiles. Shaping phase change aerogels into 2D films may be accompanied by more attractive features (e.g., low area density and superior flexibility) (Figure 20).

Despite the recent advances in aerogel-based composite PCMs for thermal energy storage, heat transfer, energy conversion, thermal management, and advanced multifunctional applications, there are still several issues that need to be further studied and addressed.

(1) The world of aerogels is exciting and fascinating. Although BN, metal, and MXene aerogels have been applied to encapsulate PCMs, there are relatively few studies, deserving

more systematic research in the future. Attempts should be made to exploit more interesting properties of aerogel-based composite PCMs by combining the properties of aerogels. (2) It is worth exploring how aerogels can bring more advanced functions to PCMs, such as BN aerogels and MXene aerogels. (3) Although PCMs can harvest thermal energy from solar energy and the efficiency of energy conversion has been greatly improved, there is a lack of practical industrial application strategies. In the future, an implementable strategy needs to be developed for practical and commercially viable large-scale applications considering the technoeconomic benefits. (4) The electric–thermal conversion efficiency of composite PCMs is still low and needs to be improved further. Metal aerogels possess high electrical conductivity, but relatively little research has been done on their energy conversion pathways, which can be tapped for application in electrothermal conversion. (5) Magnetic–thermal energy conversion is still in its infancy, and much further research is needed. (6) Thermoelectric conversion technology, as a green energy conversion technology, can realize the direct conversion from thermal energy to electric energy, which is highly valued by the country and researchers. Although solar-electric and heat-electric conversion routes have been described in articles, the development of high-performance composite PCMs for thermoelectric conversion is still imminent. (7) High-enthalpy lightweight composite PCMs are worth investigating for thermal energy storage. It is possible to take advantage of aerogels to obtain composite PCMs with high energy density by regulating the structure and properties of aerogels, which is worthy of further development, while the combination of sensible and latent heat can also be considered. (8) Most aerogel-based composite PCMs are 3D monolithic blocks or 0D microspheres. More strategies need to shape phase change aerogels into 1D fibers or 2D films, which leads to more attractive properties for thermal management systems of microelectronic devices, wearable thermal management, and shape memory composites. (9) At present, the utilization of advanced functions of PCMs is still in the initial stages. Researchers should deeply grasp the inherent properties of PCMs and explore the applications of PCMs in advanced functions, not limited to energy storage applications of PCMs. For example, real-time optical communication using the real-time evolution of optical transparency during crystallization. Specifically, materials with a change in optical transparency through melting/crystallization should be designed and prepared. The infrared signals of composite PCMs during heating and subsequent cooling were detected to convey specific information through the dynamic evolution of phase change enthalpy. (10) Currently, the preparation methods of composite PCMs are relatively traditional and require bold innovation, such as combining advanced 3D printing technology.

AUTHOR INFORMATION

Corresponding Authors

Xiao Chen − *Institute of Advanced Materials, Beijing Normal University, Beijing 100875, P.R. China;* orcid.org/0000-0001-6062-5596; Email: xiaochen@bnu.edu.cn

Ge Wang − *Beijing Advanced Innovation Center for Materials Genome Engineering, Beijing Key Laboratory of Function Materials for Molecule & Structure Construction, School of Materials Science and Engineering, University of Science and Technology Beijing, Beijing 100083, P.R. China; Shunde Graduate School, University of Science and Technology Beijing, Shunde 528399, P.R. China;* orcid.org/0000-0002-4069-4284; Email: gewang@ustb.edu.cn

Authors

Panpan Liu − *Institute of Advanced Materials, Beijing Normal University, Beijing 100875, P.R. China*

Yang Li − *Institute of Advanced Materials, Beijing Normal University, Beijing 100875, P.R. China*

Piao Cheng − *Institute of Advanced Materials, Beijing Normal University, Beijing 100875, P.R. China*

Zhaodi Tang − *Beijing Advanced Innovation Center for Materials Genome Engineering, Beijing Key Laboratory of Function Materials for Molecule & Structure Construction, School of Materials Science and Engineering, University of Science and Technology Beijing, Beijing 100083, P.R. China*

Junjun Lv − *Beijing Advanced Innovation Center for Materials Genome Engineering, Beijing Key Laboratory of Function Materials for Molecule & Structure Construction, School of Materials Science and Engineering, University of Science and Technology Beijing, Beijing 100083, P.R. China*

Waseem Aftab − *Beijing Key Laboratory for Theory and Technology of Advanced Battery Materials, School of Materials Science and Engineering, Peking University, Beijing 100871, P.R. China*

Complete contact information is available at:
https://pubs.acs.org/10.1021/acsnano.2c05067

Notes

The authors declare no competing financial interest.

VOCABULARY

aerogel, an ultralightweight solid material with an 3D porous nanostructured skeleton; phase change material, a material for the storage and release of latent heat during the isothermal phase change process; latent heat, the absorbed or released heat of a material changing one phase to another under isothermal process; thermal conductivity, the transferred heat of a material through a unit of heat transfer surface in unit time and unit temperature gradient; energy conversion, the process of converting energy from one form to another

REFERENCES

(1) Chen, X.; Gao, H.; Tang, Z.; Dong, W.; Li, A.; Wang, G. Optimization Strategies of Composite Phase Change Materials for Thermal Energy Storage, Transfer, Conversion and Utilization. *Energy Environ. Sci.* **2020**, *13* (12), 4498−4535.

(2) Pierre, A. C.; Pajonk, G. M. Chemistry of Aerogels and Their Applications. *Chem. Rev.* **2002**, *102* (11), 4243−4266.

(3) Prakash, S. S.; Brinker, C. J.; Hurd, A. J.; Rao, S. M. Silica Aerogel Films Prepared at Ambient Pressure by Using Surface Derivatization to Induce Reversible Drying Shrinkage. *Nature* **1995**, *374* (6521), 439−443.

(4) Xia, D.; Li, H.; Mannering, J.; Huang, P.; Zheng, X.; Kulak, A.; Baker, D.; Iruretagoyena, D.; Menzel, R. Electrically Heatable Graphene Aerogels as Nanoparticle Supports in Adsorptive Desulfurization and High-Pressure Co_2 Capture. *Adv. Funct. Mater.* **2020**, *30* (40), 2002788.

(5) Xu, X.; Zhang, Q.; Hao, M.; Hu, Y.; Lin, Z.; Peng, L.; Wang, T.; Ren, X.; Wang, C.; Zhao, Z.; et al. Double-Negative-Index Ceramic Aerogels for Thermal Superinsulation. *Science* **2019**, *363* (6428), 723−727.

(6) Yang, J.; Li, Y.; Zheng, Y.; Xu, Y.; Zheng, Z.; Chen, X.; Liu, W. Versatile Aerogels for Sensors. *Small* **2019**, *15* (41), 1902826.

(7) Im, H.; Kim, T.; Song, H.; Choi, J.; Park, J. S.; Ovalle-Robles, R.; Yang, H. D.; Kihm, K. D.; Baughman, R. H.; Lee, H. H.; et al. High-Efficiency Electrochemical Thermal Energy Harvester Using Carbon Nanotube Aerogel Sheet Electrodes. *Nat. Commun.* **2016**, *7* (1), 10600.

(8) Liu, C.; Zhang, J.; Liu, J.; Tan, Z.; Cao, Y.; Li, X.; Rao, Z. Highly Efficient Thermal Energy Storage Using a Hybrid Hypercrosslinked Polymer. *Angew. Chem., Int. Ed.* **2021**, *133* (25), 14097−14106.

(9) Cottrill, A. L.; Liu, A. T.; Kunai, Y.; Koman, V. B.; Kaplan, A.; Mahajan, S. G.; Liu, P.; Toland, A. R.; Strano, M. S. Ultra-High Thermal Effusivity Materials for Resonant Ambient Thermal Energy Harvesting. *Nat. Commun.* **2018**, *9* (1), 664.

(10) Chatterjee, R.; Beysens, D.; Anand, S. Delaying Ice and Frost Formation Using Phase-Switching Liquids. *Adv. Mater.* **2019**, *31* (17), 1807812.

(11) Zhang, S.; Li, Q.; Yang, N.; Shi, Y.; Ge, W.; Wang, W.; Huang, W.; Song, X.; Dong, X. Phase-Change Materials Based Nanoparticles for Controlled Hypoxia Modulation and Enhanced Phototherapy. *Adv. Funct. Mater.* **2019**, *29* (49), 1906805.

(12) Tang, J.; Chen, X.; Zhang, L.; Yang, M.; Wang, P.; Dong, W.; Wang, G.; Yu, F.; Tao, J. Alkylated Meso-Macroporous Metal-Organic Framework Hollow Tubes as Nanocontainers of Octadecane for Energy Storage and Thermal Regulation. *Small* **2018**, *14* (35), 1801970.

(13) Chen, X.; Gao, H.; Yang, M.; Dong, W.; Huang, X.; Li, A.; Dong, C.; Wang, G. Highly Graphitized 3d Network Carbon for Shape-Stabilized Composite PCMs with Superior Thermal Energy Harvesting. *Nano Energy* **2018**, *49*, 86−94.

(14) Ji, H.; Sellan, D. P.; Pettes, M. T.; Kong, X.; Ji, J.; Shi, L.; Ruoff, R. S. Enhanced Thermal Conductivity of Phase Change Materials with Ultrathin-Graphite Foams for Thermal Energy Storage. *Energy Environ. Sci.* **2014**, *7* (3), 1185−1192.

(15) Aftab, W.; Huang, X.; Wu, W.; Liang, Z.; Mahmood, A.; Zou, R. Nanoconfined Phase Change Materials for Thermal Energy Applications. *Energy Environ. Sci.* **2018**, *11* (6), 1392−1424.

(16) Sheng, Z.; Ding, Y.; Li, G.; Fu, C.; Hou, Y.; Lyu, J.; Zhang, K.; Zhang, X. Solid-Liquid Host-Guest Composites: The Marriage of Porous Solids and Functional Liquids. *Adv. Mater.* **2021**, *33*, 2104851.

(17) Qiu, J.; Fan, X.; Shi, Y.; Zhang, S.; Jin, X.; Wang, W.; Tang, B. PEG/3D Graphene Oxide Network Form-Stable Phase Change Materials with Ultrahigh Filler Content. *J. Mater. Chem. A* **2019**, *7* (37), 21371−21377.

(18) Hu, N.; Li, Z.-R.; Xu, Z.-W.; Fan, L.-W. Rapid Charging for Latent Heat Thermal Energy Storage: A State-of-the-Art Review of Close-Contact Melting. *Renew. Sust. Energy Rev.* **2022**, *155*, 111918.

(19) Wu, S.; Li, T.; Tong, Z.; Chao, J.; Zhai, T.; Xu, J.; Yan, T.; Wu, M.; Xu, Z.; Bao, H.; et al. High-Performance Thermally Conductive Phase Change Composites by Large-Size Oriented Graphite Sheets for Scalable Thermal Energy Harvesting. *Adv. Mater.* **2019**, *31* (49), 1905099.

(20) Cheng, P.; Chen, X.; Gao, H.; Zhang, X.; Tang, Z.; Li, A.; Wang, G. Different Dimensional Nanoadditives for Thermal Conductivity Enhancement of Phase Change Materials: Fundamentals and Applications. *Nano Energy* **2021**, *85*, 105948.

(21) Wu, S.; Yan, T.; Kuai, Z.; Pan, W. Thermal Conductivity Enhancement on Phase Change Materials for Thermal Energy Storage: A Review. *Energy Storage Mater.* **2020**, *25*, 251−295.

(22) Li, A.; Dong, C.; Dong, W.; Atinafu, D. G.; Gao, H.; Chen, X.; Wang, G. Hierarchical 3D Reduced Graphene Porous-Carbon-Based PCMs for Superior Thermal Energy Storage Performance. *ACS Appl. Mater. Interfaces* **2018**, *10* (38), 32093−32101.

(23) Yuan, K.; Shi, J.; Aftab, W.; Qin, M.; Usman, A.; Zhou, F.; Lv, Y.; Gao, S.; Zou, R. Engineering the Thermal Conductivity of Functional Phase-Change Materials for Heat Energy Conversion, Storage, and Utilization. *Adv. Funct. Mater.* **2020**, *30* (8), 1904228.

(24) Wang, C.; Dong, W.; Li, A.; Atinafu, D. G.; Wang, G.; Lu, Y. The Reinforced Photothermal Effect of Conjugated Dye/Graphene Oxide-Based Phase Change Materials: Fluorescence Resonance Energy Transfer and Applications in Solar-Thermal Energy Storage. *Chem. Eng. J.* **2022**, *428*, 130605.

(25) Li, Y.; Li, Y.; Huang, X.; Zheng, H.; Lu, G.; Xi, Z.; Wang, G. Graphene-CoO/PEG Composite Phase Change Materials with Enhanced Solar-to-Thermal Energy Conversion and Storage Capacity. *Compos. Sci. Technol.* **2020**, *195*, 108197.

(26) Tang, Z.; Gao, H.; Chen, X.; Zhang, Y.; Li, A.; Wang, G. Advanced Multifunctional Composite Phase Change Materials Based on Photo-Responsive Materials. *Nano Energy* **2021**, *80*, 105454.

(27) Chen, X.; Tang, Z.; Gao, H.; Chen, S.; Wang, G. Phase Change Materials for Electro-Thermal Conversion and Storage: From Fundamental Understanding to Engineering Design. *iScience* **2020**, *23* (6), 101208.

(28) Wang, W.; Tang, B.; Ju, B.; Gao, Z.; Xiu, J.; Zhang, S. Fe_3O_4-Functionalized Graphene Nanosheet Embedded Phase Change Material Composites: Efficient Magnetic-and Sunlight-Driven Energy Conversion and Storage. *J. Mater. Chem. A* **2017**, *5* (3), 958−968.

(29) Wang, W.; Umair, M. M.; Qiu, J.; Fan, X.; Cui, Z.; Yao, Y.; Tang, B. Electromagnetic and Solar Energy Conversion and Storage Based on Fe_3O_4-Functionalised Graphene/Phase Change Material Nanocomposites. *Energy Convers. Manage.* **2019**, *196*, 1299−1305.

(30) Tao, P.; Chang, C.; Tong, Z.; Bao, H.; Song, C.; Wu, J.; Shang, W.; Deng, T. Magnetically-Accelerated Large-Capacity Solar-Thermal Energy Storage within High-Temperature Phase-Change Materials. *Energy Environ. Sci.* **2019**, *12* (5), 1613−1621.

(31) Shi, J.; Qin, M.; Aftab, W.; Zou, R. Flexible Phase Change Materials for Thermal Energy Storage. *Energy Storage Mater.* **2021**, *41*, 321−342.

(32) Shi, T.; Zheng, Z.; Liu, H.; Wu, D.; Wang, X. Flexible and Foldable Composite Films Based on Polyimide/Phosphorene Hybrid Aerogel and Phase Change Material for Infrared Stealth and Thermal Camouflage. *Compos. Sci. Technol.* **2022**, *217*, 109127.

(33) Cai, Y.; Wei, Q.; Huang, F.; Lin, S.; Chen, F.; Gao, W. Thermal Stability, Latent Heat and Flame Retardant Properties of the Thermal Energy Storage Phase Change Materials Based on Paraffin/High Density Polyethylene Composites. *Renew. Energy* **2009**, *34* (10), 2117−2123.

(34) Pakdel, E.; Naebe, M.; Sun, L.; Wang, X. Advanced Functional Fibrous Materials for Enhanced Thermoregulating Performance. *ACS Appl. Mater. Interfaces* **2019**, *11* (14), 13039−13057.

(35) Tao, Z.; Chen, X.; Yang, M.; Xu, X.; Sun, Y.; Li, Y.; Wang, J.; Wang, G. Three-Dimensional RGO@Sponge Framework/Paraffin Wax Composite Shape-Stabilized Phase Change Materials for Solar-Thermal Energy Conversion and Storage. *Sol. Energy Mater. Sol. Cells* **2020**, *215*, 110600.

(36) Woods, J.; Mahvi, A.; Goyal, A.; Kozubal, E.; Odukomaiya, A.; Jackson, R. Rate Capability and Ragone Plots for Phase Change Thermal Energy Storage. *Nat. Energy* **2021**, *6* (3), 295−302.

(37) Sharma, A.; Tyagi, V. V.; Chen, C.; Buddhi, D. Review on Thermal Energy Storage with Phase Change Materials and Applications. *Renew. Sust. Energy Rev.* **2009**, *13* (2), 318−345.

(38) Aftab, W.; Usman, A.; Shi, J.; Yuan, K.; Qin, M.; Zou, R. Phase Change Material-Integrated Latent Heat Storage Systems for Sustainable Energy Solutions. *Energy Environ. Sci.* **2021**, *14* (8), 4268−4291.

(39) Yuan, Y.; Zhang, N.; Tao, W.; Cao, X.; He, Y. Fatty Acids as Phase Change Materials: A Review. *Renew. Sust. Energy Rev.* **2014**, *29*, 482−498.

(40) Sharma, R.; Ganesan, P.; Tyagi, V.; Metselaar, H.; Sandaran, S. Developments in Organic Solid-Liquid Phase Change Materials and Their Applications in Thermal Energy Storage. *Energy Convers. Manage.* **2015**, *95*, 193−228.

(41) Pielichowska, K.; Pielichowski, K. Phase Change Materials for Thermal Energy Storage. *Prog. Mater. Sci.* **2014**, *65*, 67−123.

(42) Chen, X.; Cheng, P.; Tang, Z.; Xu, X.; Gao, H.; Wang, G. Carbon-Based Composite Phase Change Materials for Thermal Energy Storage, Transfer, and Conversion. *Adv. Sci.* **2021**, *8* (9), 2001274.

(43) Chen, X.; Gao, H.; Tang, Z.; Wang, G. Metal-Organic Framework-Based Phase Change Materials for Thermal Energy Storage. *Cell Rep. Phys. Sci.* **2020**, *1*, 100218.

(44) Sun, M.-H.; Huang, S.-Z.; Chen, L.-H.; Li, Y.; Yang, X.-Y.; Yuan, Z.-Y.; Su, B.-L. Applications of Hierarchically Structured Porous Materials from Energy Storage and Conversion, Catalysis, Photocatalysis, Adsorption, Separation, and Sensing to Biomedicine. *Chem. Soc. Rev.* **2016**, *45* (12), 3479−3563.

(45) Umair, M. M.; Zhang, Y.; Iqbal, K.; Zhang, S.; Tang, B. Novel Strategies and Supporting Materials Applied to Shape-Stabilize Organic Phase Change Materials for Thermal Energy Storage-a Review. *Appl. Energy* **2019**, *235*, 846−873.

(46) Wu, M.; Wu, S.; Cai, Y.; Wang, R.; Li, T. Form-Stable Phase Change Composites: Preparation, Performance, and Applications for Thermal Energy Conversion, Storage and Management. *Energy Storage Mater.* **2021**, *42*, 380−417.

(47) Gao, H.; Wang, J.; Chen, X.; Wang, G.; Huang, X.; Li, A.; Dong, W. Nanoconfinement Effects on Thermal Properties of Nanoporous Shape-Stabilized Composite Pcms: A Review. *Nano Energy* **2018**, *53*, 769−797.

(48) Yang, Z.; Jia, S.; Niu, Y.; Lv, X.; Fu, H.; Zhang, Y.; Liu, D.; Wang, B.; Li, Q. Bean-Pod-Inspired 3D-Printed Phase Change Microlattices for Solar-Thermal Energy Harvesting and Storage. *Small* **2021**, *17*, 2101093.

(49) Ma, J.; Ma, T.; Cheng, J.; Zhang, J. 3D Printable, Recyclable and Adjustable Comb/Bottlebrush Phase Change Polysiloxane Networks toward Sustainable Thermal Energy Storage. *Energy Storage. Mater.* **2021**, *39*, 294−304.

(50) Liu, P.; Chen, X.; Wang, G. Advanced 3D-Printed Phase Change Materials. *Matter* **2021**, *4* (11), 3374−3376.

(51) Zhang, Y.; Zhu, G.; Dong, B.; Wang, F.; Tang, J.; Stadler, F. J.; Yang, G.; Hong, S.; Xing, F. Interfacial Jamming Reinforced Pickering Emulgel for Arbitrary Architected Nanocomposite with Connected Nanomaterial Matrix. *Nat. Commun.* **2021**, *12*, 111.

(52) Wei, P.; Cipriani, C. E.; Pentzer, E. B. Thermal Energy Regulation with 3D Printed Polymer-Phase Change Material Composites. *Matter* **2021**, *4* (6), 1975−1989.

(53) Rahmanian, V.; Pirzada, T.; Wang, S.; Khan, S. A. Cellulose-Based Hybrid Aerogels: Strategies toward Design and Functionality. *Adv. Mater.* **2021**, *33*, 2102892.

(54) Kistler, S. S. Coherent Expanded Aerogels and Jellies. *Nature* **1931**, *127* (3211), 741−741.

(55) Pekala, R. Organic Aerogels from the Polycondensation of Resorcinol with Formaldehyde. *J. Mater. Sci.* **1989**, *24* (9), 3221−3227.

(56) Aliev, A. E.; Oh, J.; Kozlov, M. E.; Kuznetsov, A. A.; Fang, S.; Fonseca, A. F.; Ovalle, R.; Lima, M. D.; Haque, M. H.; Gartstein, Y. N.; et al. Giant-Stroke, Superelastic Carbon Nanotube Aerogel Muscles. *Science* **2009**, *323* (5921), 1575−1578.

(57) Nardecchia, S.; Carriazo, D.; Ferrer, M. L.; Gutiérrez, M. C.; del Monte, F. Three Dimensional Macroporous Architectures and Aerogels Built of Carbon Nanotubes and/or Graphene: Synthesis and Applications. *Chem. Soc. Rev.* **2013**, *42* (2), 794−830.

(58) Wu, Z. Y.; Liang, H. W.; Hu, B. C.; Yu, S. H. Emerging Carbon-Nanofiber Aerogels: Chemosynthesis Versus Biosynthesis. *Angew. Chem., Int. Ed.* **2018**, *57* (48), 15646−15662.

(59) Randall, J. P.; Meador, M. A. B.; Jana, S. C. Tailoring Mechanical Properties of Aerogels for Aerospace Applications. *ACS Appl. Mater. Interfaces* **2011**, *3* (3), 613−626.

(60) Lee, J.-H.; Park, S.-J. Recent Advances in Preparations and Applications of Carbon Aerogels: A Review. *Carbon* **2020**, *163*, 1−18.

(61) Wang, T.; Long, M.-C.; Zhao, H.-B.; Liu, B.-W.; Shi, H.-G.; An, W.-L.; Li, S.-L.; Xu, S.-M.; Wang, Y.-Z. An Ultralow-Temperature Superelastic Polymer Aerogel with High Strength as a Great Thermal Insulator under Extreme Conditions. *J. Mater. Chem. A* **2020**, *8* (36), 18698−18706.

(62) Bigall, N. C.; Herrmann, A. K.; Vogel, M.; Rose, M.; Simon, P.; Carrillo-Cabrera, W.; Dorfs, D.; Kaskel, S.; Gaponik, N.; Eychmüller, A. Hydrogels and Aerogels from Noble Metal Nanoparticles. *Angew. Chem., Int. Ed.* **2009**, *48* (51), 9731−9734.

(63) Du, R.; Fan, X.; Jin, X.; Hübner, R.; Hu, Y.; Eychmüller, A. Emerging Noble Metal Aerogels: State of the Art and a Look Forward. *Matter* **2019**, *1* (1), 39−56.

(64) Bi, H.; Yin, Z.; Cao, X.; Xie, X.; Tan, C.; Huang, X.; Chen, B.; Chen, F.; Yang, Q.; Bu, X.; et al. Carbon Fiber Aerogel Made from Raw Cotton: A Novel, Efficient and Recyclable Sorbent for Oils and Organic Solvents. *Adv. Mater.* **2013**, *25* (41), 5916−5921.

(65) Gu, P.; Liu, W.; Hou, Q.; Ni, Y. Lignocellulose-Derived Hydrogel/Aerogel-Based Flexible Quasi-Solid-State Supercapacitors with High-Performance: A Review. *J. Mater. Chem. A* **2021**, *9* (25), 14233−14264.

(66) Wang, J.; Liu, D.; Li, Q.; Chen, C.; Chen, Z.; Song, P.; Hao, J.; Li, Y.; Fakhrhoseini, S.; Naebe, M.; et al. Lightweight, Superelastic yet Thermoconductive Boron Nitride Nanocomposite Aerogel for Thermal Energy Regulation. *ACS Nano* **2019**, *13* (7), 7860−7870.

(67) Zhang, X.; Lv, R.; Wang, A.; Guo, W.; Liu, X.; Luo, J. Mxene Aerogel Scaffolds for High-Rate Lithium Metal Anodes. *Angew. Chem., Int. Ed.* **2018**, *130* (46), 15248−15253.

(68) Du, A.; Zhou, B.; Zhang, Z.; Shen, J. A Special Material or a New State of Matter: A Review and Reconsideration of the Aerogel. *Materials* **2013**, *6* (3), 941−968.

(69) Roig, A.; Molins, E.; Rodríguez, E.; Martínez, S.; Moreno-Mañas, M.; Vallribera, A. Superhydrophobic Silica Aerogels by Fluorination at the Gel Stage. *Chem. Commun.* **2004**, No. 20, 2316−2317.

(70) Zhu, C.; Han, T. Y.-J.; Duoss, E. B.; Golobic, A. M.; Kuntz, J. D.; Spadaccini, C. M.; Worsley, M. A. Highly Compressible 3D Periodic Graphene Aerogel Microlattices. *Nat. Commun.* **2015**, *6*, 6962.

(71) Chen, Y.; Zhang, L.; Yang, Y.; Pang, B.; Xu, W.; Duan, G.; Jiang, S.; Zhang, K. Recent Progress on Nanocellulose Aerogels: Preparation, Modification, Composite Fabrication, Applications. *Adv. Mater.* **2021**, *33* (11), 2005569.

(72) Gao, W.; Wen, D. Recent Advances of Noble Metal Aerogels in Biosensing. *View* **2021**, *2*, 20200124.

(73) Feng, J.; Su, B.-L.; Xia, H.; Zhao, S.; Gao, C.; Wang, L.; Ogbeide, O.; Feng, J.; Hasan, T. Printed Aerogels: Chemistry, Processing, and Applications. *Chem. Soc. Rev.* **2021**, *50* (6), 3842−3888.

(74) Tetik, H.; Wang, Y.; Sun, X.; Cao, D.; Shah, N.; Zhu, H.; Qian, F.; Lin, D. Additive Manufacturing of 3D Aerogels and Porous Scaffolds: A Review. *Adv. Funct. Mater.* **2021**, *31* (45), 2103410.

(75) Tetik, H.; Orangi, J.; Yang, G.; Zhao, K.; Mujib, S. B.; Singh, G.; Beidaghi, M.; Lin, D. 3D Printed MXene Aerogels with Truly 3D Macrostructure and Highly Engineered Microstructure for Enhanced Electrical and Electrochemical Performance. *Adv. Mater.* **2021**, *34* (2), 2104980.

(76) Zhao, S.; Siqueira, G.; Drdova, S.; Norris, D.; Ubert, C.; Bonnin, A.; Galmarini, S.; Ganobjak, M.; Pan, Z.; Brunner, S.; et al. Additive Manufacturing of Silica Aerogels. *Nature* **2020**, *584* (7821), 387−392.

(77) Howe, N.; Bundell, S. 3D Printing Some of the World's Lightest Materials. *Nature* **2020**, DOI: 10.1038/d41586-020-02448-5.

(78) Liu, R.-L.; Ji, W.-J.; He, T.; Zhang, Z.-Q.; Zhang, J.; Dang, F.-Q. Fabrication of Nitrogen-Doped Hierarchically Porous Carbons through a Hybrid Dual-Template Route for CO_2 Capture and Haemoperfusion. *Carbon* **2014**, *76*, 84−95.

(79) Fu, X.; Choi, J.-Y.; Zamani, P.; Jiang, G.; Hoque, M. A.; Hassan, F. M.; Chen, Z. Co-N Decorated Hierarchically Porous Graphene Aerogel for Efficient Oxygen Reduction Reaction in Acid. *ACS Appl. Mater. Interfaces* **2016**, *8* (10), 6488−6495.

(80) Huang, X.; Chen, X.; Li, A.; Atinafu, D.; Gao, H.; Dong, W.; Wang, G. Shape-Stabilized Phase Change Materials Based on Porous Supports for Thermal Energy Storage Applications. *Chem. Eng. J.* **2019**, *356*, 641−661.

(81) Li, Y.; Huang, X.; Hai, G.; Lv, J.; Tao, Z.; Wang, G. Crystallization of C18 in Mesoporous Silica: Effect of Surface Functionalization and Nanoconfinement. *Chem. Eng. J.* **2022**, *428*, 131075.

(82) Lu, X.; Arduini-Schuster, M.; Kuhn, J.; Nilsson, O.; Fricke, J.; Pekala, R. Thermal Conductivity of Monolithic Organic Aerogels. *Science* **1992**, *255* (5047), 971−972.

(83) Baetens, R.; Jelle, B. P.; Gustavsen, A. Aerogel Insulation for Building Applications: A State-of-the-Art Review. *Energy Build.* **2011**, *43* (4), 761−769.

(84) Xie, Y.; Xu, S.; Xu, Z.; Wu, H.; Deng, C.; Wang, X. Interface-Mediated Extremely Low Thermal Conductivity of Graphene Aerogel. *Carbon* **2016**, *98*, 381−390.

(85) Wang, B.; Li, G.; Xu, L.; Liao, J.; Zhang, X. Nanoporous Boron Nitride Aerogel Film and Its Smart Composite with Phase Change Materials. *ACS Nano* **2020**, *14* (12), 16590−16599.

(86) Zhuo, H.; Hu, Y.; Tong, X.; Chen, Z.; Zhong, L.; Lai, H.; Liu, L.; Jing, S.; Liu, Q.; Liu, C.; et al. A Supercompressible, Elastic, and Bendable Carbon Aerogel with Ultrasensitive Detection Limits for Compression Strain, Pressure, and Bending Angle. *Adv. Mater.* **2018**, *30* (18), 1706705.

(87) Peng, X.; Wu, K.; Hu, Y.; Zhuo, H.; Chen, Z.; Jing, S.; Liu, Q.; Liu, C.; Zhong, L. A Mechanically Strong and Sensitive CNT/RGO-CNF Carbon Aerogel for Piezoresistive Sensors. *J. Mater. Chem. A* **2018**, *6* (46), 23550−23559.

(88) Li, J.; Li, J.; Meng, H.; Xie, S.; Zhang, B.; Li, L.; Ma, H.; Zhang, J.; Yu, M. Ultra-Light, Compressible and Fire-Resistant Graphene Aerogel as a Highly Efficient and Recyclable Absorbent for Organic Liquids. *J. Mater. Chem. A* **2014**, *2* (9), 2934−2941.

(89) Mu, B.; Li, M. Fabrication and Thermal Properties of Tetradecanol/Graphene Aerogel Form-Stable Composite Phase Change Materials. *Sci. Rep.* **2018**, *8*, 8878.

(90) Worsley, M. A.; Pauzauskie, P. J.; Olson, T. Y.; Biener, J.; Satcher, J. H., Jr; Baumann, T. F. Synthesis of Graphene Aerogel with High Electrical Conductivity. *J. Am. Chem. Soc.* **2010**, *132* (40), 14067−14069.

(91) Xia, D.; Xu, Y.; Mannering, J.; Ma, X.; Ismail, M.; Borman, D.; Baker, D. L.; Pourkashanian, M.; Menzel, R. Tuning the Electrical and Solar Thermal Heating Efficiencies of Nanocarbon Aerogels. *Chem. Mater.* **2021**, *33* (1), 392−402.

(92) Fu, Y.; Wang, G.; Mei, T.; Li, J.; Wang, J.; Wang, X. Accessible Graphene Aerogel for Efficiently Harvesting Solar Energy. *ACS Sustain. Chem. Eng.* **2017**, *5* (6), 4665−4671.

(93) Mao, J.; Iocozzia, J.; Huang, J.; Meng, K.; Lai, Y.; Lin, Z. Graphene Aerogels for Efficient Energy Storage and Conversion. *Energy Environ. Sci.* **2018**, *11* (4), 772−799.

(94) Li, C.; Yang, J.; Pachfule, P.; Li, S.; Ye, M.-Y.; Schmidt, J.; Thomas, A. Ultralight Covalent Organic Framework/Graphene Aerogels with Hierarchical Porosity. *Nat. Commun.* **2020**, *11*, 4712.

(95) Xia, Y.; Cui, W.; Zhang, H.; Xu, F.; Sun, L.; Zou, Y.; Chu, H.; Yan, E. Synthesis of Three-Dimensional Graphene Aerogel Encapsulated N-Octadecane for Enhancing Phase-Change Behavior and Thermal Conductivity. *J. Mater. Chem. A* **2017**, *5* (29), 15191−15199.

(96) Ye, S.; Zhang, Q.; Hu, D.; Feng, J. Core-Shell-Like Structured Graphene Aerogel Encapsulating Paraffin: Shape-Stable Phase Change Material for Thermal Energy Storage. *J. Mater. Chem. A* **2015**, *3* (7), 4018−4025.

(97) Cheng, P.; Gao, H.; Chen, X.; Chen, Y.; Han, M.; Xing, L.; Liu, P.; Wang, G. Flexible Monolithic Phase Change Material Based on Carbon Nanotubes/Chitosan/Poly (Vinyl Alcohol). *Chem. Eng. J.* **2020**, *397*, 125330.

(98) Sun, H.; Xu, Z.; Gao, C. Multifunctional, Ultra-Flyweight, Synergistically Assembled Carbon Aerogels. *Adv. Mater.* **2013**, *25* (18), 2554−2560.

(99) Zhao, J.; Luo, W.; Kim, J.-K.; Yang, J. Graphene Oxide Aerogel Beads Filled with Phase Change Material for Latent Heat Storage and Release. *ACS Appl. Energy Mater.* **2019**, *2* (5), 3657−3664.

(100) Wei, D.; Wu, C.; Jiang, G.; Sheng, X.; Xie, Y. Lignin-Assisted Construction of Well-Defined 3D Graphene Aerogel/PEG Form-Stable Phase Change Composites Towards Efficient Solar Thermal Energy Storage. *Sol. Energy Mater. Sol. Cells* **2021**, *224*, 111013.

(101) Li, M.; Mu, B. Effect of Different Dimensional Carbon Materials on the Properties and Application of Phase Change Materials: A Review. *Appl. Energy* **2019**, *242*, 695−715.

(102) Li, A.; Wang, J.; Dong, C.; Dong, W.; Atinafu, D. G.; Chen, X.; Gao, H.; Wang, G. Core-Sheath Structural Carbon Materials for Integrated Enhancement of Thermal Conductivity and Capacity. *Appl. Energy* **2018**, *217*, 369−376.

(103) Yavari, F.; Fard, H. R.; Pashayi, K.; Rafiee, M. A.; Zamiri, A.; Yu, Z.; Ozisik, R.; Borca-Tasciuc, T.; Koratkar, N. Enhanced Thermal Conductivity in a Nanostructured Phase Change Composite Due to Low Concentration Graphene Additives. *J. Phys. Chem. C* **2011**, *115* (17), 8753−8758.

(104) Su, M.; Han, G.; Gao, J.; Feng, Y.; He, C.; Ma, J.; Liu, C.; Shen, C. Carbon Welding on Graphene Skeleton for Phase Change Composites with High Thermal Conductivity for Solar-to-Heat Conversion. *Chem. Eng. J.* **2022**, *427*, 131665.

(105) Zhong, Y.; Zhou, M.; Huang, F.; Lin, T.; Wan, D. Effect of Graphene Aerogel on Thermal Behavior of Phase Change Materials for Thermal Management. *Sol. Energy Mater. Sol. Cells* **2013**, *113*, 195−200.

(106) Mu, B.; Li, M. Synthesis of Novel Form-Stable Composite Phase Change Materials with Modified Graphene Aerogel for Solar Energy Conversion and Storage. *Sol. Energy Mater. Sol. Cells* **2019**, *191*, 466−475.

(107) Yang, J.; Li, X.; Han, S.; Yang, R.; Min, P.; Yu, Z.-Z. High-Quality Graphene Aerogels for Thermally Conductive Phase Change Composites with Excellent Shape Stability. *J. Mater. Chem. A* **2018**, *6* (14), 5880−5886.

(108) Zhang, G.; Koman, V. B.; Shikdar, T.; Oliver, R. J.; Perez-Lodeiro, N.; Strano, M. S. High Thermal Effusivity Nanocarbon Materials for Resonant Thermal Energy Harvesting. *Small* **2021**, *17*, 2006752.

(109) Burger, N.; Laachachi, A.; Ferriol, M.; Lutz, M.; Toniazzo, V.; Ruch, D. Review of Thermal Conductivity in Composites: Mechanisms, Parameters and Theory. *Prog. Polym. Sci.* **2016**, *61*, 1−28.

(110) Liang, K.; Shi, L.; Zhang, J.; Cheng, J.; Wang, X. Fabrication of Shape-Stable Composite Phase Change Materials Based on Lauric Acid and Graphene/Graphene Oxide Complex Aerogels for Enhancement of Thermal Energy Storage and Electrical Conduction. *Thermochim. Acta* **2018**, *664*, 1−15.

(111) Yang, J.; Qi, G.-Q.; Liu, Y.; Bao, R.-Y.; Liu, Z.-Y.; Yang, W.; Xie, B.-H.; Yang, M.-B. Hybrid Graphene Aerogels/Phase Change Material Composites: Thermal Conductivity, Shape-Stabilization and Light-to-Thermal Energy Storage. *Carbon* **2016**, *100*, 693−702.

(112) Yang, J.; Li, X.; Han, S.; Zhang, Y.; Min, P.; Koratkar, N.; Yu, Z.-Z. Air-Dried, High-Density Graphene Hybrid Aerogels for Phase Change Composites with Exceptional Thermal Conductivity and Shape Stability. *J. Mater. Chem. A* **2016**, *4* (46), 18067−18074.

(113) Liu, P.; An, F.; Lu, X.; Li, X.; Min, P.; Shu, C.; Li, W.; Yu, Z.-Z. Highly Thermally Conductive Phase Change Composites with Excellent Solar-Thermal Conversion Efficiency and Satisfactory Shape Stability on the Basis of High-Quality Graphene-Based Aerogels. *Compos. Sci. Technol.* **2021**, *201*, 108492.

(114) Yang, J.; Qi, G.-Q.; Bao, R.-Y.; Yi, K.; Li, M.; Peng, L.; Cai, Z.; Yang, M.-B.; Wei, D.; Yang, W. Hybridizing Graphene Aerogel into Three-Dimensional Graphene Foam for High-Performance Composite Phase Change Materials. *Energy Storage Mater.* **2018**, *13*, 88−95.

(115) Han, Z.; Fina, A. Thermal Conductivity of Carbon Nanotubes and Their Polymer Nanocomposites: A Review. *Prog. Polym. Sci.* **2011**, *36* (7), 914−944.

(116) Cao, Q.; He, F.; Li, Y.; He, Z.; Fan, J.; Wang, R.; Hu, W.; Zhang, K.; Yang, W. Graphene-Carbon Nanotube Hybrid Aerogel/ Polyethylene Glycol Phase Change Composite for Thermal Management. *Fuller. Nanotub. Car. N.* **2020**, *28* (8), 656−662.

(117) Chen, G.; Su, Y.; Jiang, D.; Pan, L.; Li, S. An Experimental and Numerical Investigation on a Paraffin Wax/Graphene Oxide/Carbon Nanotubes Composite Material for Solar Thermal Storage Applications. *Appl. Energy* **2020**, *264*, 114786.

(118) Cao, Q.; He, F.; Xie, C.; Fan, J.; Wu, J.; Zhang, K.; Yang, Z.; Yang, W. Paraffin-Based Shape-Stable Phase Change Materials with Graphene/Carbon Nanotube Three-Dimensional Network Structure. *Fuller. Nanotub. Car. N.* **2019**, *27* (6), 492−497.

(119) Li, T.; Wu, M.; Wu, S.; Xiang, S.; Xu, J.; Chao, J.; Yan, T.; Deng, T.; Wang, R. Highly Conductive Phase Change Composites Enabled by Vertically-Aligned Reticulated Graphite Nanoplatelets for High-Temperature Solar Photo/Electro-Thermal Energy Conversion, Harvesting and Storage. *Nano Energy* **2021**, *89*, 106338.

(120) Ren, W.; Cao, L.; Zhang, D. Composite Phase Change Material Based on Reduced Graphene Oxide/Expanded Graphite Aerogel with Improved Thermal Properties and Shape-Stability. *Int. J. Energy Res.* **2020**, *44* (1), 242−256.

(121) Deng, Y.; Li, J.; Qian, T.; Guan, W.; Li, Y.; Yin, X. Thermal Conductivity Enhancement of Polyethylene Glycol/Expanded Vermiculite Shape-Stabilized Composite Phase Change Materials with Silver Nanowire for Thermal Energy Storage. *Chem. Eng. J.* **2016**, *295*, 427−435.

(122) Liu, L.; Zheng, K.; Yan, Y.; Cai, Z.; Lin, S.; Hu, X. Graphene Aerogels Enhanced Phase Change Materials Prepared by One-Pot Method with High Thermal Conductivity and Large Latent Energy Storage. *Sol. Energy Mater. Sol. Cells* **2018**, *185*, 487−493.

(123) Renteria, J. D.; Ramirez, S.; Malekpour, H.; Alonso, B.; Centeno, A.; Zurutuza, A.; Cocemasov, A. I.; Nika, D. L.; Balandin, A. A. Strongly Anisotropic Thermal Conductivity of Free-Standing Reduced Graphene Oxide Films Annealed at High Temperature. *Adv. Funct. Mater.* **2015**, *25* (29), 4664−4672.

(124) Huang, J.; Zhang, B.; Valdiserri, P.; Huang, X.; Yin, G.; Cui, Y. Thermal Flow Self-Assembled Anisotropic Chemically Derived Graphene Aerogels and Their Thermal Conductivity Enhancement. *Nanomaterials* **2019**, *9* (9), 1226.

(125) Min, P.; Liu, J.; Li, X.; An, F.; Liu, P.; Shen, Y.; Koratkar, N.; Yu, Z. Z. Thermally Conductive Phase Change Composites Featuring Anisotropic Graphene Aerogels for Real-Time and Fast-Charging Solar-Thermal Energy Conversion. *Adv. Funct. Mater.* **2018**, *28* (51), 1805365.

(126) Li, G.; Zhang, X.; Wang, J.; Fang, J. From Anisotropic Graphene Aerogels to Electron-and Photo-Driven Phase Change Composites. *J. Mater. Chem. A* **2016**, *4* (43), 17042−17049.

(127) Li, C.; Zhang, D.; Ren, W. Phase Change Materials Composite Based on Hybrid Aerogel with Anisotropic Microstructure. *Materials* **2021**, *14* (4), 777.

(128) Zhang, L.; Shi, Z.; Zhang, B.; Huang, J. Silver Attached Graphene-Based Aerogel Composite Phase Change Material and the Enhancement of Thermal Conductivity. *Materials* **2020**, *13* (15), 3271.

(129) Huang, J.; Zhang, B.; He, M.; Huang, X.; Wu, G.; Yin, G.; Cui, Y. Preparation of Anisotropic Reduced Graphene Oxide/BN/Paraffin Composite Phase Change Materials and Investigation of Their Thermal Properties. *J. Mater. Sci.* **2020**, *55* (17), 7337−7350.

(130) Xie, M.; Huang, J.; Ling, Z.; Fang, X.; Zhang, Z. Improving the Heat Storage/Release Rate and Photo-Thermal Conversion Performance of an Organic PCM/Expanded Graphite Composite Block. *Sol. Energy Mater. Sol. Cells* **2019**, *201*, 110081.

(131) Tahan Latibari, S.; Sadrameli, S. M. Carbon Based Material Included-Shaped Stabilized Phase Change Materials for Sunlight-Driven Energy Conversion and Storage: An Extensive Review. *Sol. Energy* **2018**, *170*, 1130−1161.

(132) Tang, L.-S.; Yang, J.; Bao, R.-Y.; Liu, Z.-Y.; Xie, B.-H.; Yang, M.-B.; Yang, W. Polyethylene Glycol/Graphene Oxide Aerogel Shape-Stabilized Phase Change Materials for Photo-to-Thermal Energy Conversion and Storage Via Tuning the Oxidation Degree of Graphene Oxide. *Energy Convers. Manage.* **2017**, *146*, 253−264.

(133) Xue, F.; Jin, X.-z.; Wang, W.-y.; Qi, X.-d.; Yang, J.-h.; Wang, Y. Melamine Foam and Cellulose Nanofiber Co-Mediated Assembly of Graphene Nanoplatelets to Construct Three-Dimensional Networks Towards Advanced Phase Change Materials. *Nanoscale* **2020**, *12* (6), 4005−4017.

(134) Xi, S.; Wang, M.; Wang, L.; Xie, H.; Yu, W. 3d Reduced Graphene Oxide Aerogel Supported TiO_{2-X} for Shape-Stable Phase Change Composites with High Photothermal Efficiency and Thermal Conductivity. *Sol. Energy Mater. Sol. Cells* **2021**, *226*, 111068.

(135) Zheng, X.; Gao, X.; Huang, Z.; Li, Z.; Fang, Y.; Zhang, Z. Form-Stable Paraffin/Graphene Aerogel/Copper Foam Composite Phase Change Material for Solar Energy Conversion and Storage. *Sol. Energy Mater. Sol. Cells* **2021**, *226*, 111083.

(136) Sootsman, J. R.; Chung, D. Y.; Kanatzidis, M. G. New and Old Concepts in Thermoelectric Materials. *Angew. Chem., Int. Ed.* **2009**, *48* (46), 8616−8639.

(137) Liu, D.; Lei, C.; Wu, K.; Fu, Q. A Multidirectionally Thermoconductive Phase Change Material Enables High and Durable Electricity Via Real-Environment Solar-Thermal-Electric Conversion. *ACS Nano* **2020**, *14* (11), 15738−15747.

(138) Zhang, Y.; Wu, K.; Fu, Q. A Structured Phase Change Material with Controllable Thermoconductive Highways Enables Unparalleled Electricity Via Solar-Thermal-Electric Conversion. *Adv. Funct. Mater.* **2021**, *32* (6), 2109255.

(139) Liu, P.; Gao, Y.; Chen, X. Magnetically Tightened Multifunctional Phase Change Materials. *Matter* **2022**, *5* (6), 1639−1642.

(140) Cao, R.; Sun, D.; Wang, L.; Yan, Z.; Liu, W.; Wang, X.; Zhang, X. Enhancing Solar-Thermal-Electric Energy Conversion Based on M-PEGMA/GO Synergistic Phase Change Aerogels. *J. Mater. Chem. A* **2020**, *8* (26), 13207−13217.

(141) Yu, C.; Yang, S. H.; Pak, S. Y.; Youn, J. R.; Song, Y. S. Graphene Embedded Form Stable Phase Change Materials for Drawing the Thermo-Electric Energy Harvesting. *Energy Convers. Manage.* **2018**, *169*, 88−96.

(142) Yu, C.; Kim, H.; Youn, J. R.; Song, Y. S. Enhancement of Structural Stability of Graphene Aerogel for Thermal Energy Harvesting. *ACS Appl. Energy Mater.* **2021**, *4* (10), 11666−11674.

(143) Wang, Y.; Ji, H.; Shi, H.; Zhang, T.; Xia, T. Fabrication and Characterization of Stearic Acid/Polyaniline Composite with Electrical Conductivity as Phase Change Materials for Thermal Energy Storage. *Energy Convers. Manage.* **2015**, *98*, 322−330.

(144) Zhang, Y.; Umair, M. M.; Zhang, S.; Tang, B. Phase Change Materials for Electron-Triggered Energy Conversion and Storage: A Review. *J. Mater. Chem. A* **2019**, *7* (39), 22218−22228.

(145) Xue, F.; Lu, Y.; Qi, X.-d.; Yang, J.-h.; Wang, Y. Melamine Foam-Templated Graphene Nanoplatelet Framework toward Phase Change Materials with Multiple Energy Conversion Abilities. *Chem. Eng. J.* **2019**, *365*, 20−29.

(146) Zhou, Y.; Wang, X.; Liu, X.; Sheng, D.; Ji, F.; Dong, L.; Xu, S.; Wu, H.; Yang, Y. Polyurethane-Based Solid-Solid Phase Change Materials with Halloysite Nanotubes-Hybrid Graphene Aerogels for Efficient Light-and Electro-Thermal Conversion and Storage. *Carbon* **2019**, *142*, 558−566.

(147) Zhou, Y.; Wang, X.; Liu, X.; Sheng, D.; Ji, F.; Dong, L.; Xu, S.; Wu, H.; Yang, Y. Multifunctional ZnO/Polyurethane-Based Solid-Solid Phase Change Materials with Graphene Aerogel. *Sol. Energy Mater. Sol. Cells* **2019**, *193*, 13−21.

(148) Hasegawa, S.; Kondo, K.; Oshinoya, Y. Experimental Verification of Heat Transport by Acoustic Wave. *Appl. Therm. Eng.* **2015**, *78*, 551−555.

(149) Oh, J.-H.; Lee, H. R.; Umrao, S.; Kang, Y. J.; Oh, I.-K. Self-Aligned and Hierarchically Porous Graphene-Polyurethane Foams for Acoustic Wave Absorption. *Carbon* **2019**, *147*, 510−518.

(150) Liu, L.; Hu, J.; Fan, X.; Zhang, Y.; Zhang, S.; Tang, B. Phase Change Materials with Fe_3O_4/GO Three-Dimensional Network Structure for Acoustic-Thermal Energy Conversion and Management. *Chem. Eng. J.* **2021**, *426*, 130789.

(151) Shi, Y.; Wang, C.; Yin, Y.; Li, Y.; Xing, Y.; Song, J. Functional Soft Composites as Thermal Protecting Substrates for Wearable Electronics. *Adv. Funct. Mater.* **2019**, *29* (45), 1905470.

(152) Sun, K.; Dong, H.; Kou, Y.; Yang, H.; Liu, H.; Li, Y.; Shi, Q. Flexible Graphene Aerogel-Based Phase Change Film for Solar-Thermal Energy Conversion and Storage in Personal Thermal Management Applications. *Chem. Eng. J.* **2021**, *419*, 129637.

(153) Li, G.; Hong, G.; Dong, D.; Song, W.; Zhang, X. Multiresponsive Graphene-Aerogel-Directed Phase-Change Smart Fibers. *Adv. Mater.* **2018**, *30* (30), 1801754.

(154) Chen, Z.; Zhuo, H.; Hu, Y.; Lai, H.; Liu, L.; Zhong, L.; Peng, X. Wood-Derived Lightweight and Elastic Carbon Aerogel for Pressure Sensing and Energy Storage. *Adv. Funct. Mater.* **2020**, *30* (17), 1910292.

(155) Long, S.; Feng, Y.; He, F.; Zhao, J.; Bai, T.; Lin, H.; Cai, W.; Mao, C.; Chen, Y.; Gan, L.; et al. Biomass-Derived, Multifunctional and Wave-Layered Carbon Aerogels toward Wearable Pressure Sensors, Supercapacitors and Triboelectric Nanogenerators. *Nano Energy* **2021**, *85*, 105973.

(156) Fang, X.; Hao, P.; Song, B.; Tuan, C.-C.; Wong, C.-P.; Yu, Z.-T. Form-Stable Phase Change Material Embedded with Chitosan-Derived Carbon Aerogel. *Mater. Lett.* **2017**, *195*, 79−81.

(157) Sheng, N.; Nomura, T.; Zhu, C.; Habazaki, H.; Akiyama, T. Cotton-Derived Carbon Sponge as Support for Form-Stabilized Composite Phase Change Materials with Enhanced Thermal Conductivity. *Sol. Energy Mater. Sol. Cells* **2019**, *192*, 8−15.

(158) Zhang, Q.; Xia, T.; Zhang, Q.; Zhu, Y.; Zhang, H.; Xu, F.; Sun, L.; Wang, X.; Xia, Y.; Lin, X. Biomass Homogeneity Reinforced Carbon Aerogels Derived Functional Phase-Change Materials for Solar-Thermal Energy Conversion and Storage. *Energy & Environmental Materials* **2021**, DOI: 10.1002/eem2.12264.

(159) Zou, Z.; Wu, W.; Wang, Y.; Drummer, D. Biomass Derived Carbon Aerogel as an Ultrastable Skeleton of Form-Stable Phase Change Materials for Efficient Thermal Energy Storage. *Mater. Res. Express.* **2020**, *7* (4), 045601.

(160) Wei, Y.; Li, J.; Sun, F.; Wu, J.; Zhao, L. Leakage-Proof Phase Change Composites Supported by Biomass Carbon Aerogels from Succulents. *Green. Chem.* **2018**, *20* (8), 1858−1865.

(161) Liu, H.; Qian, Z.; Wang, Q.; Wu, D.; Wang, X. Development of Renewable Biomass-Derived Carbonaceous Aerogel/Mannitol Phase-Change Composites for High Thermal-Energy-Release Efficiency and Shape Stabilization. *ACS Appl. Energy Mater.* **2021**, *4* (2), 1714−1730.

(162) Wang, C.; Liang, W.; Yang, Y.; Liu, F.; Sun, H.; Zhu, Z.; Li, A. Biomass Carbon Aerogels Based Shape-Stable Phase Change Composites with High Light-to-Thermal Efficiency for Energy Storage. *Renew. Energy* **2020**, *153*, 182−192.

(163) Wu, Y.; Ming, T.; Li, X.; Pan, T.; Peng, K.; Luo, X. Numerical Simulations on the Temperature Gradient and Thermal Stress of a Thermoelectric Power Generator. *Energy Convers. Manage.* **2014**, *88*, 915−927.

(164) Niu, Z.; Yuan, W. Highly Efficient Thermo-and Sunlight-Driven Energy Storage for Thermo-Electric Energy Harvesting Using Sustainable Nanocellulose-Derived Carbon Aerogels Embedded Phase Change Materials. *ACS Sustain. Chem. Eng.* **2019**, *7* (20), 17523−17534.

(165) Li, Y.; Samad, Y. A.; Polychronopoulou, K.; Alhassan, S. M.; Liao, K. From Biomass to High Performance Solar-Thermal and Electric-Thermal Energy Conversion and Storage Materials. *J. Mater. Chem. A* **2014**, *2* (21), 7759−7765.

(166) Yang, H.; Chao, W.; Di, X.; Yang, Z.; Yang, T.; Yu, Q.; Liu, F.; Li, J.; Li, G.; Wang, C. Multifunctional Wood Based Composite Phase Change Materials for Magnetic-Thermal and Solar-Thermal Energy Conversion and Storage. *Energy Convers. Manage.* **2019**, *200*, 112029.

(167) Sun, K.; Kou, Y.; Dong, H.; Ye, S.; Zhao, D.; Liu, J.; Shi, Q. The Design of Phase Change Materials with Carbon Aerogel Composites for Multi-Responsive Thermal Energy Capture and Storage. *J. Mater. Chem. A* **2021**, *9* (2), 1213−1220.

(168) Song, S.; Ai, H.; Zhu, W.; Lv, L.; Feng, R.; Dong, L. Carbon Aerogel Based Composite Phase Change Material Derived from Kapok Fiber: Exceptional Microwave Absorbility and Efficient Solar/Magnetic to Thermal Energy Storage Performance. *Compos. Part. B-Eng.* **2021**, *226*, 109330.

(169) Tao, Z.; Yang, M.; Wu, L.; Yan, J.; Yang, F.; Lin, J.; Wang, J.; Wang, G. Phase Change Material Based on Polypyrrole/Fe_3O_4-Functionalized Hollow Kapok Fiber Aerogel Matrix for Solar/Magnetic-Thermal Energy Conversion and Storage. *Chem. Eng. J.* **2021**, *423*, 130180.

(170) Jia, Z.; Zhang, M.; Liu, B.; Wang, F.; Wei, G.; Su, Z. Graphene Foams for Electromagnetic Interference Shielding: A Review. *ACS Appl. Nano Mater.* **2020**, *3* (7), 6140−6155.

(171) Linhares, T.; Pessoa de Amorim, M. T.; Duraes, L. Silica Aerogel Composites with Embedded Fibres: A Review on Their Preparation, Properties and Applications. *J. Mater. Chem. A* **2019**, *7* (40), 22768−22802.

(172) Wang, J.; Yang, M.; Lu, Y.; Jin, Z.; Tan, L.; Gao, H.; Fan, S.; Dong, W.; Wang, G. Surface Functionalization Engineering Driven Crystallization Behavior of Polyethylene Glycol Confined in Mesoporous Silica for Shape-Stabilized Phase Change Materials. *Nano Energy* **2016**, *19*, 78−87.

(173) Yu, Y.; Xu, J.; Wang, G.; Zhang, R.; Peng, X. Preparation of Paraffin/SiO_2 Aerogel Stable-Stabilized Phase Change Composites for High-Humidity Environment. *J. Mater. Sci.* **2020**, *55* (4), 1511−1524.

(174) Huang, X.; Liu, Z.; Xia, W.; Zou, R.; Han, R. P. Alkylated Phase Change Composites for Thermal Energy Storage Based on Surface-Modified Silica Aerogels. *J. Mater. Chem. A* **2015**, *3* (5), 1935−1940.

(175) Wu, X.; Ding, J.; Kong, Y.; Sun, Z.; Shao, G.; Li, B.; Wu, J.; Zhong, Y.; Shen, X.; Cui, S. Synthesis of a Novel Three-Dimensional Na_2SO_4@SiO_2@Al_2O_3-SiO_2 Phase Change Material Doped Aerogel Composite with High Thermal Resistance and Latent Heat. *Ceram. Int.* **2018**, *44* (17), 21855−21865.

(176) Xiangfa, Z.; Hanning, X.; Jian, F.; Changrui, Z.; Yonggang, J. Preparation, Properties and Thermal Control Applications of Silica Aerogel Infiltrated with Solid-Liquid Phase Change Materials. *J. Exp. Nanosci.* **2012**, *7* (1), 17−26.

(177) Shaid, A.; Wang, L.; Islam, S.; Cai, J. Y.; Padhye, R. Preparation of Aerogel-Eicosane Microparticles for Thermoregulatory Coating on Textile. *Appl. Therm. Eng.* **2016**, *107*, 602−611.

(178) Wang, F.; Gao, S.; Pan, J.; Li, X.; Liu, J. Short-Chain Modified SiO_2 with High Absorption of Organic PCM for Thermal Protection. *Nanomaterials* **2019**, *9* (4), 657.

(179) Gao, H.; Bo, L.; Liu, P.; Chen, D.; Li, A.; Ou, Y.; Dong, C.; Wang, J.; Chen, X.; Hou, C.; et al. Ambient Pressure Dried Flexible Silica Aerogel for Construction of Monolithic Shape-Stabilized Phase Change Materials. *Sol. Energy Mater. Sol. Cells* **2019**, *201*, 110122.

(180) Liu, P.; Gao, H.; Chen, X.; Chen, D.; Lv, J.; Han, M.; Cheng, P.; Wang, G. In Situ One-Step Construction of Monolithic Silica Aerogel-Based Composite Phase Change Materials for Thermal Protection. *Compos. Part. B-Eng.* **2020**, *195*, 108072.

(181) Yan, D.; Tang, B.; Zhang, S. Preparation and Performances of Sunlight-Induced Phase Change PEG/SiO_2-Dye Composite for Solar Energy Conversion and Storage. *Sol. Energy Mater. Sol. Cells* **2020**, *215*, 110657.

(182) Zhang, M.; Xiao, Q.; Chen, C.; Li, L.; Yuan, W. Developing a Heat-Insulating Composite Phase Change Material with Light-to-Thermal Conversion Performance from Graphene Oxide/Silica Hybrid Aerogel. *Appl. Therm. Eng.* **2020**, *174*, 115303.

(183) Zhao, L.; Bhatia, B.; Yang, S.; Strobach, E.; Weinstein, L. A.; Cooper, T. A.; Chen, G.; Wang, E. N. Harnessing Heat Beyond 200°C from Unconcentrated Sunlight with Nonevacuated Transparent Aerogels. *ACS Nano* **2019**, *13* (7), 7508−7516.

(184) Lyu, J.; Li, G.; Liu, M.; Zhang, X. Aerogel-Directed Energy-Storage Films with Thermally Stimulant Multiresponsiveness. *Langmuir* **2019**, *35* (4), 943−949.

(185) Li, H.; Li, J.; Thomas, A.; Liao, Y. Ultra-High Surface Area Nitrogen-Doped Carbon Aerogels Derived from a Schiff-Base Porous Organic Polymer Aerogel for CO_2 Storage and Supercapacitors. *Adv. Funct. Mater.* **2019**, *29* (40), 1904785.

(186) Zheng, Q.; Fang, L.; Guo, H.; Yang, K.; Cai, Z.; Meador, M. A. B.; Gong, S. Highly Porous Polymer Aerogel Film-Based Triboelectric Nanogenerators. *Adv. Funct. Mater.* **2018**, *28* (13), 1706365.

(187) Li, M.; Qin, Z.; Cui, Y.; Yang, C.; Deng, C.; Wang, Y.; Kang, J. S.; Xia, H.; Hu, Y. Ultralight and Flexible Monolithic Polymer Aerogel with Extraordinary Thermal Insulation by a Facile Ambient Process. *Adv. Mater. Interfaces* **2019**, *6* (13), 1900314.

(188) Li, T.; Song, J.; Zhao, X.; Yang, Z.; Pastel, G.; Xu, S.; Jia, C.; Dai, J.; Chen, C.; Gong, A.; et al. Anisotropic, Lightweight, Strong, and Super Thermally Insulating Nanowood with Naturally Aligned Nanocellulose. *Sci. Adv.* **2018**, *4* (3), eaar3724.

(189) Ferreira, F. V.; Otoni, C. G.; De France, K. J.; Barud, H. S.; Lona, L. M.F.; Cranston, E. D.; Rojas, O. J. Porous Nanocellulose Gels and Foams: Breakthrough Status in the Development of Scaffolds for Tissue Engineering. *Mater. Today* **2020**, *37*, 126−141.

(190) De France, K. J.; Hoare, T.; Cranston, E. D. Review of Hydrogels and Aerogels Containing Nanocellulose. *Chem. Mater.* **2017**, *29* (11), 4609−4631.

(191) Song, J.; Chen, C.; Yang, Z.; Kuang, Y.; Li, T.; Li, Y.; Huang, H.; Kierzewski, I.; Liu, B.; He, S.; et al. Highly Compressible, Anisotropic Aerogel with Aligned Cellulose Nanofibers. *ACS Nano* **2018**, *12* (1), 140−147.

(192) Wang, H.; Deng, Y.; Wu, F.; Jin, H.; Liu, Y.; Zheng, J. Facile in-Situ Fabrication of Latent Heat Enhanced Cellulose Aerogel-Based Form-Stable Composite Phase Change Materials Based on Dopamine Modification Strategy. *Sol. Energy Mater. Sol. Cells* **2021**, *230*, 111236.

(193) Song, M.; Jiang, J.; Zhu, J.; Zheng, Y.; Yu, Z.; Ren, X.; Jiang, F. Lightweight, Strong, and Form-Stable Cellulose Nanofibrils Phase Change Aerogel with High Latent Heat. *Carbohyd Polym.* **2021**, *272*, 118460.

(194) Du, X.; Qiu, J.; Deng, S.; Du, Z.; Cheng, X.; Wang, H. Alkylated Nanofibrillated Cellulose/Carbon Nanotubes Aerogels Supported Form-Stable Phase Change Composites with Improved N-Alkanes Loading Capacity and Thermal Conductivity. *ACS Appl. Mater. Interfaces* **2020**, *12* (5), 5695−5703.

(195) Yang, J.; Zhang, E.; Li, X.; Zhang, Y.; Qu, J.; Yu, Z.-Z. Cellulose/Graphene Aerogel Supported Phase Change Composites with High Thermal Conductivity and Good Shape Stability for Thermal Energy Storage. *Carbon* **2016**, *98*, 50−57.

(196) Wei, X.; Xue, F.; Qi, X.-d.; Yang, J.-h.; Zhou, Z.-w.; Yuan, Y.-p.; Wang, Y. Photo-and Electro-Responsive Phase Change Materials Based on Highly Anisotropic Microcrystalline Cellulose/Graphene Nanoplatelet Structure. *Appl. Energy* **2019**, *236*, 70−80.

(197) Zhang, Q.; Chen, B.; Wu, K.; Nan, B.; Lu, M.; Lu, M. Peg-Filled Kapok Fiber/Sodium Alginate Aerogel Loaded Phase Change Composite Material with High Thermal Conductivity and Excellent Shape Stability. *Compos. Part. A Appl. Sci. Manuf.* **2021**, *143*, 106279.

(198) Liu, H.; Sun, K.; Shi, X.; Yang, H.; Dong, H.; Kou, Y.; Das, P.; Wu, Z.-S.; Shi, Q. Two-Dimensional Materials and Their Derivatives for High Performance Phase Change Materials: Emerging Trends and Challenges. *Energy Storage Mater.* **2021**, *42*, 845−870.

(199) Chang, C.; Nie, X.; Li, X.; Tao, P.; Fu, B.; Wang, Z.; Xu, J.; Ye, Q.; Zhang, J.; Song, C.; et al. Bioinspired Roll-to-Roll Solar-Thermal Energy Harvesting within Form-Stable Flexible Composite Phase Change Materials. *J. Mater. Chem. A* **2020**, *8* (40), 20970−20978.

(200) Aftab, W.; Khurram, M.; Jinming, S.; Tabassum, H.; Liang, Z.; Usman, A.; Guo, W.; Huang, X.; Wu, W.; Yao, R.; et al. Highly Efficient Solar-Thermal Storage Coating Based on Phosphorene Encapsulated Phase Change Materials. *Energy Storage Mater.* **2020**, *32*, 199−207.

(201) Tang, Z.; Gao, H.; Chen, X.; Zhang, Y.; Li, A.; Wang, G. Advanced Multifunctional Composite Phase Change Materials Based on Photo-Responsive Materials. *Nano Energy* **2021**, *80*, 105454.

(202) Fan, X.; Yang, Y.; Shi, X.; Liu, Y.; Li, H.; Liang, J.; Chen, Y. A MXene-Based Hierarchical Design Enabling Highly Efficient and Stable Solar-Water Desalination with Good Salt Resistance. *Adv. Funct. Mater.* **2020**, *30* (52), 2007110.

(203) Tang, L.; Zhao, X.; Feng, C.; Bai, L.; Yang, J.; Bao, R.; Liu, Z.; Yang, M.; Yang, W. Bacterial Cellulose/MXene Hybrid Aerogels for Photodriven Shape-Stabilized Composite Phase Change Materials. *Sol. Energy Mater. Sol. Cells* **2019**, *203*, 110174.

(204) Du, X.; Wang, J.; Jin, L.; Deng, S.; Dong, Y.; Lin, S. Dopamine-Decorated $Ti_3C_2T_X$ MXene/Cellulose Nanofiber Aerogels Supported Form-Stable Phase Change Composites with Superior Solar-Thermal Conversion Efficiency and Extremely High Thermal Storage Density. *ACS Appl. Mater. Interfaces* **2022**, *14* (13), 15225−15234.

(205) Du, X.; Zhou, M.; Deng, S.; Du, Z.; Cheng, X.; Wang, H. Poly (Ethylene Glycol)-Grafted Nanofibrillated Cellulose/Graphene Hybrid Aerogels Supported Phase Change Composites with Superior Energy Storage Capacity and Solar-Thermal Conversion Efficiency. *Cellulose* **2020**, *27* (8), 4679−4690.

(206) Huang, H.; Shi, T.; He, R.; Wang, J.; Chu, P. K.; Yu, X. F. Phase-Changing Microcapsules Incorporated with Black Phosphorus for Efficient Solar Energy Storage. *Adv. Sci.* **2020**, *7* (23), 2000602.

(207) Du, X.; Qiu, J.; Deng, S.; Du, Z.; Cheng, X.; Wang, H. Flame-Retardant and Form-Stable Phase Change Composites Based on Black Phosphorus Nanosheets/Cellulose Nanofiber Aerogels with Extremely High Energy Storage Density and Superior Solar-Thermal Conversion Efficiency. *J. Mater. Chem. A* **2020**, *8* (28), 14126−14134.

(208) Wang, X.; Liu, Q.; Wu, S.; Xu, B.; Xu, H. Multilayer Polypyrrole Nanosheets with Self-Organized Surface Structures for Flexible and Efficient Solar-Thermal Energy Conversion. *Adv. Mater.* **2019**, *31* (19), 1807716.

(209) Xu, J.; Tan, Y.; Du, X.; Du, Z.; Cheng, X.; Wang, H. Cellulose Nanofibril/Polypyrrole Hybrid Aerogel Supported Form-Stable Phase Change Composites with Superior Energy Storage Density and Improved Photothermal Conversion Efficiency. *Cellulose* **2020**, *27* (16), 9547−9558.

(210) Zou, Y.; Chen, X.; Yang, P.; Liang, G.; Yang, Y.; Gu, Z.; Li, Y. Regulating the Absorption Spectrum of Polydopamine. *Sci. Adv.* **2020**, *6* (36), eabb4696.

(211) Tan, Y.; Du, X.; Du, Z.; Wang, H.; Cheng, X. Form-Stable Phase Change Composites Based on Nanofibrillated Cellulose/Polydopamine Hybrid Aerogels with Extremely High Energy Storage Density and Improved Photothermal Conversion Efficiency. *RSC Adv.* **2021**, *11* (10), 5712−5721.

(212) Wang, Y.; Li, X.; Cheng, H.; Wang, B.; Feng, X.; Mao, Z.; Sui, X. Facile Fabrication of Robust and Stretchable Cellulose Nanofibers/Polyurethane Hybrid Aerogels. *ACS Sustain. Chem. Eng.* **2020**, *8* (24), 8977−8985.

(213) Guo, W.; Liu, J.; Zhang, P.; Song, L.; Wang, X.; Hu, Y. Multi-Functional Hydroxyapatite/Polyvinyl Alcohol Composite Aerogels with Self-Cleaning, Superior Fire Resistance and Low Thermal Conductivity. *Compos. Sci. Technol.* **2018**, *158*, 128−136.

(214) Yang, L.; Yang, J.; Tang, L.-S.; Feng, C.-P.; Bai, L.; Bao, R.-Y.; Liu, Z.-Y.; Yang, M.-B.; Yang, W. Hierarchically Porous Pva Aerogel for Leakage-Proof Phase Change Materials with Superior Energy Storage Capacity. *Energy Fuels* **2020**, *34* (2), 2471−2479.

(215) Hong, H.; Pan, Y.; Sun, H.; Zhu, Z.; Ma, C.; Wang, B.; Liang, W.; Yang, B.; Li, A. Superwetting Polypropylene Aerogel Supported Form-Stable Phase Change Materials with Extremely High Organics Loading and Enhanced Thermal Conductivity. *Sol. Energy Mater. Sol. Cells* **2018**, *174*, 307−313.

(216) Hasegawa, G.; Shimizu, T.; Kanamori, K.; Maeno, A.; Kaji, H.; Nakanishi, K. Highly Flexible Hybrid Polymer Aerogels and Xerogels Based on Resorcinol-Formaldehyde with Enhanced Elastic Stiffness and Recoverability: Insights into the Origin of Their Mechanical Properties. *Chem. Mater.* **2017**, *29* (5), 2122−2134.

(217) Zhao, H.-B.; Yuan, L.; Fu, Z.-B.; Wang, C.-Y.; Yang, X.; Zhu, J.-Y.; Qu, J.; Chen, H.-B.; Schiraldi, D. A. Biomass-Based Mechanically Strong and Electrically Conductive Polymer Aerogels and Their Application for Supercapacitors. *ACS Appl. Mater. Interfaces* **2016**, *8* (15), 9917−9924.

(218) Liu, Q.; Yan, K.; Chen, J.; Xia, M.; Li, M.; Liu, K.; Wang, D.; Wu, C.; Xie, Y. Recent Advances in Novel Aerogels through the Hybrid Aggregation of Inorganic Nanomaterials and Polymeric Fibers for Thermal Insulation. *Aggregate* **2021**, *2* (2), e30.

(219) Wang, J.; Zhang, X. Binary Crystallized Supramolecular Aerogels Derived from Host-Guest Inclusion Complexes. *ACS Nano* **2015**, *9* (11), 11389−11397.

(220) Liu, Z.; Lyu, J.; Fang, D.; Zhang, X. Nanofibrous Kevlar Aerogel Threads for Thermal Insulation in Harsh Environments. *ACS Nano* **2019**, *13* (5), 5703−5711.

(221) Wang, Y.; Cui, Y.; Shao, Z.; Gao, W.; Fan, W.; Liu, T.; Bai, H. Multifunctional Polyimide Aerogel Textile Inspired by Polar Bear Hair for Thermoregulation in Extreme Environments. *Chem. Eng. J.* **2020**, *390*, 124623.

(222) Zheng, Z.; Shi, T.; Liu, H.; Wu, D.; Wang, X. Polyimide/ Phosphorene Hybrid Aerogel-Based Composite Phase Change Materials for High-Efficient Solar Energy Capture and Photothermal Conversion. *Appl. Therm. Eng.* **2022**, *207*, 118173.

(223) Zheng, Z.; Liu, H.; Wu, D.; Wang, X. Polyimide/MXene Hybrid Aerogel-Based Phase-Change Composites for Solar-Driven Seawater Desalination. *Chem. Eng. J.* **2022**, *440*, 135862.

(224) Cao, Y.; Weng, M.; Mahmoud, M.; Elnaggar, A. Y.; Zhang, L.; El Azab, I. H.; Chen, Y.; Huang, M.; Huang, J.; Sheng, X. Flame-Retardant and Leakage-Proof Phase Change Composites Based on MXene/Polyimide Aerogels toward Solar Thermal Energy Harvesting. *Adv. Compos. Hybrid. Ma.* **2022**, 1−15.

(225) Zhou, M.; Xie, D.; Zhou, K.; Gong, K.; Yin, L.; Qian, X.; Shi, C. 3D Porous Aerogel Based-Phase Change Materials with Excellent Flame Retardancy and Shape Stability for Both Thermal and Light Energy Storage. *Sol. Energy Mater. Sol. Cells* **2022**, *236*, 111537.

(226) Lyu, J.; Liu, Z.; Wu, X.; Li, G.; Fang, D.; Zhang, X. Nanofibrous Kevlar Aerogel Films and Their Phase-Change Composites for Highly Efficient Infrared Stealth. *ACS Nano* **2019**, *13* (2), 2236−2245.

(227) Zhang, X.; Li, N.; Hu, Z.; Yu, J.; Wang, Y.; Zhu, J. Direct Fabrication of Poly (P-Phenylene Terephthalamide) Aerogel and Its Composites with Great Thermal Insulation and Infrared Stealth. *Chem. Eng. J.* **2020**, *388*, 124310.

(228) Shi, T.; Zheng, Z.; Liu, H.; Wu, D.; Wang, X. Flexible and Foldable Composite Films Based on Polyimide/Phosphorene Hybrid Aerogel and Phase Change Material for Infrared Stealth and Thermal Camouflage. *Compos. Sci. Technol.* **2022**, *217*, 109127.

(229) Cheng, Q.; Liu, Y.; Lyu, J.; Lu, Q.; Zhang, X.; Song, W. 3D Printing-Directed Auxetic Kevlar Aerogel Architectures with Multiple Functionalization Options. *J. Mater. Chem. A* **2020**, *8* (28), 14243− 14253.

(230) Bao, Y.; Lyu, J.; Liu, Z.; Ding, Y.; Zhang, X. Bending Stiffness-Directed Fabricating of Kevlar Aerogel-Confined Organic Phase-Change Fibers. *ACS Nano* **2021**, *15* (9), 15180−15190.

(231) Cai, Y.; Hu, Y.; Song, L.; Tang, Y.; Yang, R.; Zhang, Y.; Chen, Z.; Fan, W. Flammability and Thermal Properties of High Density Polyethylene/Paraffin Hybrid as a Form-Stable Phase Change Material. *J. Appl. Polym. Sci.* **2006**, *99* (4), 1320−1327.

(232) Yang, Y.; Lyu, J.; Chen, J.; Liao, J.; Zhang, X. Flame-Retardant Host-Guest Films for Efficient Thermal Management of Cryogenic Devices. *Adv. Funct. Mater.* **2021**, *31*, 2102232.

(233) Cai, B.; Hübner, R.; Sasaki, K.; Zhang, Y.; Su, D.; Ziegler, C.; Vukmirovic, M. B.; Rellinghaus, B.; Adzic, R. R.; Eychmüller, A. Core-Shell Structuring of Pure Metallic Aerogels Towards Highly Efficient Platinum Utilization for the Oxygen Reduction Reaction. *Angew. Chem., Int. Ed.* **2018**, *57* (11), 2963−2966.

(234) Son, H. W.; Heu, C. S.; Lee, H. S.; Kim, S. H.; Mok, J. Y.; Kang, S.-W.; Kim, D. R. Enhanced Thermal Performance of Lithium Nitrate Phase Change Material by Porous Copper Oxide Nanowires

(235) Cai, B.; Dianat, A.; Hübner, R.; Liu, W.; Wen, D.; Benad, A.; Sonntag, L.; Gemming, T.; Cuniberti, G.; Eychmüller, A. Multi-metallic Hierarchical Aerogels: Shape Engineering of the Building Blocks for Efficient Electrocatalysis. *Adv. Mater.* **2017**, *29* (11), 1605254.

(236) Zhang, L.; An, L.; Wang, Y.; Lee, A.; Schuman, Y.; Ural, A.; Fleischer, A. S.; Feng, G. Thermal Enhancement and Shape Stabilization of a Phase-Change Energy-Storage Material Via Copper Nanowire Aerogel. *Chem. Eng. J.* **2019**, *373*, 857−869.

(237) Salamanca-Riba, L. G.; Isaacs, R. A.; LeMieux, M. C.; Wan, J.; Gaskell, K.; Jiang, Y.; Wuttig, M.; Mansour, A. N.; Rashkeev, S. N.; Kuklja, M. M.; et al. Synthetic Crystals of Silver with Carbon: 3D Epitaxy of Carbon Nanostructures in the Silver Lattice. *Adv. Funct. Mater.* **2015**, *25* (30), 4768−4777.

(238) Zhang, L.; Liu, X.; Deb, A.; Feng, G. Ice-Templating Synthesis of Hierarchical and Anisotropic Silver-Nanowire-Fabric Aerogel and Its Application for Enhancing Thermal Energy Storage Composites. *ACS Sustain. Chem. Eng.* **2019**, *7* (24), 19910−19917.

(239) Zhang, L.; Feng, G. A One-Step-Assembled Three-Dimensional Network of Silver/Polyvinylpyrrolidone (PVP) Nanowires and Its Application in Energy Storage. *Nanoscale* **2020**, *12* (19), 10573− 10583.

(240) Yi, H.; Xia, L.; Song, S. Three-Dimensional Montmorillonite/ Ag Nanowire Aerogel Supported Stearic Acid as Composite Phase Change Materials for Superior Solar-Thermal Energy Harvesting and Storage. *Compos. Sci. Technol.* **2022**, *217*, 109121.

(241) Song, L.; Ci, L.; Lu, H.; Sorokin, P. B.; Jin, C.; Ni, J.; Kvashnin, A. G.; Kvashnin, D. G.; Lou, J.; Yakobson, B. I.; et al. Large Scale Growth and Characterization of Atomic Hexagonal Boron Nitride Layers. *Nano Lett.* **2010**, *10* (8), 3209−3215.

(242) Zhang, K.; Feng, Y.; Wang, F.; Yang, Z.; Wang, J. Two Dimensional Hexagonal Boron Nitride (2d-Hbn): Synthesis, Properties and Applications. *J. Mater. Chem. C* **2017**, *5* (46), 11992−12022.

(243) Han, W.; Ge, C.; Zhang, R.; Ma, Z.; Wang, L.; Zhang, X. Boron Nitride Foam as a Polymer Alternative in Packaging Phase Change Materials: Synthesis, Thermal Properties and Shape Stability. *Appl. Energy* **2019**, *238*, 942−951.

(244) Jia, X.; Li, Q.; Ao, C.; Hu, R.; Xia, T.; Xue, Z.; Wang, Q.; Deng, X.; Zhang, W.; Lu, C. High Thermal Conductive Shape-Stabilized Phase Change Materials of Polyethylene Glycol/Boron Nitride@Chitosan Composites for Thermal Energy Storage. *Compos. Part. A Appl. Sci. Manuf.* **2020**, *129*, 105710.

(245) Yang, J.; Tang, L.-S.; Bao, R.-Y.; Bai, L.; Liu, Z.-Y.; Yang, W.; Xie, B.-H.; Yang, M.-B. An Ice-Templated Assembly Strategy to Construct Graphene Oxide/Boron Nitride Hybrid Porous Scaffolds in Phase Change Materials with Enhanced Thermal Conductivity and Shape Stability for Light-Thermal-Electric Energy Conversion. *J. Mater. Chem. A* **2016**, *4* (48), 18841−18851.

(246) Bao, J.; Edwards, M.; Huang, S.; Zhang, Y.; Fu, Y.; Lu, X.; Yuan, Z.; Jeppson, K.; Liu, J. Two-Dimensional Hexagonal Boron Nitride as Lateral Heat Spreader in Electrically Insulating Packaging. *J. Phys. D* **2016**, *49* (26), 265501.

(247) Wang, M.; Zhang, T.; Mao, D.; Yao, Y.; Zeng, X.; Ren, L.; Cai, Q.; Mateti, S.; Li, L. H.; Zeng, X.; et al. Highly Compressive Boron Nitride Nanotube Aerogels Reinforced with Reduced Graphene Oxide. *ACS Nano* **2019**, *13* (7), 7402−7409.

(248) Xue, F.; Jin, X.-z.; Xie, X.; Qi, X.-d.; Yang, J.-h.; Wang, Y. Constructing Reduced Graphene Oxide/Boron Nitride Frameworks in Melamine Foam Towards Synthesizing Phase Change Materials Applied in Thermal Management of Microelectronic Devices. *Nanoscale* **2019**, *11* (40), 18691−18701.

(249) Lei, C.; Wu, K.; Wu, L.; Liu, W.; Du, R.; Chen, F.; Fu, Q. Phase Change Material with Anisotropically High Thermal Conductivity and Excellent Shape Stability Due to Its Robust Cellulose/ Bnnss Skeleton. *J. Mater. Chem. A* **2019**, *7* (33), 19364−19373.

(250) Wan, L.; Liu, C.; Cao, D.; Sun, X.; Zhu, H. High Phase Change Enthalpy Enabled by Nanocellulose Enhanced Shape Stable

Boron Nitride Aerogel. *ACS Appl. Polym. Mater.* **2020**, *2* (7), 3001−3009.

(251) Kashfipour, M. A.; Dent, R. S.; Mehra, N.; Yang, X.; Gu, J.; Zhu, J. Directional Xylitol Crystal Propagation in Oriented Micro-Channels of Boron Nitride Aerogel for Isotropic Heat Conduction. *Compos. Sci. Technol.* **2019**, *182*, 107715.

(252) Dai, Y.; Wu, X.; Liu, Z.; Zhang, H.-B.; Yu, Z.-Z. Highly Sensitive, Robust and Anisotropic MXene Aerogels for Efficient Broadband Microwave Absorption. *Compos. Part. B-Eng.* **2020**, *200*, 108263.

(253) Liu, A.; Liang, X.; Ren, X.; Guan, W.; Gao, M.; Yang, Y.; Yang, Q.; Gao, L.; Li, Y.; Ma, T. Recent Progress in MXene-Based Materials: Potential High-Performance Electrocatalysts. *Adv. Funct. Mater.* **2020**, *30* (38), 2003437.

(254) Naguib, M.; Kurtoglu, M.; Presser, V.; Lu, J.; Niu, J.; Heon, M.; Hultman, L.; Gogotsi, Y.; Barsoum, M. W. Two-Dimensional Nanocrystals: Two-Dimensional Nanocrystals Produced by Exfoliation of Ti$_3$AlC$_2$. *Adv. Mater.* **2011**, *23* (37), 4207−4207.

(255) Zhang, Q.; Yi, G.; Fu, Z.; Yu, H.; Chen, S.; Quan, X. Vertically Aligned Janus MXene-Based Aerogels for Solar Desalination with High Efficiency and Salt Resistance. *ACS Nano* **2019**, *13* (11), 13196−13207.

(256) Lin, P.; Xie, J.; He, Y.; Lu, X.; Li, W.; Fang, J.; Yan, S.; Zhang, L.; Sheng, X.; Chen, Y. MXene Aerogel-Based Phase Change Materials toward Solar Energy Conversion. *Sol. Energy Mater. Sol. Cells* **2020**, *206*, 110229.

(257) Liu, X.; Lin, F.; Zhang, X.; Liu, M.; Sun, Z.; Zhang, L.; Min, X.; Mi, R.; Huang, Z. Paraffin/Ti$_3$C$_2$T$_X$ MXene@Gelatin Aerogels Composite Phase-Change Materials with High Solar-Thermal Conversion Efficiency and Enhanced Thermal Conductivity for Thermal Energy Storage. *Energy Fuels* **2021**, *35* (3), 2805−2814.

(258) Luo, Y.; Xie, Y.; Jiang, H.; Chen, Y.; Zhang, L.; Sheng, X.; Xie, D.; Wu, H.; Mei, Y. Flame-Retardant and Form-Stable Phase Change Composites Based on MXene with High Thermostability and Thermal Conductivity for Thermal Energy Storage. *Chem. Eng. J.* **2021**, *420*, 130466.

(259) Hu, W.-w.; Shi, X.-y.; Gao, M.-h.; Huang, C.-h.; Huang, T.; Zhang, N.; Yang, J.-h.; Qi, X.-d.; Wang, Y. Light-Actuated Shape Memory and Self-Healing Phase Change Composites Supported by MXene/Waterborne Polyurethane Aerogel for Superior Solar-Thermal Energy Storage. *Compos. Commun.* **2021**, *28*, 100980.

(260) Xia, L.; Zhang, P.; Wang, R. Preparation and Thermal Characterization of Expanded Graphite/Paraffin Composite Phase Change Material. *Carbon* **2010**, *48* (9), 2538−2548.

(261) Xiao, X.; Zhang, P. Morphologies and Thermal Characterization of Paraffin/Carbon Foam Composite Phase Change Material. *Sol. Energy Mater. Sol. Cells* **2013**, *117*, 451−461.

(262) Qi, G.; Yang, J.; Bao, R.; Xia, D.; Cao, M.; Yang, W.; Yang, M.; Wei, D. Hierarchical Graphene Foam-Based Phase Change Materials with Enhanced Thermal Conductivity and Shape Stability for Efficient Solar-to-Thermal Energy Conversion and Storage. *Nano Res.* **2017**, *10* (3), 802−813.

(263) Yang, J.; Tang, L.-S.; Bai, L.; Bao, R.-Y.; Liu, Z.-Y.; Xie, B.-H.; Yang, M.-B.; Yang, W. High-Performance Composite Phase Change Materials for Energy Conversion Based on Macroscopically Three-Dimensional Structural Materials. *Mater. Horizons* **2019**, *6* (2), 250−273.

(264) Zhao, Y.; Min, X.; Huang, Z.; Liu, Y. g.; Wu, X.; Fang, M. Honeycomb-Like Structured Biological Porous Carbon Encapsulating Peg: A Shape-Stable Phase Change Material with Enhanced Thermal Conductivity for Thermal Energy Storage. *Energy Build.* **2018**, *158*, 1049−1062.

(265) Wang, W.; Yang, X.; Fang, Y.; Ding, J. Preparation and Performance of Form-Stable Polyethylene Glycol/Silicon Dioxide Composites as Solid-Liquid Phase Change Materials. *Appl. Energy* **2009**, *86* (2), 170−174.

(266) Li, Y.; Yu, S.; Chen, P.; Rojas, R.; Hajian, A.; Berglund, L. Cellulose Nanofibers Enable Paraffin Encapsulation and the

Formation of Stable Thermal Regulation Nanocomposites. *Nano Energy* **2017**, *34*, 541−548.

(267) Sarı, A. Form-Stable Paraffin/High Density Polyethylene Composites as Solid-Liquid Phase Change Material for Thermal Energy Storage: Preparation and Thermal Properties. *Energy Convers. Manage.* **2004**, *45* (13−14), 2033−2042.

(268) Wu, W.; Wu, W.; Wang, S. Form-Stable and Thermally Induced Flexible Composite Phase Change Material for Thermal Energy Storage and Thermal Management Applications. *Appl. Energy* **2019**, *236*, 10−21.

(269) Xiao, X.; Zhang, P.; Li, M. Preparation and Thermal Characterization of Paraffin/Metal Foam Composite Phase Change Material. *Appl. Energy* **2013**, *112*, 1357−1366.

(270) Qian, Z.; Shen, H.; Fang, X.; Fan, L.; Zhao, N.; Xu, J. Phase Change Materials of Paraffin in H-BN Porous Scaffolds with Enhanced Thermal Conductivity and Form Stability. *Energy Build.* **2018**, *158*, 1184−1188.

(271) Fan, X.; Liu, L.; Jin, X.; Wang, W.; Zhang, S.; Tang, B. MXene Ti$_3$C$_2$T$_X$ for Phase Change Composite with Superior Photothermal Storage Capability. *J. Mater. Chem. A* **2019**, *7* (23), 14319−14327.

(272) Karaipekli, A.; Biçer, A.; Sarı, A.; Tyagi, V. V. Thermal Characteristics of Expanded Perlite/Paraffin Composite Phase Change Material with Enhanced Thermal Conductivity Using Carbon Nanotubes. *Energy Convers. Manage.* **2017**, *134*, 373−381.